WL-TM-92-313-FIBE

AN ASSESSMENT OF THE B-747'S CAPABILITY TO OPERATE ON ROUGH SURFACES

ELIJAH W. TURNER
JOHN T. RIECHERS

Loads and Criteria Group
Structural Integrity Branch

MAY 1992

FLIGHT DYNAMICS DIRECTORATE
WRIGHT LABORATORY
AIR FORCE SYSTEMS COMMAND
WRIGHT-PATTERSON AFB OHIO 45433-6553

FOREWORD

This report was prepared by Mr Elijah W. Turner and Mr John T. Riechers, Aerospace Engineers in the Loads and Criteria Group, Structural Integrity Branch, Structures Division, Flight Dynamics Directorate, Wright Laboratory at Wright-Patterson AFB OH. The work described herein is a part of the Air Force Systems Command program to determine the effect of operating aircraft from runways that have been bomb damaged and repaired. The work was conducted under Project 20545001. The Rapid Runway Repair program is managed by Air Force Engineering Support Center (AFESC/RDCR) at Tyndall AFB FL. The HAVE BOUNCE program is managed by Aeronautical Systems Divisions (ASD/TAA) at Wright-Patterson AFB. The HAVE BOUNCE Technical Manager is Mr John T. Riechers, WL/FIREB.

This report covers work done from May 1981 through September 1985. This manuscript was released by the authors in May 1992 for publication as a WL Technical Memorandum.

This report has been reviewed and approved.

Elijah W. Turner
Elijah W. Turner
Loads & Criteria Group
Structural Integrity Branch

John T. Riechers
John T. Riechers
Loads & Criteria Group
Structural Integrity Branch

This memorandum has been reviewed and approved.

James L. Rudd, Chief
Structural Integrity Branch
Structures Division

William P. Johnson, Tech Mgr
Loads & Criteria Group
Structural Integrity Branch

ABSTRACT

A study has been conducted to determine the capability of the Boeing 747 to operate on rough runways; specifically, runways that have been damaged by bombing and repaired rapidly using current Air Force procedures. The quality of the repairs has been determined that will allow the aircraft to operate from the repaired surface without being subjected to loads on the landing gears that exceed design limit load.

This study indicates that the B-747 is capable of taking off on a repaired runway at 836,000 lbs gross weight provided that repairs in the first 500 feet of the takeoff roll are at least class B. Repairs further down the runway only need to be class E. If the aircraft will traverse two repairs, tables are provided that give the minimum spacing between repairs. Consideration is not given to traversing more than two repairs.

Analysis indicates that the ability of the nose gear to withstand loads produced by traversing repair profiles can be significantly improved by increasing the precharge pressure in the shock strut. A nose gear precharge of 185 psi will reduce the peak loads sufficiently to permit a class C repair to be at any position on the runway, including the first 500 feet. Increasing the precharge pressure to 272 psi will permit class E repairs to be located anywhere.

At the maximum landing gross weight of 666000 lbs, none of the repairs A through E produced loads that exceeded design limit load during taxi at any speed. The landing touchdown, however, was not considered in this study. Until such time as an analysis becomes available, it should be considered that no repairs can be located in the touchdown area.

TABLE OF CONTENTS

LIST OF TABLES

LIST OF ILLUSTRATIONS

LIST OF ILLUSTRATIONS (Cont.)

LIST OF ILLUSTRATIONS (Cont.)

LIST OF ILLUSTRATIONS (Cont.)

1. INTRODUCTION

The US Air Force is concerned with the ability to use runways in as short a time as possible after they are bomb damaged. The Air Force Engineering Support Center (AFESC) located at Tyndall AFB FL. is in charge of developing methods for rapidly repairing runways and taxiways. The project, RAPID RUNWAY REPAIR (RRR), involves present and future methods for repairing runways and defining the quality of repairs needed for safe aircraft operations. The quality which is required is aircraft dependent. Fighter aircraft, in general, require smoother repairs than transport or bomber aircraft.

The Aeronautical Systems Division (ASD) and Wright Laboratory (WL) are assisting AFESC by providing validated computer programs which simulate aircraft operations on repaired, bomb damaged runways. The computer programs for particular aircraft are developed through contracts, or in-house efforts at WL. This project is called HAVE BOUNCE. The program is managed at ASD and WL is providing technical support. Headquarters USAF has selected a variety of fighter and transport aircraft to be evaluated.

The approach is to develop a mathematical model of each aircraft and simulate the aircraft traversing discrete runway roughness profiles. The computer programs must have the capability of predicting loads at critical locations on the aircraft. WL has monitored the technical aspects of the contractor's programs and performed some simulations in-house using a WL developed computer program called TAXI.

Some of the selected aircraft have been tested at the Air Force Flight Test Center (AFFTC) at Edwards AFB CA. These test have been compared to the computer simulations which have permitted the mathematical model to be corrected and validated, thus providing increased confidence in the accuracy of the simulations. There are no plans to test the B-747 aircraft, hence only analytical tools will be available for developing surface roughness criteria for bomb damage repair. The Boeing Company has performed some simulations of the B-747 taxiing over discrete repair profiles. These were compared to simulations produced at the WL and are presented in this report. The comparison has provided a level of confidence in the Boeing and WL simulations. It is not known if AFESC will utilize the program developed at WL to develop final repair roughness criteria or contract for a more detailed computer program to be developed.

2. ANALYSIS

2.1 General Arrangement Of B-747

The 747 family of aircraft consists of seven models, six of which are included in the Civil Reserve Air Force (CRAF). The B-747-200F is certified to a maximum gross weight of 836000 lbs and is the most critical aircraft for rough runway operations. The maximum landing weight of this aircraft is 666000 lbs. This report is directed to determining the capabilities of these two configurations of the B-747-200F. Figure 1 presents two views of the B-747 aircraft.

The landing gear system consists of five single-stage, vertical-post shock struts with oleo-pneumatic shock absorbing characteristics. The nose gear, shown in Figure 2, is a single axle, dual wheel arrangement. The main landing gear systems as shown in Figures 3 and 4 respectively. They have two posts on the wings and two on the body. Each main gear post has a bogie arrangement with twin tandem axles. The landing gear footprint is shown in Figure 5.

2.2 Repair Profiles

The procedure for repairing bomb damage to runways consists of filling the crater to within 24 inches of the surface with material discharged from the crater and compacting with heavy equipment. The remaining 24 inches is filled with crushed limestone and compacted with vibratory compactors. The surface is filled, compacted and graded to a specified degree of flatness. The entire area of the damage is then covered with articulated aluminum planks that are 1 1/2 inches thick, 24 inches wide and 6 or 12 feet long. Planks of triangular cross section 2 foot wide are used as ramps to get get the aircraft on and off of the mat. The planks are joined along the long side to form an assembly which is nominally 54 by 78 feet. The AM-2 mat, as it is called, can be assembled to the side of the crater while the crater is being filled and compacted. The mat can then be pulled over the compacted crater by a tractor to complete the repair.

In order to investigate a realistic variety of repairs, 4 repair profiles have been selected. They are referred to as SINGLE BUMP, DOUBLE BUMP, SINGLE MAT and SEVERE BUMP WITH SETTLING. These configurations are presented in Figure 6.

2.3 Computer Program

A digital computer program developed in-house at the Flight Dynamics Directorate was used in the analysis. Computer program TAXI was used to simulate the B-747 traversing discrete profiles

and produced nose, wing and body gear loads as a function of time. Options are available within the program to cycle through a number of time history solutions recording only the maximum value of each solution. Use of this option provided aircraft response in the velocity domain.

For the condition of free roll, thrust is equal to the sum of aerodynamic drag and rolling friction on the runway. This is slightly conservative, because there would normally be some thrust on the engine and engine thrust creates a nose up pitching moment. Therefore, to neglect it increases the loads on the nose gear. For the condition of braking with reverse thrust, the moment due to forward thrust is zero, but the contribution due to reverse thrust is considered. This is consistant with the real situation.

The aircraft structure was modeled with 18 flexible modes of vibration, together with rigid body pitch and vertical translation. Structural damping was assumed to be 3 percent of critical damping. Lift and moment aerodynamic loads were modeled as a function of the angle of attack and aerodynamic drag was modeled using a 0.055 drag coefficient. Damping was added to rigid body pitch and vertical translation modes to obtain realistic amplitude decay rates over time periods of 5 to 10 seconds. The rigid body damping simulates aerodynamic and tire damping that were not explicitly modeled.

The landing gear shock struts were modeled to include bearing friction, hydraulic forces due to discharge of oil through an orifice and pneumatic forces from a nitrogen charged strut. Bearing friction was modeled as a force opposing the direction of stroke of the strut. The magnitude of the force was equal to the smaller of 0.1 times the bearing normal force, or the unbalance force on the strut relative to static equilibrium. Modeling in this way allows the strut to stop momentarily when it reverses direction and not begin moving again until the unbalance force exceeds a static friction of 0.2 times the normal bearing force. The pneumatic force within the cylinder was modeled as a reversible isothermal compression. The hydraulic force was modeled using a hydraulic discharge coefficient in conjunction with a variable orifice area. The orifice area is controlled by the position of the shock strut by means of a contoured metering pen that passes through the center of the orifice.

The tires were modeled using parabolic springs and drag components due to rolling friction that were assumed to act at the axle. The drag components were 0.05 times the normal force in the tire. When braking conditions were simulated, the magnitude of the drag force was assumed to have an additional component for the wing and body gears equal to 0.45 times the normal strut force. The reverse thrust resulting from all four engines was assumed to be a vector located 70.8 inches below the center of gravity of the aircraft. This results in a nose down pitching moment which creates additional load on the nose gear. The magnitude of the

reverse thrust is a function of the aircraft forward velocity. Tabular data was obtained from the Boeing Company and two parabolic curves were fitted to the data to produce the reverse thrust versus velocity presented in Figure 7a.

Specific items that were not modeled in the computer program TAXI and for which no allowance has been made include the following:

Hydraulic damper which arrests the pitch of the articulating trucks on each of the main and wing gears

The effect of wing lift spoilers

The action of the wheel anti-skid mechanisms

The effects of cylinder expansion and oil compressibility

2.4 Simulations

The heavy gross weight of 836000 lbs was analyzed for free roll over various profiles. This weight is larger than the maximum landing weight. Therefore, the aircraft should not be subjected to significant braking loads at this gross weight except under the emergency condition of an aborted take-off. Since use of the CRAF aircraft over repaired bomb damaged runways is an unlikely event, it is not reasonable to consider this event to occur in conjunction with another unlikely event, an aborted takeoff. Therefore, braking at 836000 lbs gross weight was not analyzed.

The maximum landing weight of 666000 lbs was analyzed for those conditions likely to occur on a normal rollout after landing. The application of brakes produces a nose down pitching moment and tends to increase nose gear loads. Reverse thrust also tends to increase nose gear loads. Although the application of heavy braking and reverse thrust is not normal operation, it is reasonably possible that they both may be required on a short runway. Therefore, this condition was analyzed.

The condition of an aircraft landing on a repair profile was not analyzed because it is not within the capabilities of the computer program TAXI.

In this investigation, there were three types of analysis performed. Each involved taxi over all 4 repair profiles at constant speed. The analyses are:

FREE ROLL: Rolling friction equal to 0.05 times aircraft weight.

BRAKED ROLL: Rolling friction on the nose gear and braking friction on each of the main gears equal to 0.50 times the normal gear force.

BRAKING WITH REVERSE THRUST: Reverse thrust as a function of aircraft velocity acting along the engine axis combined with braking the same as in the braked roll.

The results of these analyses are presented in two forms: velocity plots and time histories. The velocity plots present maximum parameter response as a function of aircraft velocity over the respective repair profile. These plots are useful in identifying the critical velocities for each response parameter. The time histories display how the parameter values vary with time during a traverse of a particular profile at constant velocity.

Velocity plots are presented for each analysis over each of the repair profiles. Time history plots are presented for the critical velocity identified from the velocity analysis. The parameters that were monitored include nose gear load, wing gear load and body gear load.

2.5 Basis For Interpreting Results

The Design Limit Load (DLL) for each gear in the vertical direction was considered to be the maximum allowable load for safe operation. It is probable that the strength of each gear exceeds the DLL, but this is not known. In the future, if there is a need to establish a higher capability, then additional analysis and test can be done. Such analysis and test, however, are beyond the scope of this effort. The DLL for the gears are given in Table 1.

TABLE 1

B-747 DESIGN LIMIT LOAD

Nose Gear Vertical Load	196700 lbs
Wing Gear Vertical Load	378000 lbs
Body Gear Vertical Load	436000 lbs

2.6 Acceleration For Takeoff

The recommended class of repairs that may be permitted on the Minimum Operating Strip (MOS) takes into consideration the velocity that the aircraft is likely to have at various positions on the strip during the takeoff roll. Certain repair profiles have critical velocities and it is necessary to restrict use of that quality of repair in an area that the aircraft is likely to

traverse at the critical velocity. Figure 7b gives the aircraft velocity as a function of position down the strip form the start of the takeoff roll.

2.7 Analysis By The Boeing Company

The Boeing Company of Seattle, Washington, performed an analysis to identify critical components of the aircraft. They identified the nose gear, wing and fuselage as being potentially critical. These results are presented in Table 2 in terms of design limit load. In considering the nose gear, wing and fuselage, the margin of safety for the nose gear was the lowest of the three components. It is presumed that if it is safe to taxi over a particular profile from a nose gear load standpoint, then it is safe from a wing and body load standpoint. This assumption was necessary because the computer program TAXI does not have the provision to monitor wing and body loads.

TABLE 2

RESULTS OF BOEING COMPANY ANALYSIS
Taxi of B-747 over Single Bump at 836000 lbs

Max Wing loads	78% DLL
Max Fuselage Loads	60% DLL
Max Inboard Nacelle Loads	23% DLL
Max Outboard Nacelle Loads	20% DLL
Max Nose Gear Load	83% DLL
Max Wing Gear Load	60% DLL
Max Body Gear Load	49% DLL

Results from the computer program TAXI were compared with results from the Boeing Company analysis. The maximum vertical gear loads as a function of taxi velocity are compared in Figure 8 for taxi over a double bump at a gross weight of 836000 lbs. Although none of the gear loads exceeded design limit loads, there are differences in the two analyses. For the nose gear, the analyses differ by 3 percent (Boeing lower), wing gear by 2 percent (Boeing lower) and body gear by 2 percent (Boeing higher). Figures 9, 10 and 11 present a comparison of the time histories of the nose, wing and body gear loads respectively for taxi over a double bump at 25 knots at a gross weight of 836000 lbs. At this velocity, the analysis differ by 6 percent for the nose gear (Boeing lower), wing gear by 1 percent (Boeing higher) and body gear by 1 percent (Boeing higher). These comparisons indicate a reasonable level of confidence in the two analyses.

2.8 Landing Analysis By The Boeing Company

The Boeing Company performed a landing analysis where discrete profiles were encountered during touchdown at various sink speeds. For a B-747 at 666000 lbs gross weight, landing with the main gears on a double bump at the most critical time during the touchdown, it was determined that design limit loads would be exceeded by the vertical bending loads on the fuselage at body balance station (BBS) 1900, for a sink rate of 7.2 feet per second.

Although a sink rate of 7.2 feet per second gives reasonable latitude, caution is advised. The presence of upheavel can add to the loads. Figure 12 illustrates that a 1 inch upheavel over a distance of 10 feet produces a slope that is equivalent to a sink rate of 2 feet per second when encountered at a forward velocity of 240 feet per second.

2.9 Load Stroke Curve

The pneumatic force in each strut is a function of the precharge pressure in the strut, the volume of the strut when it is fully extended and the area of the pneumatic piston in the strut. Use of parameter values taken from engineering drawings of the shock struts produced values that were slightly different for those used in the analysis by the Boeing Company. To eliminate these differences as much as possible, small changes in the precharge pressure, strut volume and piston area were made so as to achieve the best possible match to the pneumatic load stroke curve used in the Boeing analysis. Figures 13, 14 and 15 present comparisons of the load stroke curves used in the two analyses for the nose, wing and body gears respectively.

2.10 Eeffect Of Structural Flexibility and Aerodynamic Loads

As a check on the reasonableness of the TAXI analysis, the effects of aircraft flexibility and aerodynamic loads were considered. A time history analysis was performed in which the flexible modes of vibration were removed from the analysis. Another analysis was performed in which the aerodynamic pressure was set equal to zero so that where would be no aerodynamic forces. Figures 16, 17 and 18 present these two analyses together with a rational analysis for taxi over a single bump at 60 knots with a gross weight of 836000 lbs, for the nose, wing and body gears respectively. The effects appear to be reasonable.

2.11 Rigid Body Damping

Damping was added to the rigid body pitch and vertical translation modes in order to account for the aerodynamic and tire damping that is not modeled explicitly in the computer program TAXI. Damping added to the rigid body modes has little effect on

the initial encounter of a repair profile, but has a significant effect on the loads from a second profile located a considerable distance from the first and encountered when the oscillation is at a critical phase. The objective was to add a reasonable amount of damping so as not to severely penalize the B-747's capability to encounter multiple repair profiles, yet to have confidence that the taxi analysis is under damped and thus produces higher (conservative) loads. Comparison of the results of the Boeing analysis and TAXI for 25 knot over a double bump indicate that they have about the same damping upon initial bump encounter. The Boeing analysis displayed a damping ratio of about -0.039 and TAXI displayed a damping ratio of about -0.034 for a period of time immediately after leaving the repair profile. It is interesting to note that data available from the C-130 test indicated a damping ratio of about -0.08 after mat encounter. For multiple repair encounter, however, the damping at lower amplitudes is of considerable importance. A Boeing computer run made to determine initial conditions, indicated that the oscillatory component of nose gear load decayed from 15000 lbs to 2000 lbs in 5 cycles. TAXI analysis indicated a decay from 15000 lbs to 2000 lbs in 7 cycles. Hence, for the same low amplitude, the Boeing analysis indicated a damping ratio of -0.06 and TAXI indicated a damping ratio of -0.04. This provides reasonable confidence that excessive damping has not been added to the TAXI analysis and that the results are expected to be conservative. The effect of rigid body damping on nose, wing and body gear loads is shown in Figures 19, 20 and 21 respectively.

3. RESULTS

3.1 Velocity Analysis

Table 3 presents a summary of results from 12 velocity analyses with respect to nose gear vertical load, the most critical structure for taxi over repair profiles. The first 12 figures following Table 3 give nose, wing and body gear loads as a function of velocity for the analyses summarized in Table 3. Two gross weights were analyzed and 4 repair profiles. For 836000 lbs gross weight, only free roll was analyzed. For 666000 lbs gross weight, only braking was analyzed, however, it was considered both with and without thrust reversal. For those conditions where the nose gear load exceeded design limit load, the condition was reanalyzed using a nose gear strut precharge pressure adequate to reduce the loads to below design limit load.

3.2 Time History Analysis

Table 3 also identifies the particular velocity which produced the maximum nose gear load, referred to as the critical velocity. For the 836000 lbs gross weight conditions, time histories are presented for taxi over each repair profile at the critical velocity, except for conditions where the nose gear precharge pressure was increased. For the 666000 lbs gross weight conditions, time histories are presented for taxi over each repair profile at the critical velocities for combined braking and thrust reversal, which were determined to be more critical than without thrust reversal.

3.3 High Pressure Strut Analysis

For taxi at 836000 lbs, class E repairs produced nose gear loads that exceed design limit load. For this condition, a variety of computer runs were made in which the nose gear precharge pressure was increased. The results of these analyses are presented in Figure 52, which indicates that a precharge pressure of 280 psi would permit the aircraft to taxi over class E repairs at any speed.

3.4 One-Minus-Cosine Profile Analysis

Although a One-Minus-Cosine profile is not considered a likely shape for a bomb damage repair profile, this shape was analyzed because it is a smooth shape that is often used in analytical comparisons. Figure 53 presents the results of a velocity analysis for an 836000 lb aircraft traversing a 3 inch high One-Minus-Cosine shaped profile with a wave length of 60 feet. Nose, wing and body gear vertical loads are presented in figure 54, 55 and 56

respectively, for traverse of the same profile at 60 knots, which is very near the critical velocity for the nose gear load.

3.5 Aircraft Traversing Multiple Repair Profiles

An aircraft traversing more than one repair profile may experience increased load if the second profile is encountered while the aircraft is at an unfavorable phase of the rigid body oscillation that resulted from the first profile. An analysis was performed to determine the minimum spacing between repair profiles if two are encountered. The spacing allows the rigid body oscillations to be attenuated so that the gear loads from the second profile do not exceede design limit. The results are summarized in Table 4. Figures 57 through 72 present velocity analysis plots of all possible pairs of the four repair profiles that were investigated. The case of encountering more than 2 profiles has so many possible combinations and spacings that it was not addressed in this analysis.

4. CONCLUSION

1 Aircraft velocity can be determined as a function of the distance traveled during the takeoff roll from Figure 7b for the B-747 at 836000 lbs gross weight. This chart can be used to determine the probable speed that an aircraft will encounter a repair profile, if the position of the repair profile is known relative to the start of the takeoff roll.

2. The maximum nose, wing and body gear loads can be determined for the B-747 traversing class A, B, C or E repair profiles at any speed up to takeoff speed for gross weights of 836000 and 666000 from velocity analysis plots provided in this report.

3. The minimum spacing between repair profiles is presented for pairs of class A, B, C and E repair profiles such that design limit load will not be exceeded for 836000 lbs gross weight.

4. The computer program TAXI, which was utilized in producing the results for this report, produced results that were similar to results produced by a computer program that was developed at the Boeing Company.

a. For the nose gear, the maximum values from a time history analyses differ by 3 percent (Boeing lower), wing gear by 2 percent (Boeing lower) and the body gear by 2 percent (Boeing higher).

b. Over a double bump at 25 knots at a gross weight of 836000 lbs, the maximum value from the time history analysis for the nose gear differed by 6 percent (Boeing lower), wing gear by 1 percent (Boeing higher) and body gear by 1 percent (Boeing higher).

c. There was a very close correlation between the Boeing Company and TAXI analyses on the stroke curves.

5. RECOMMENDATIONS

1. It appears that the B-747 has significant capability to negotiate rough runways. If it is considered likely that it will be used in this manner, then it is recommended that a flight test program be initiated to validate or refine the roughness criteria set forth in this document.

2. Following validation of the computer model, it is recommended that a more extensive analysis be conducted to define the capability to operate over multiple repair profiles.

3. If enhancement of the B-747's rough runway capability is desirable, the pratical aspects of the high pressure nose gear strut should be investigated.

6. REFERENCES

1. Gerardi, Anthony G., "Digital Simulation of Flexible Aircraft Response to Symmetrical and Asymmetrical Runway Roughness," AFFDL-TR-77-37, Air Force Flight Dynamics Laboratory, Wright-Patterson AFB OH 45433, August 1977.

2. "TASK II RESULTS, INTERIM REPORT, HAVE BOUNCE (747)," Contract Number F33615-81-C-2095, Boeing Military Airplane Company, Seattle, Washington, February 1982, updated August 1983.

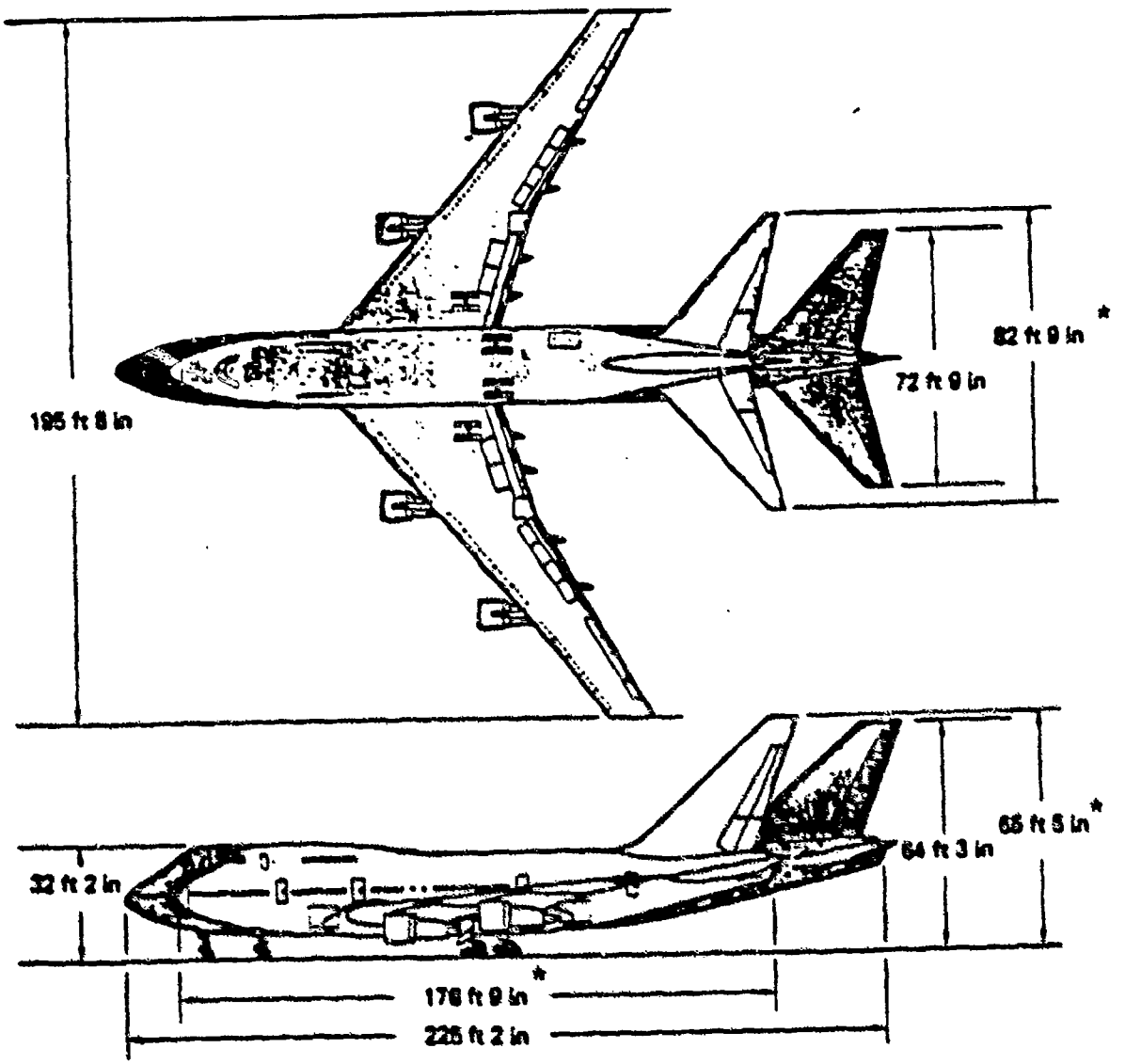

Figure 1 External Dimensions of B747

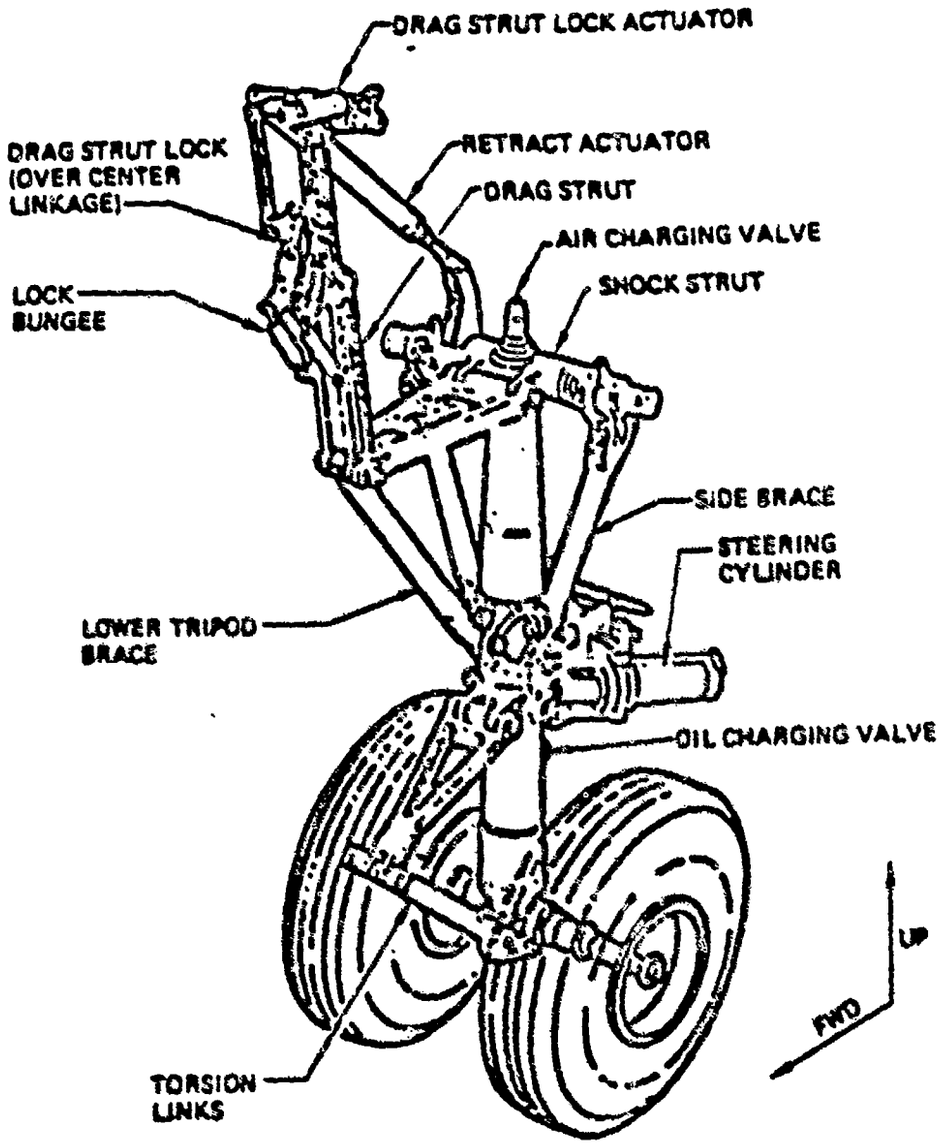

Figure 2 Nose Landing Gear Configuration

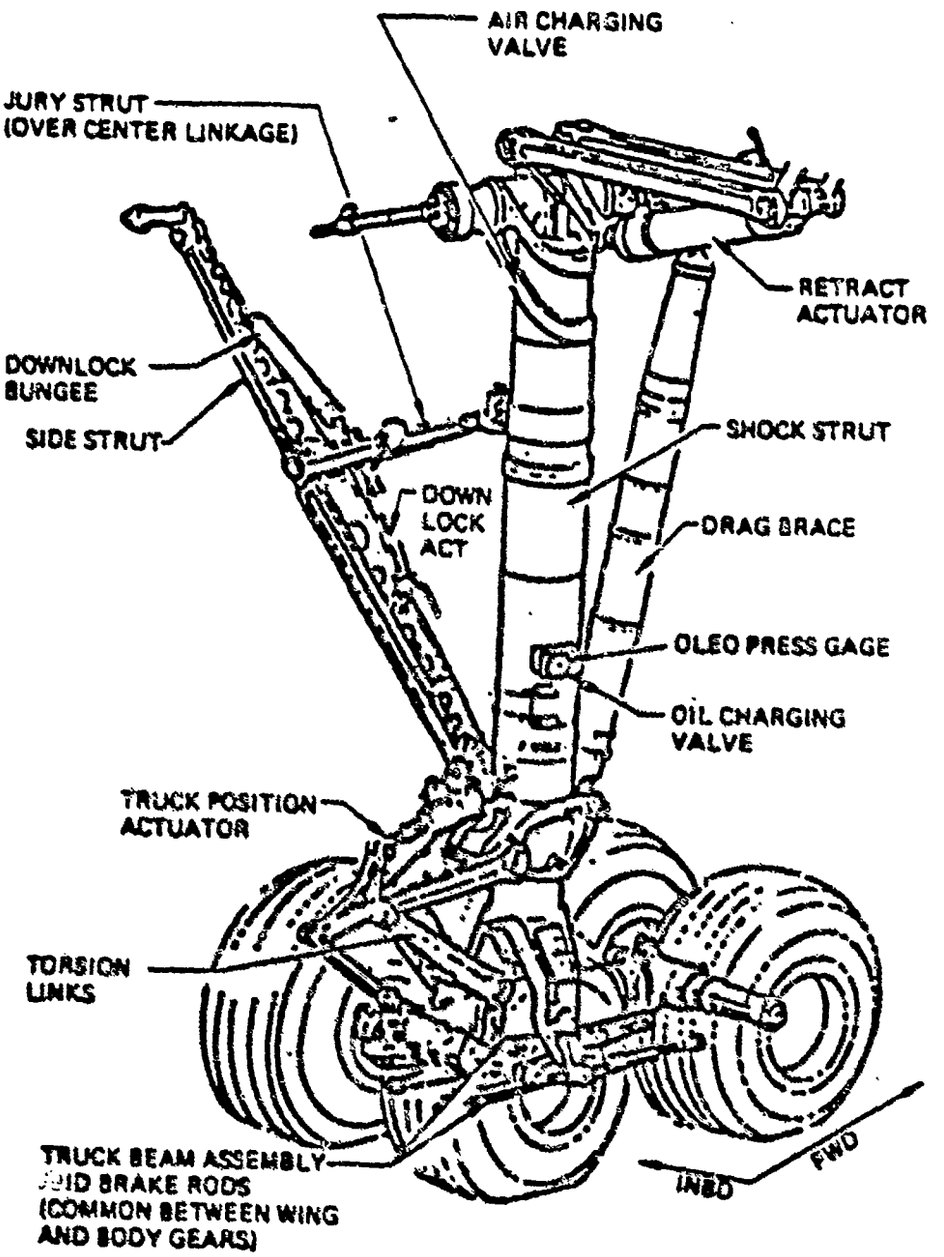

Figure 3 Wing Landing Gear Configuration

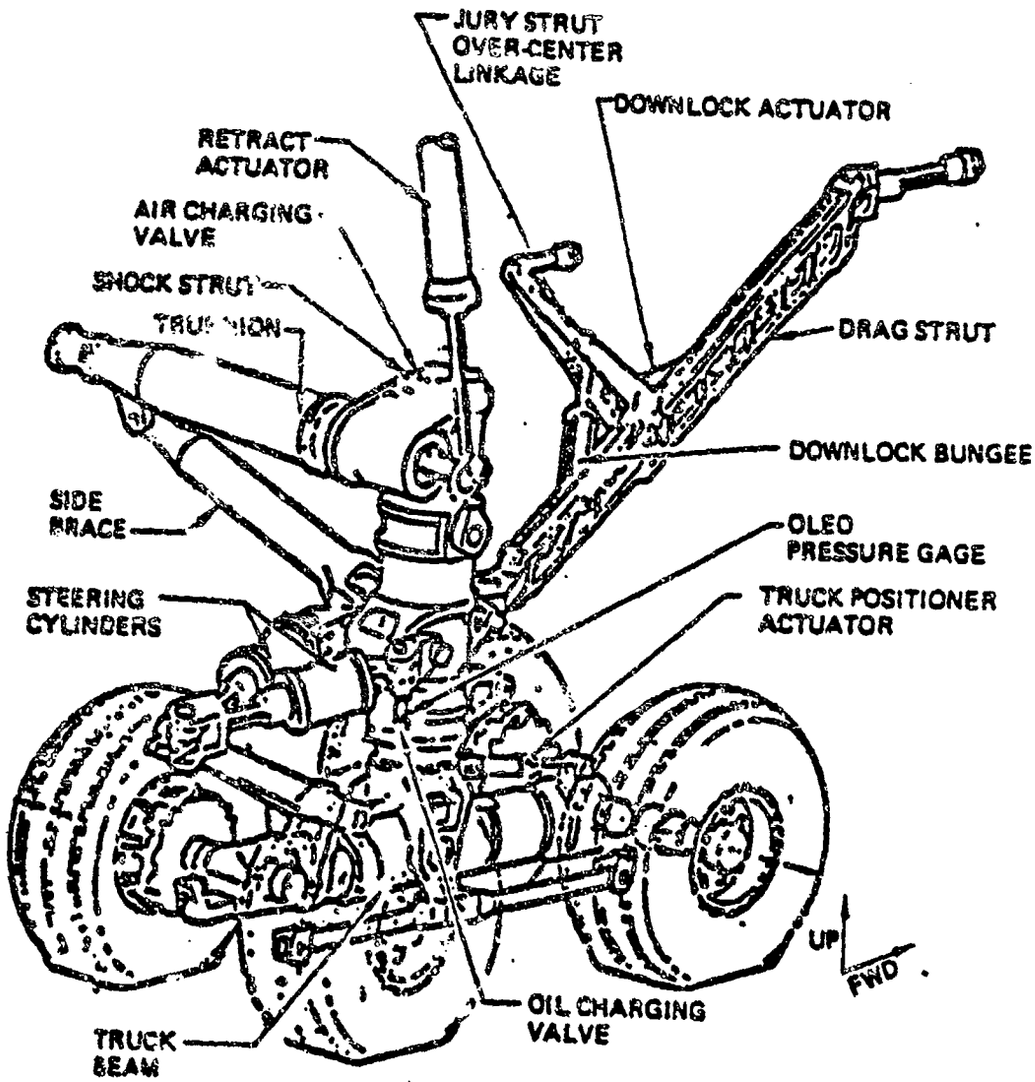

Figure 4 Body Landing Gear Configuration

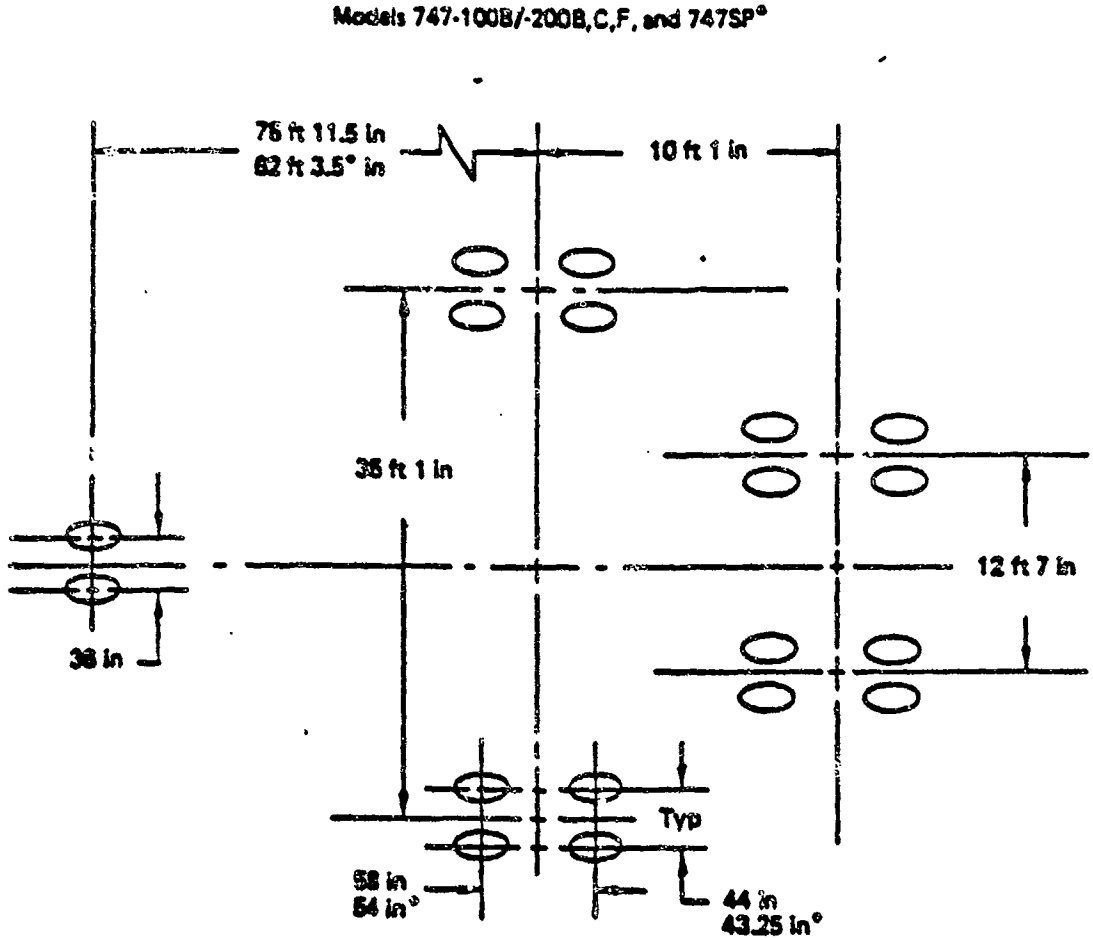

Figure 5 Landing Gear Footprint

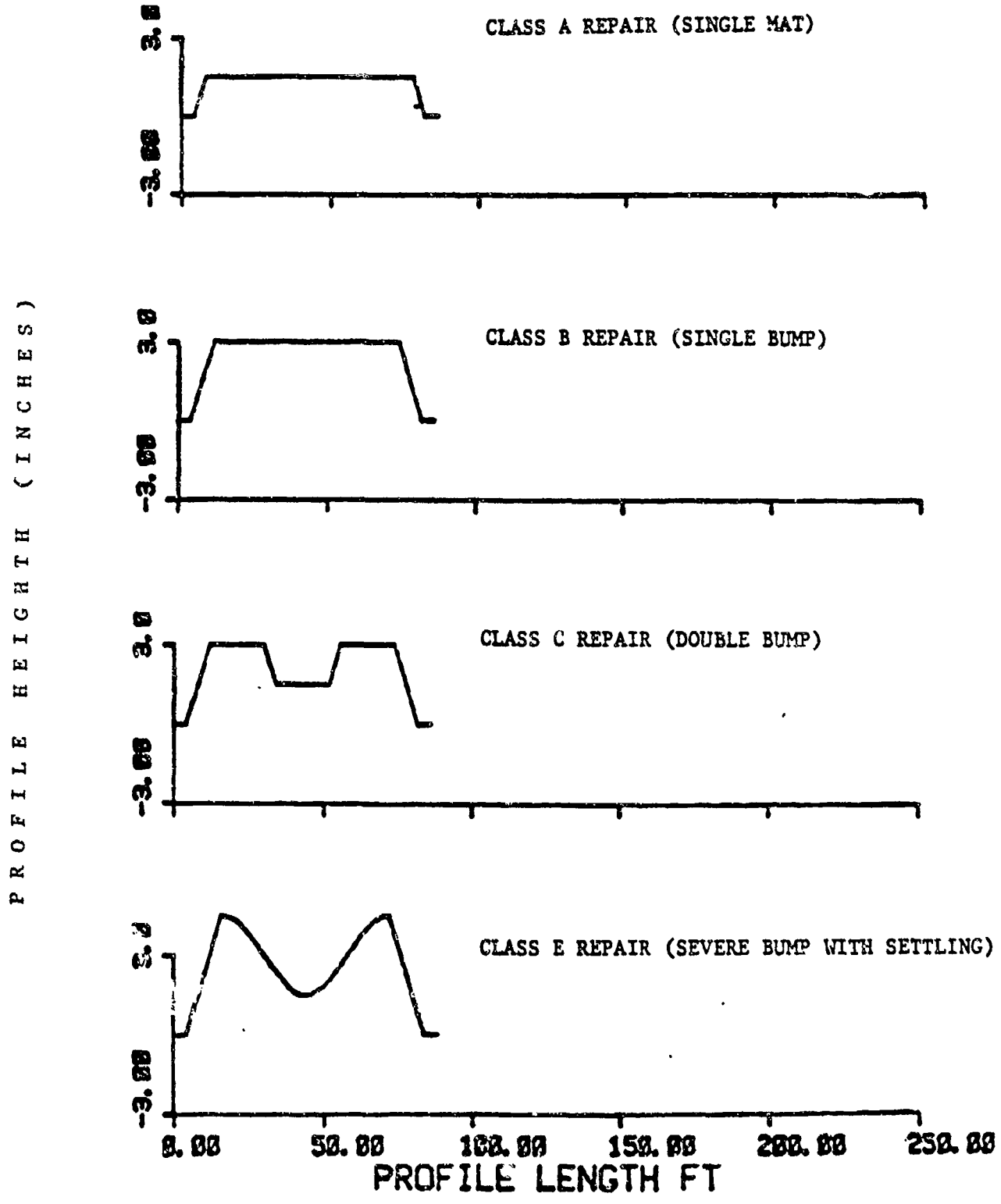

Figure 6 Bomb Damage Repair Profiles

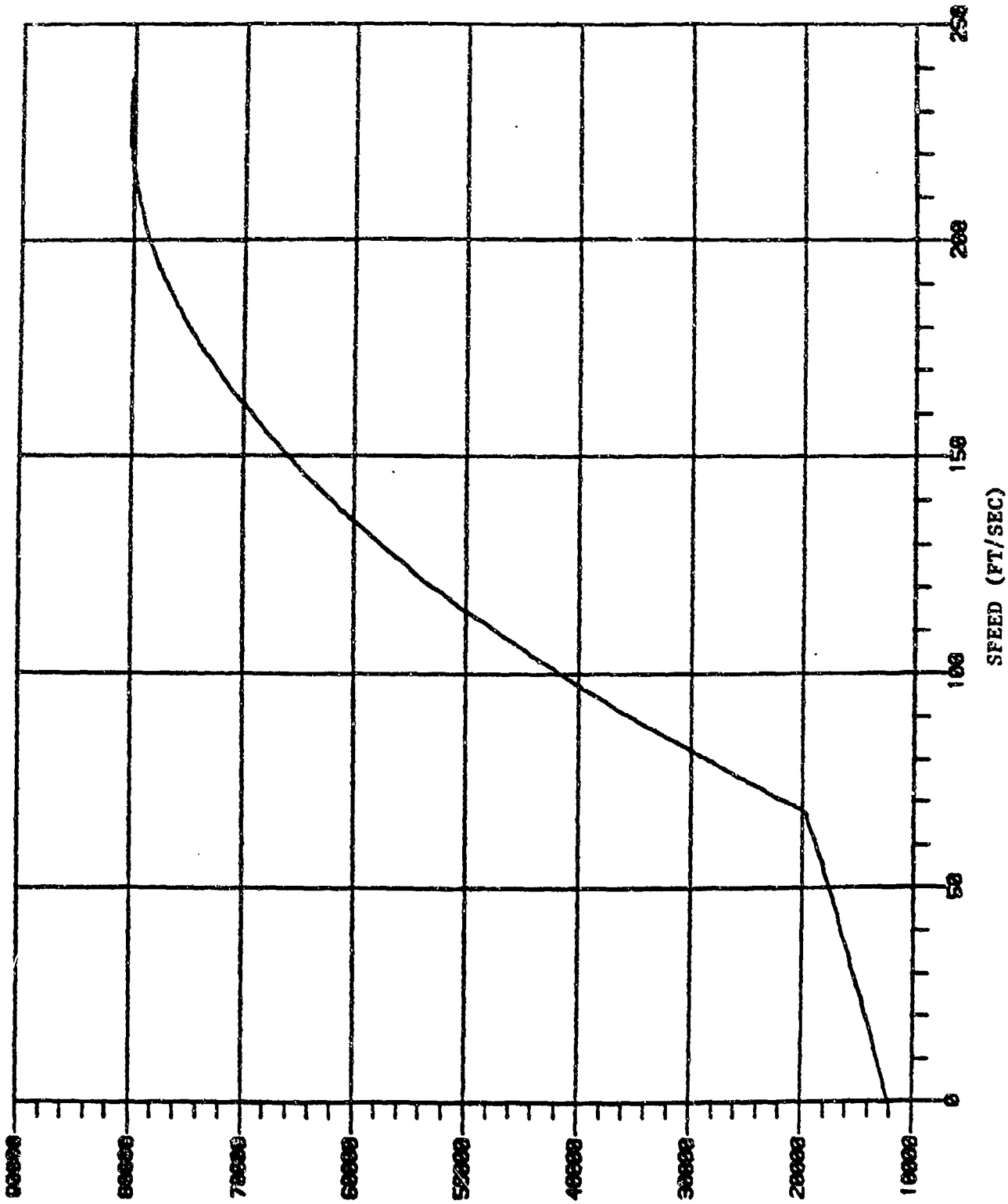

Figure 7a Reverse Thrust vs Speed

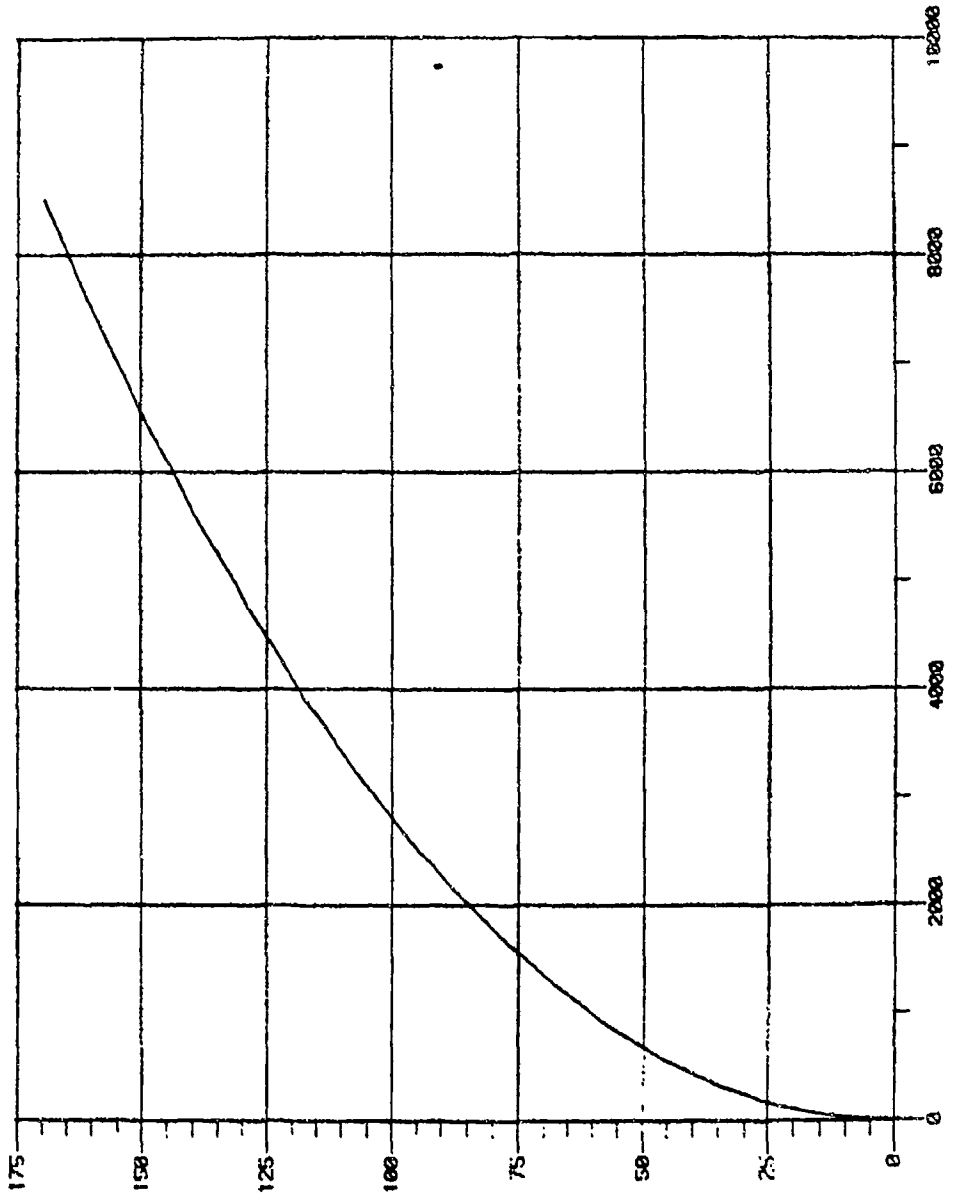

Figure 7b Takeoff Velocity Time History

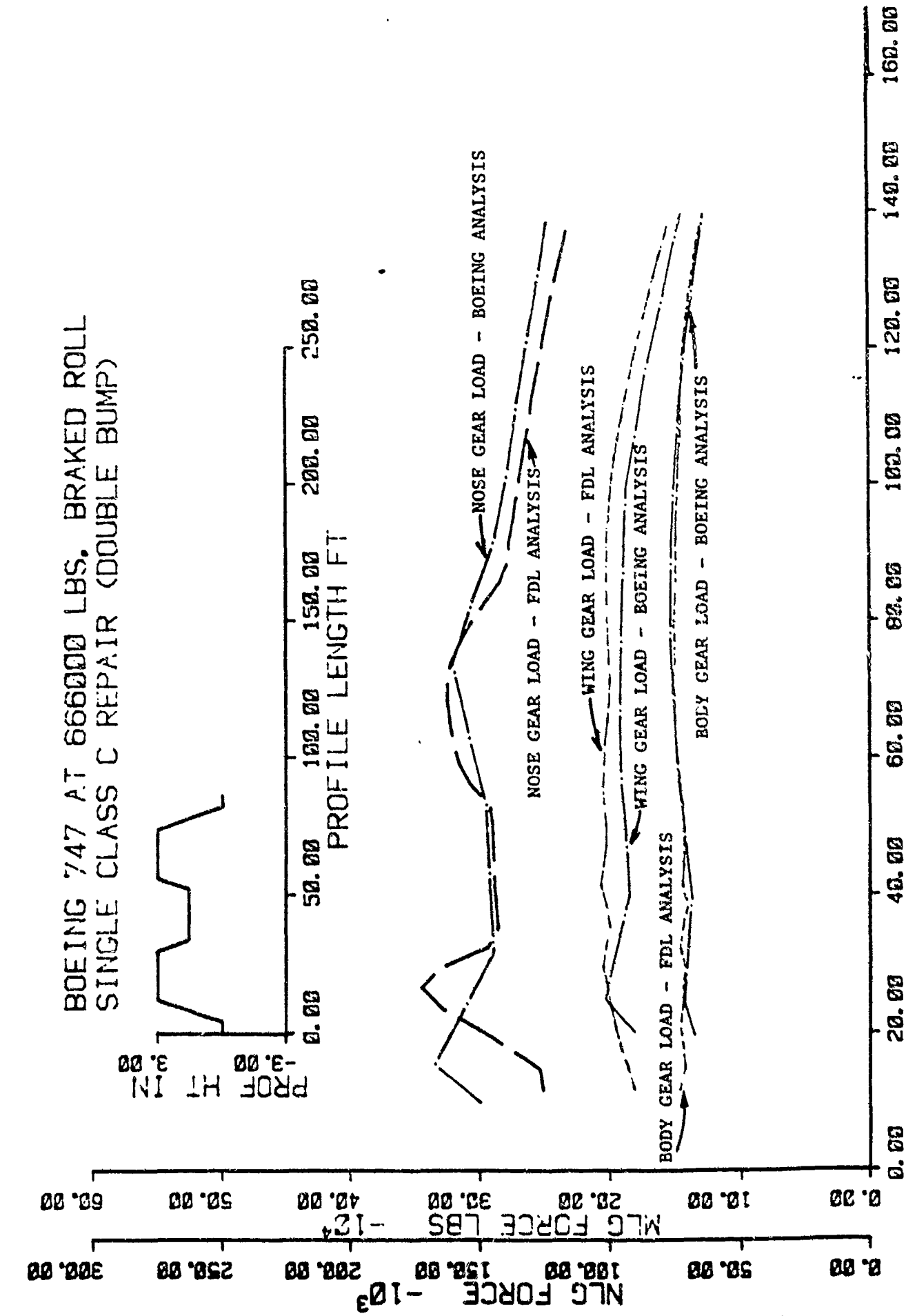

Figure 8 Velocity Plot-Comparison of Boeing and FDL Analysis

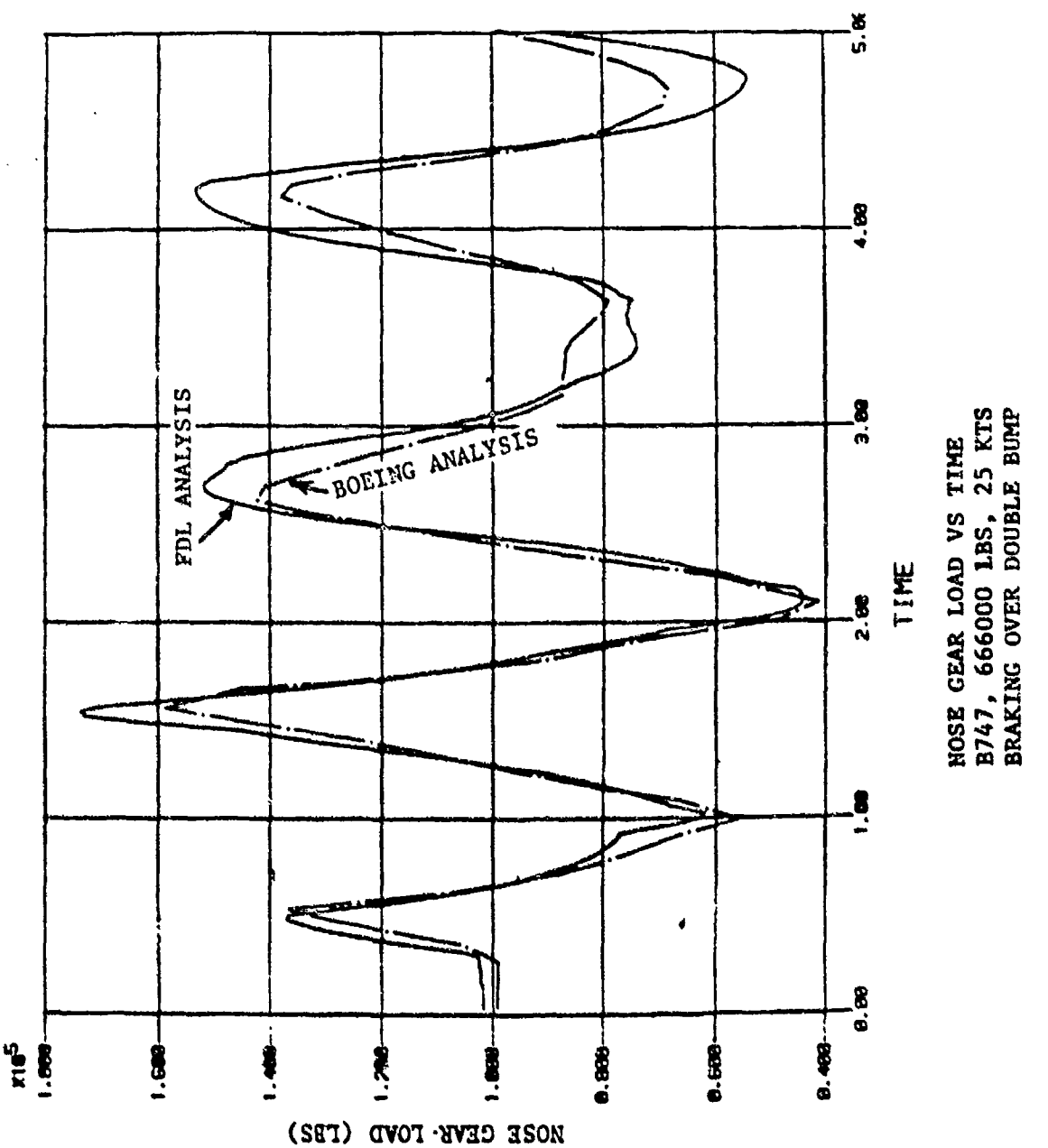

Figure 9 Nose Gear Load vs Time-Comparison of Boeing and FDL Analysis

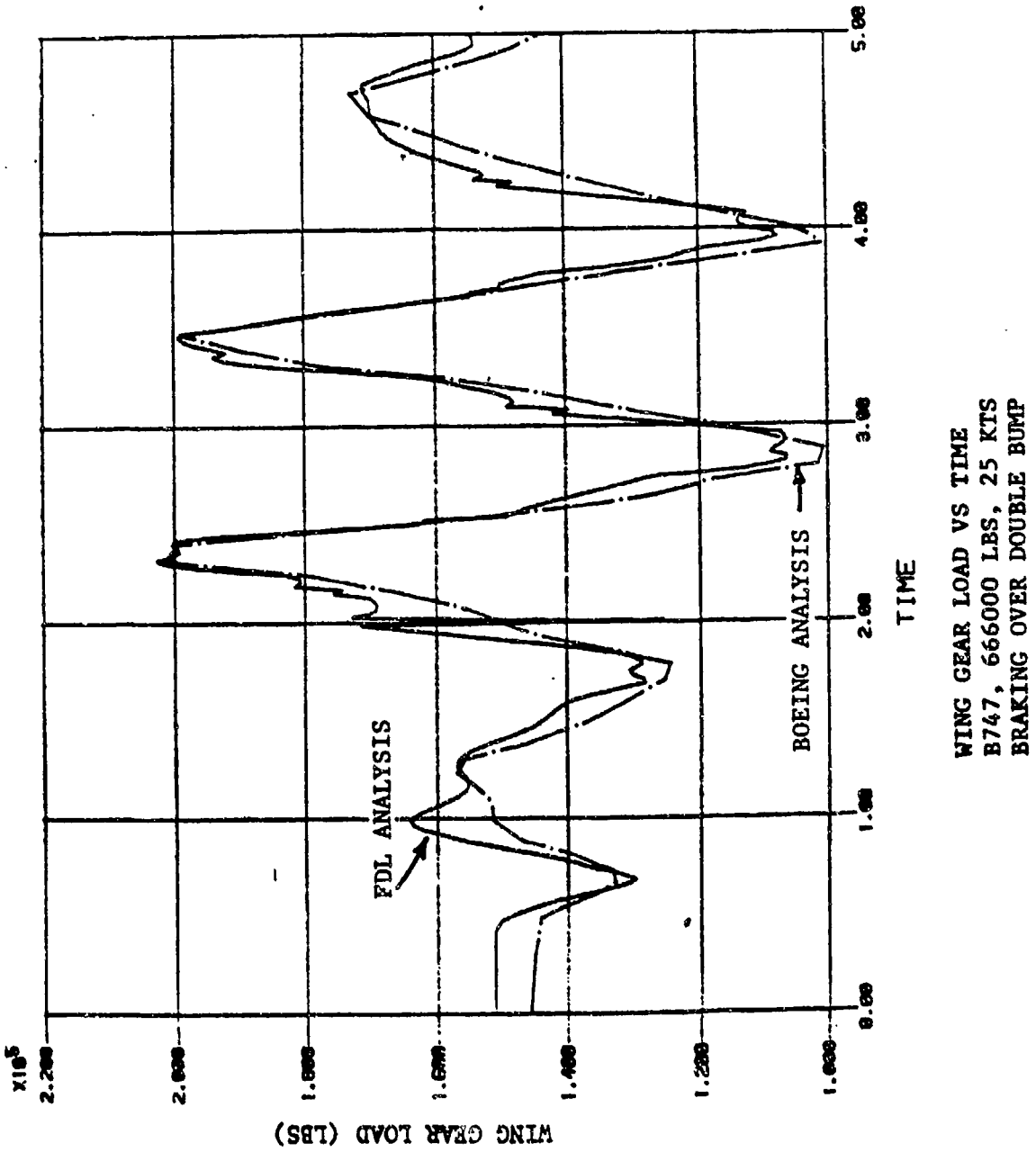

Figure 10 Wing Gear Load vs Time-Comparison of Boeing and FDL Analysis

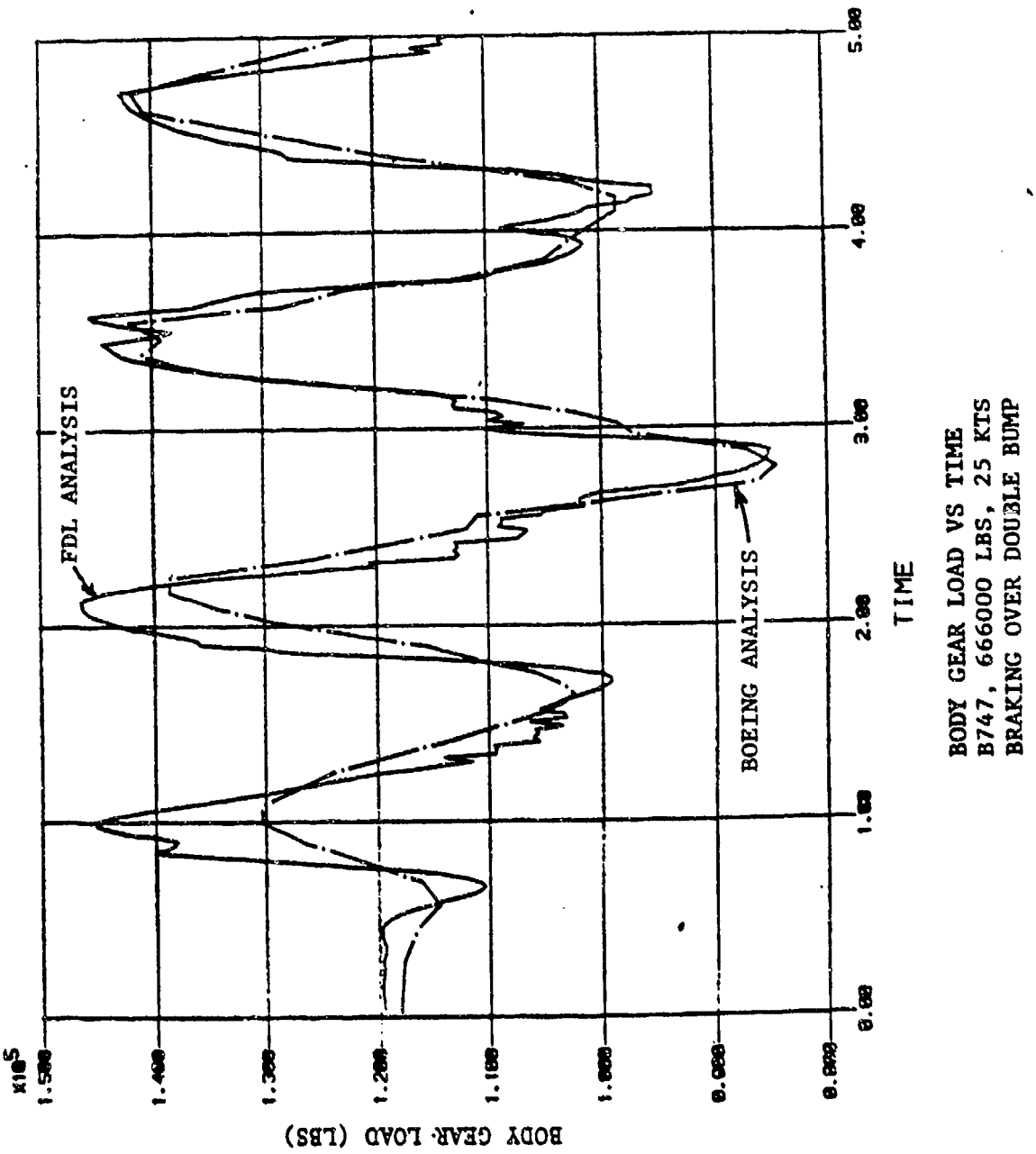

Figure 11 Body Gear Load vs Time Comparison of Boeing and FDL Analysis

VERTICAL LOADS:

UPHEAVAL: AT 240 FPS (142 KTS). UPHEAVAL IN 10 FEET WILL PRODUCE A 2 FPS EQUIVALENT SINK SPEED

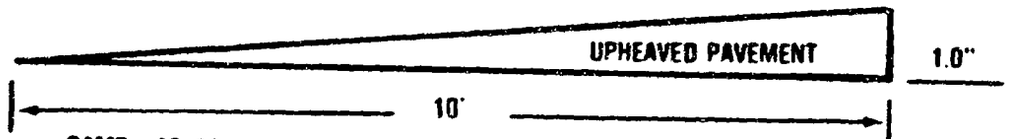

RAMP: AT 240 FPS, AN AM-2 RAMP WILL PRODUCE AN 8 FPS EQUIVALENT SINK SPEED

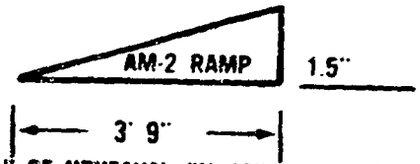

AN AM-2 RAMP ON 1" OF UPHEAVAL (IN 10') WILL PRODUCE AN EQUIVALENT 10 FPS SINK SPEED WHICH IS DESIGN LIMIT FOR MOST AIRCRAFT.

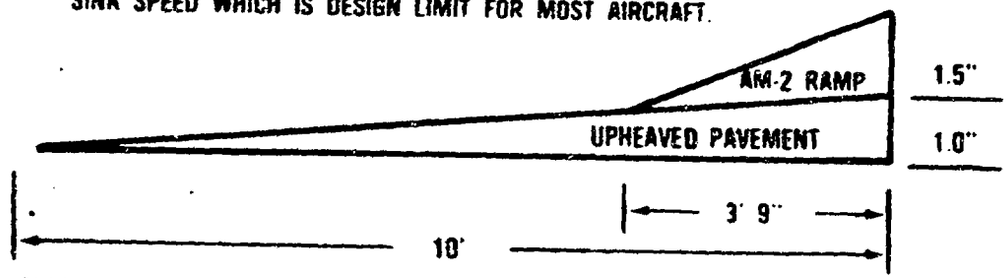

THEREFORE A TOUCHDOWN SINK SPEED OR A DYNAMIC LOAD COUPLED WITH THE ABOVE COULD PRODUCE EXCESSIVE VERTICAL LOADS.

DRAG LOADS: SIMILARLY DRAG LOADS WILL BE INCREASED IN PORPORTION TO THE ANGLE OF THE RAMP OR UPHEAVAL PAVEMENT.

Figure 12 Effects of Upheavel on Landing Sink Rate

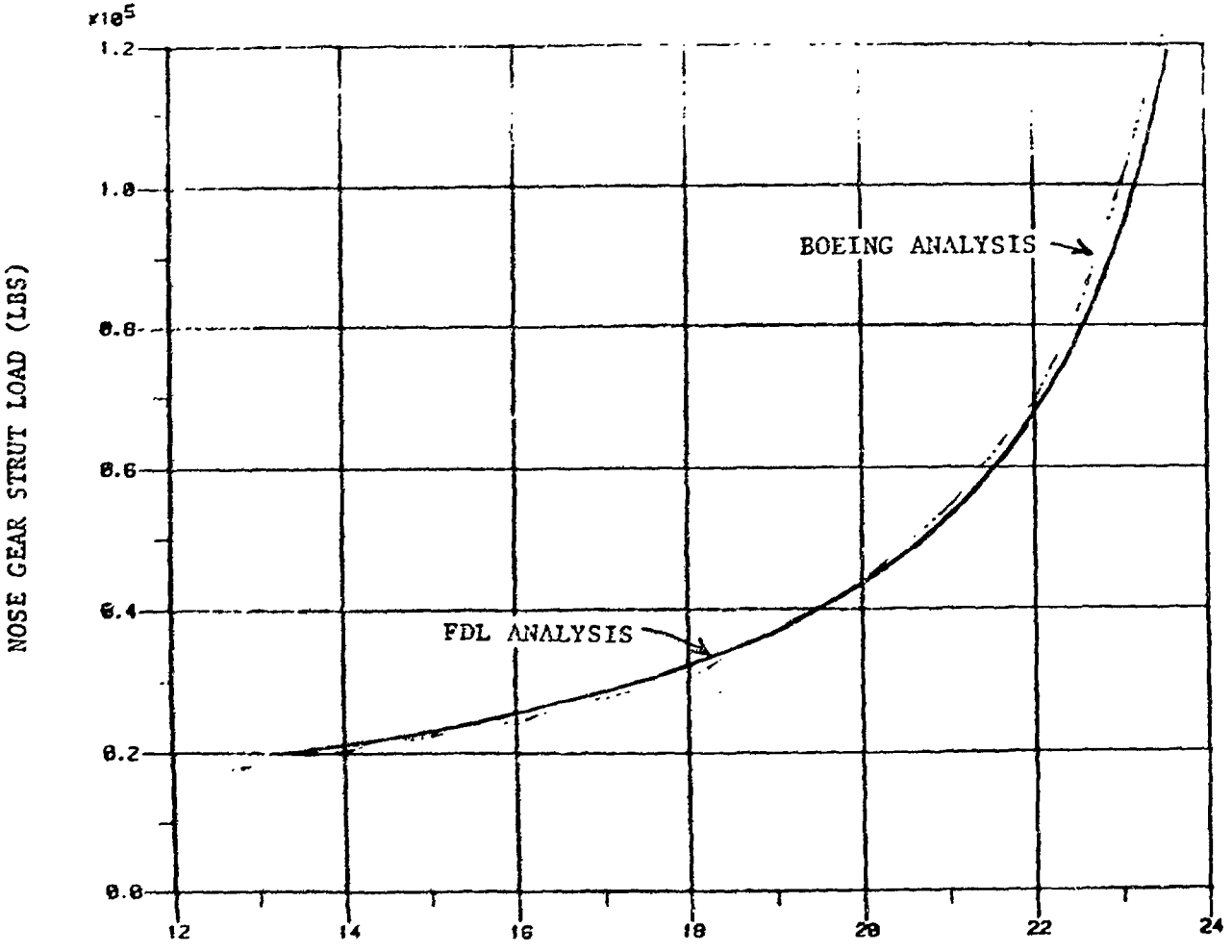

B747 NOSE GEAR LOAD STROKE CURVE

Figure 13 Nose Gear Load Stroke Curve

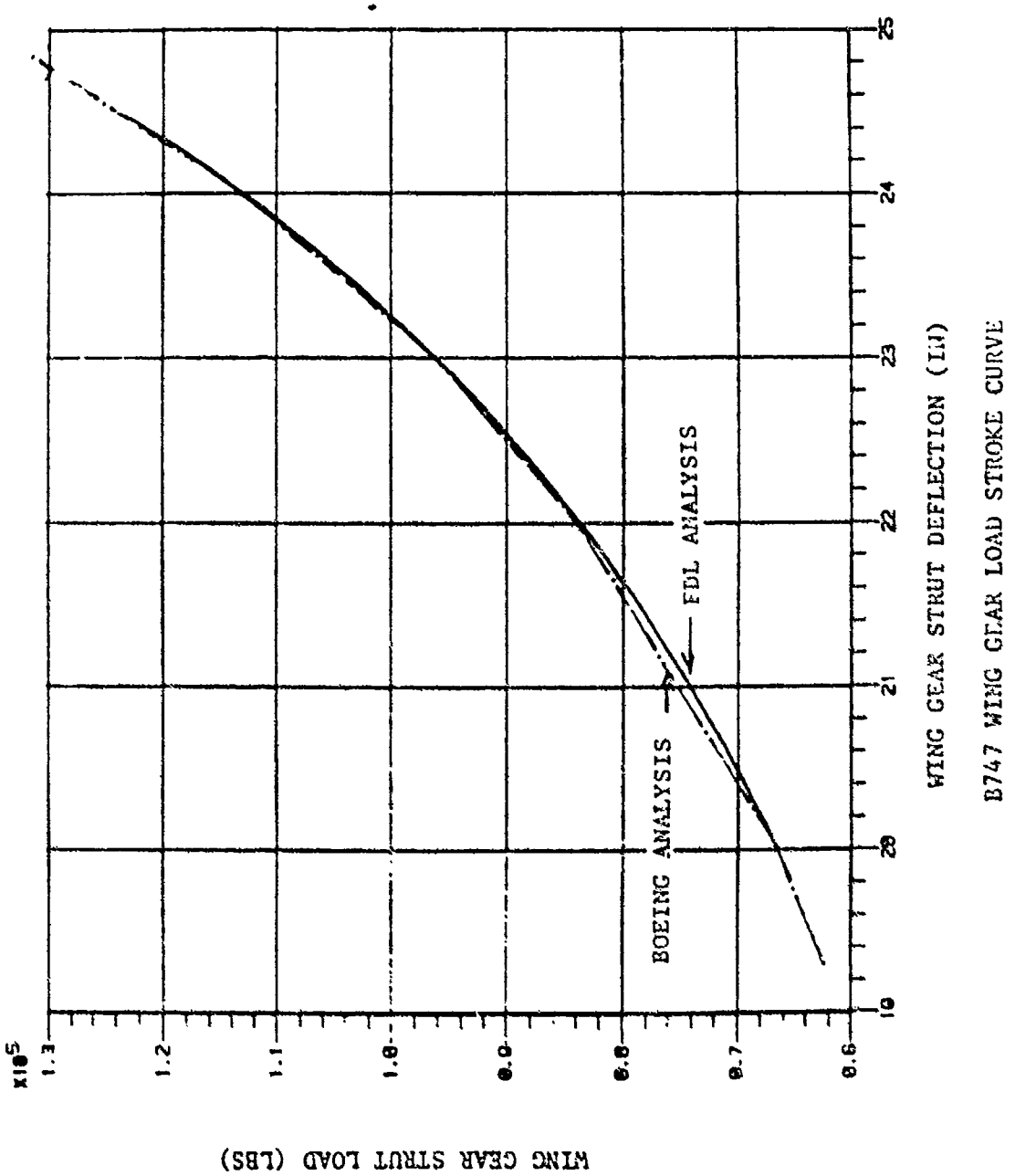

Figure 14 Wing Gear Load Stroke Curve

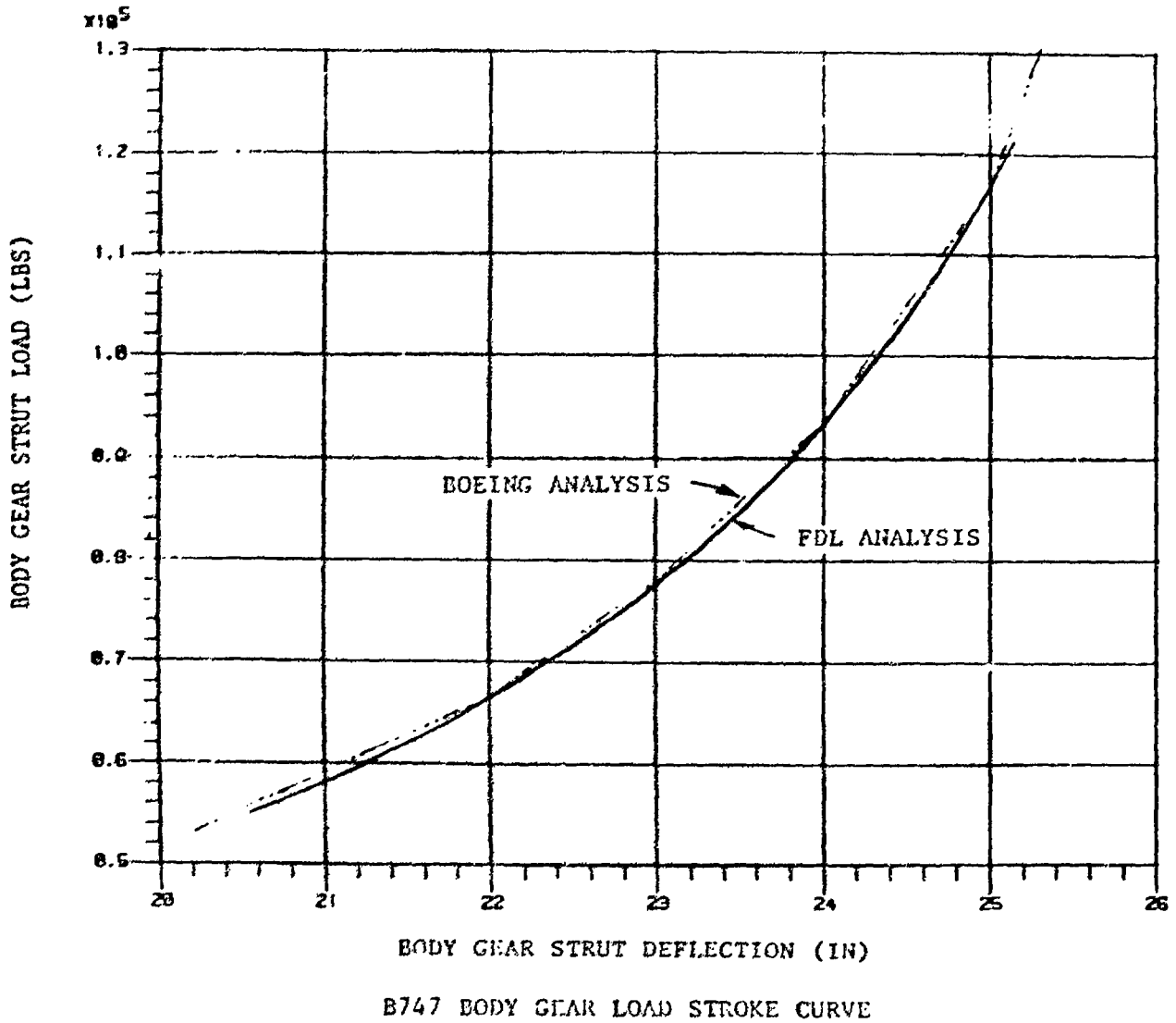

Figure 15 Body Gear Load Stroke Curve

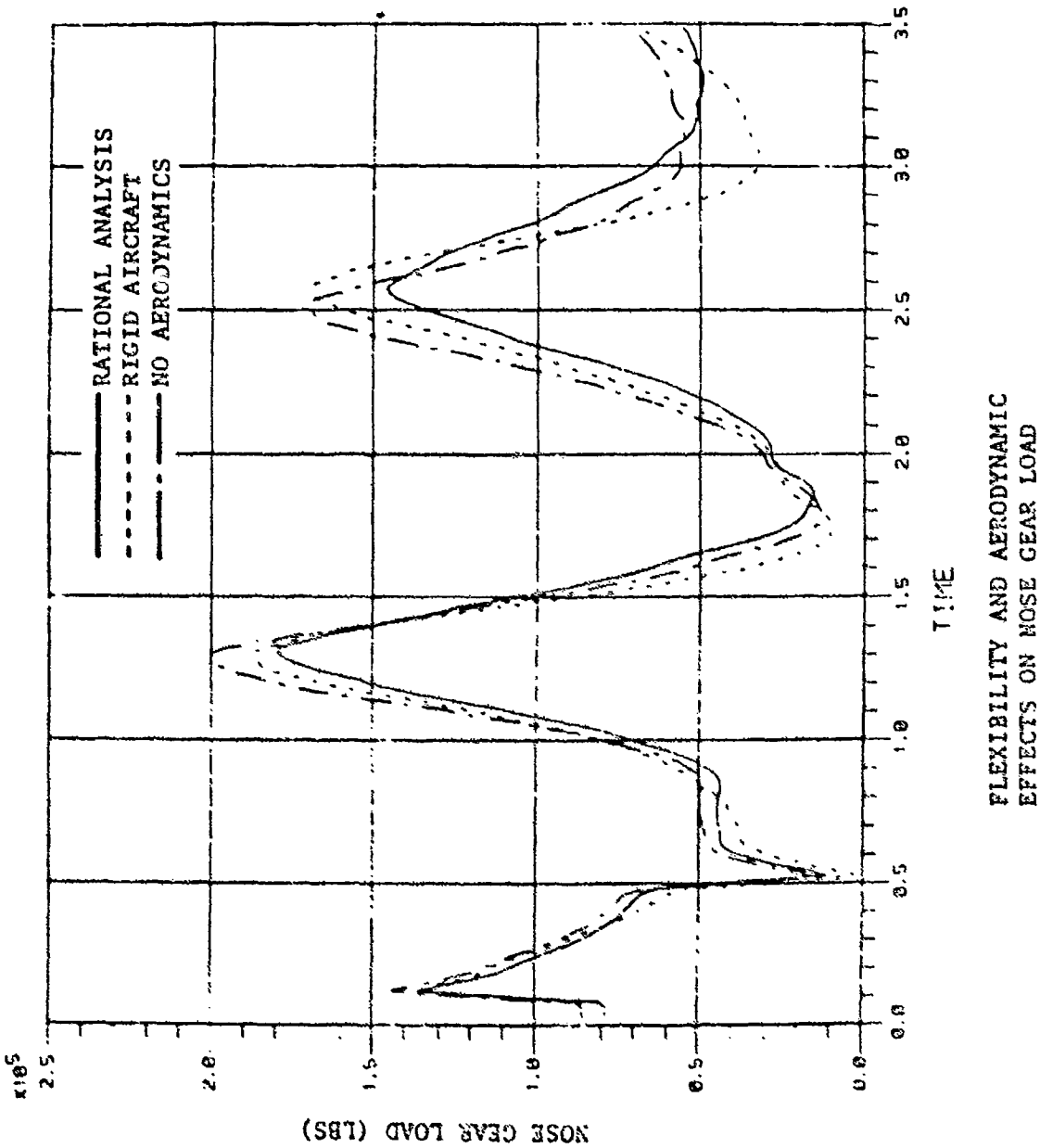

Figure 16 Effect of Flexibility and Aerodynamics on Nose Gear Load

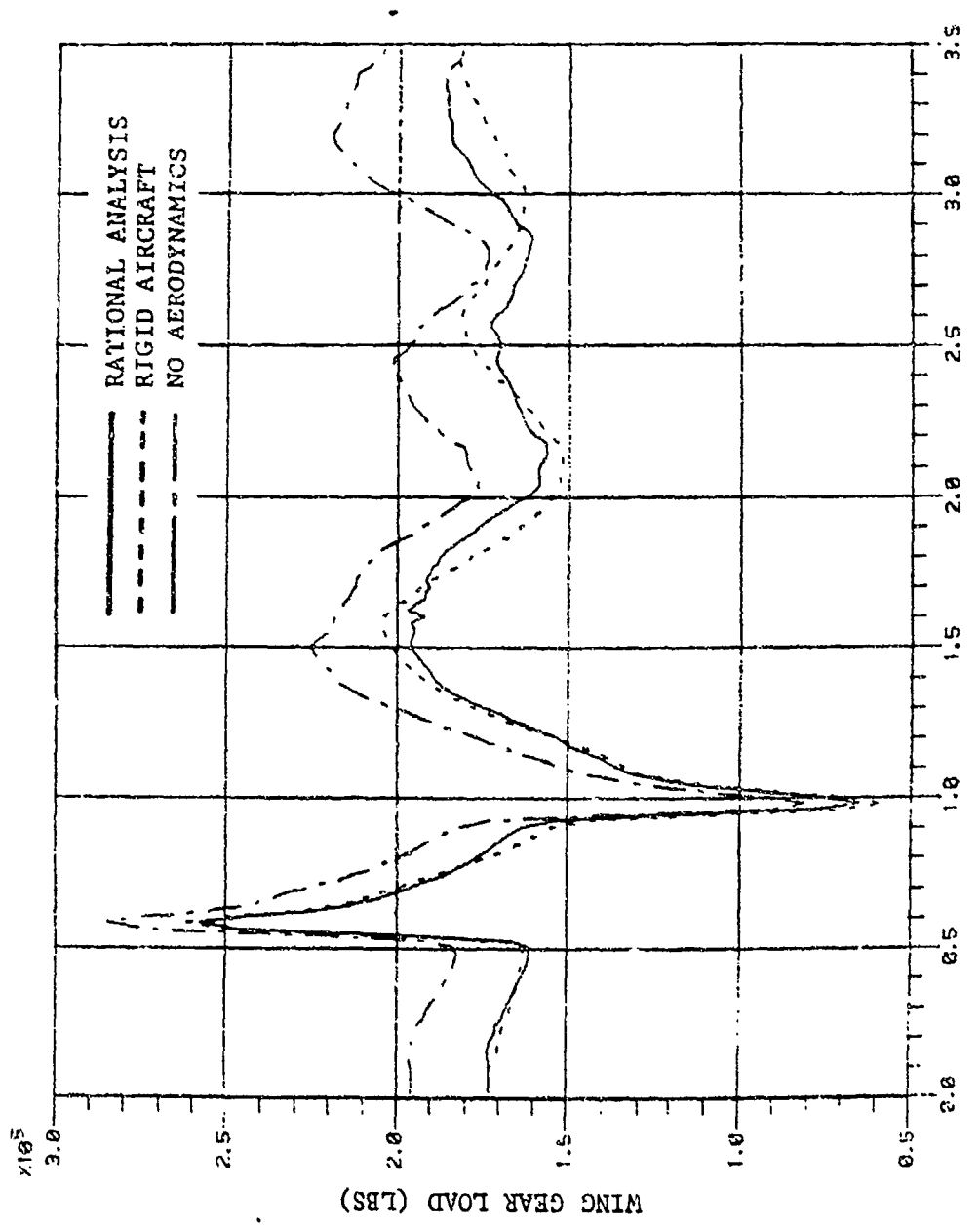

Figure 17 Effect of Flexibility and Aerodynamics on Wing Gear Load

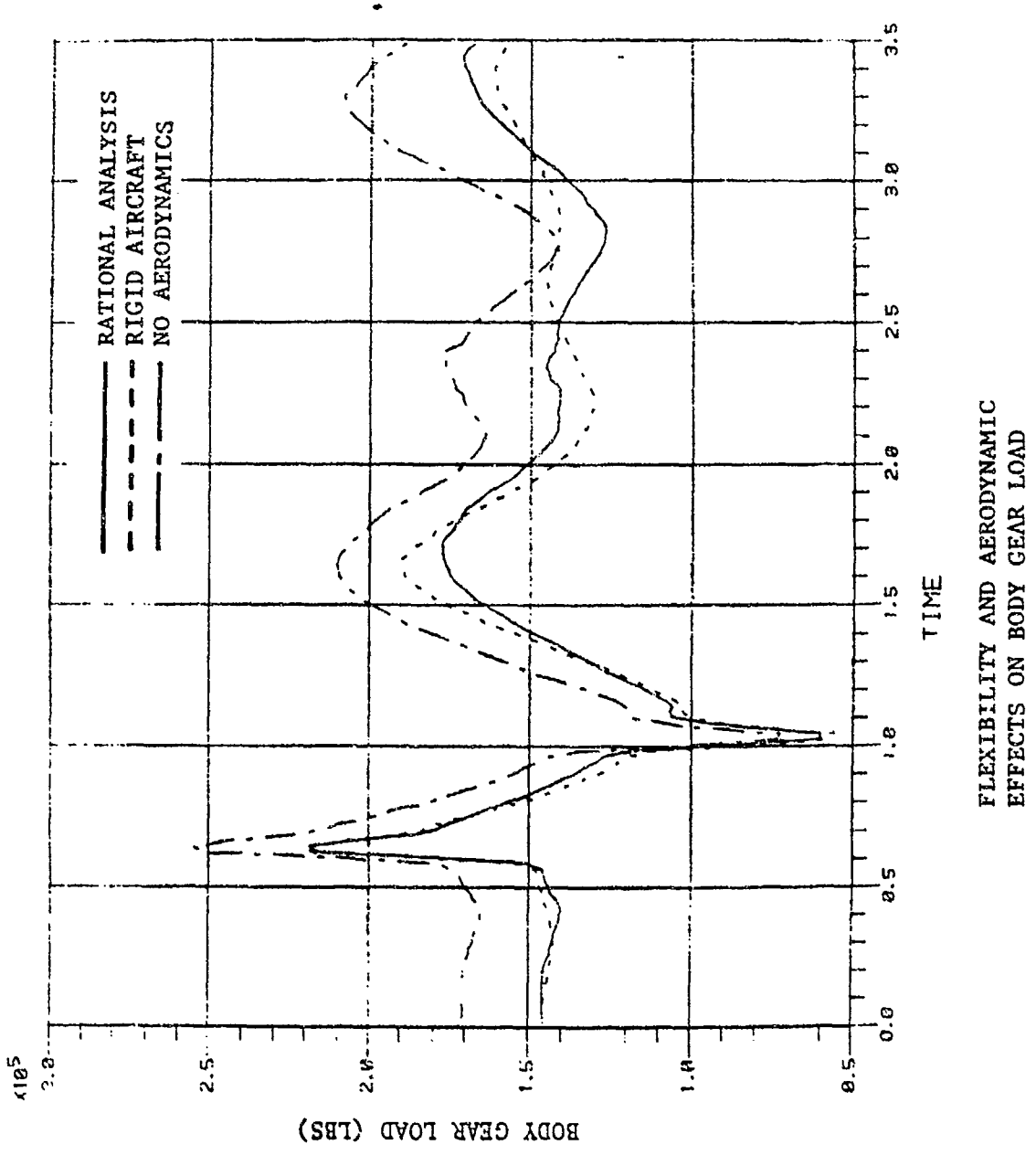

Figure 18 Effect of Flexibility and Aerodynamics on Body Gear Load

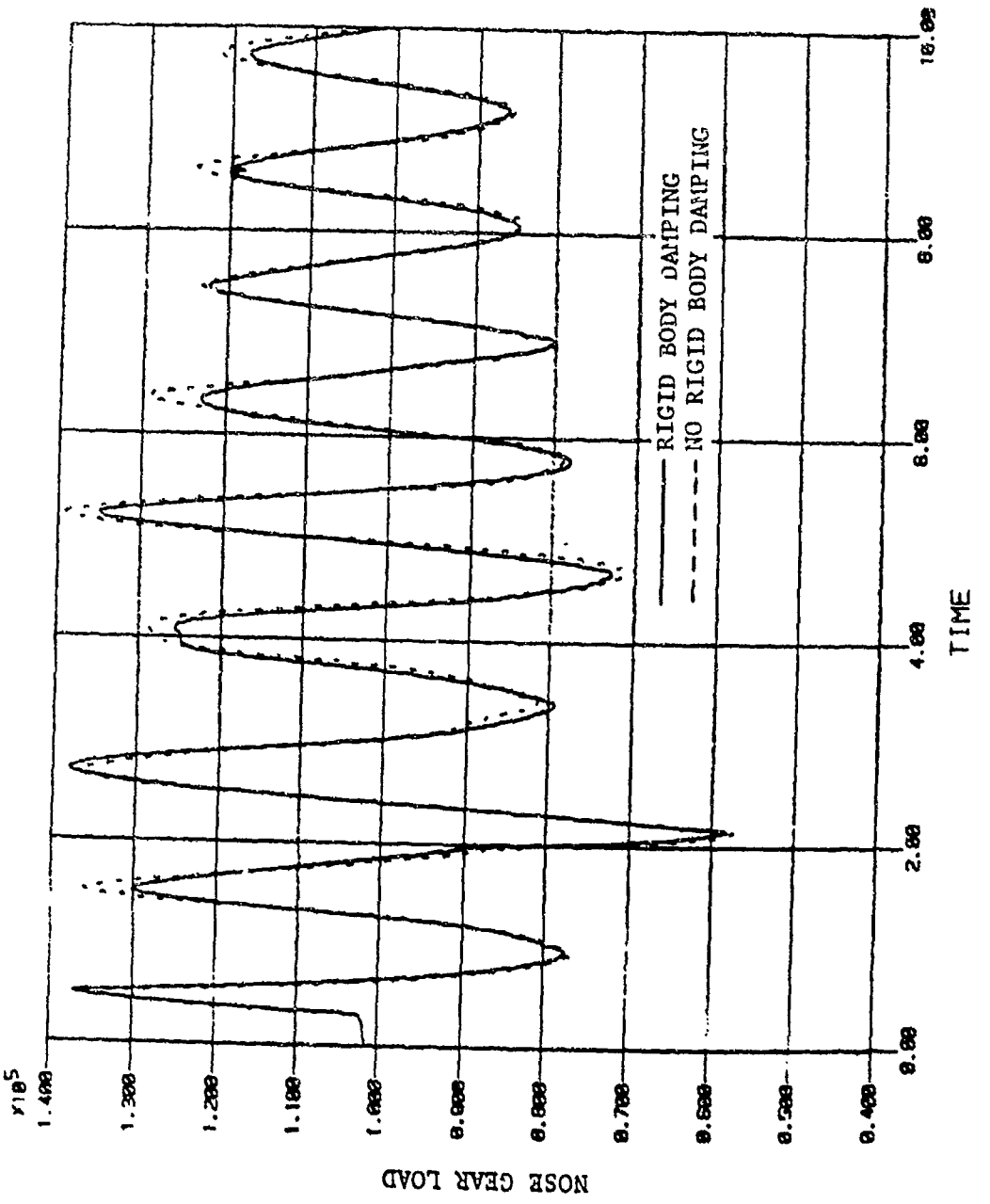

Figure 19 Effect of Rigid Body Damping on Nose Gear Load

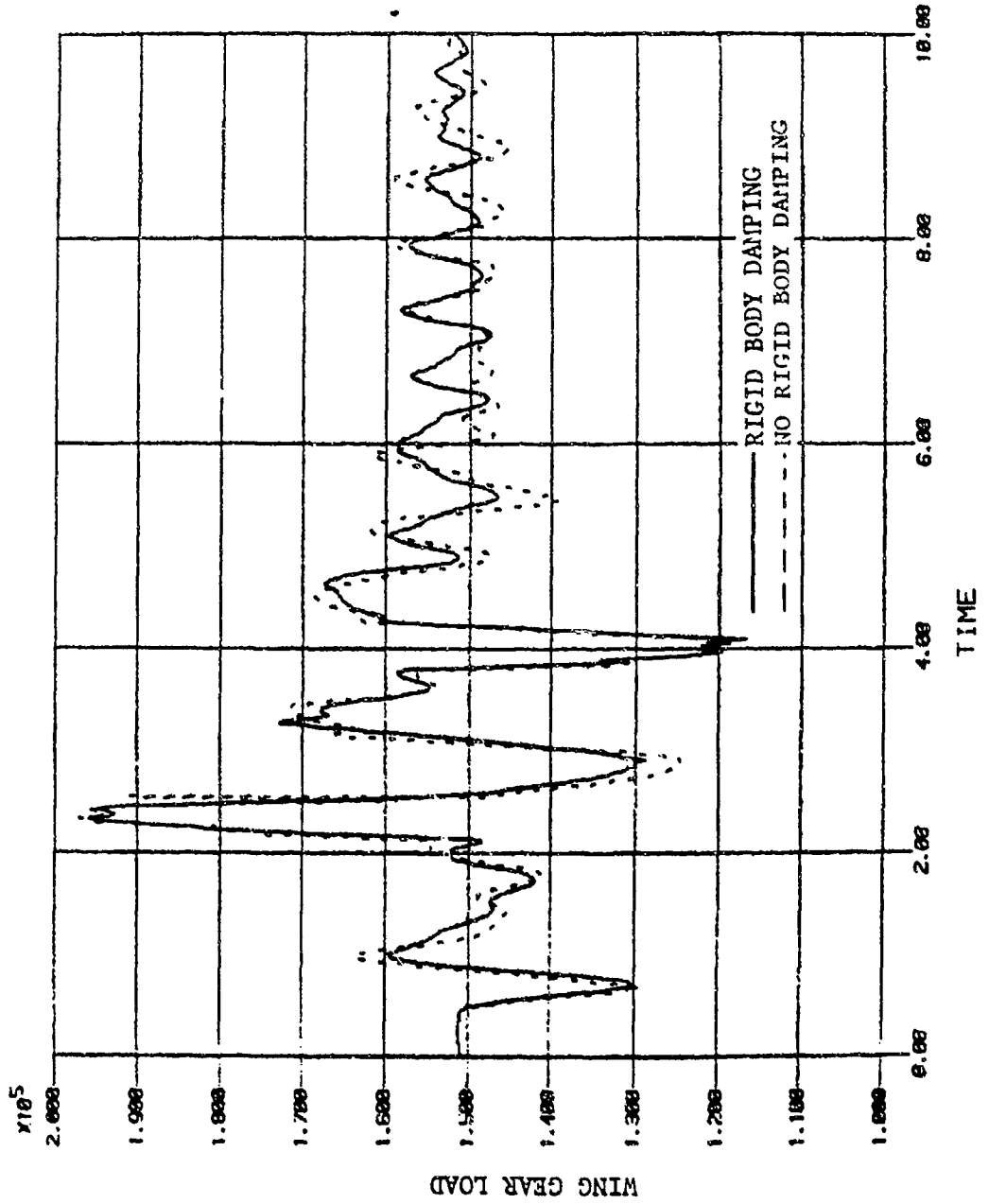

Figure 20 Effect of Rigid Body Damping on Wing Gear Load

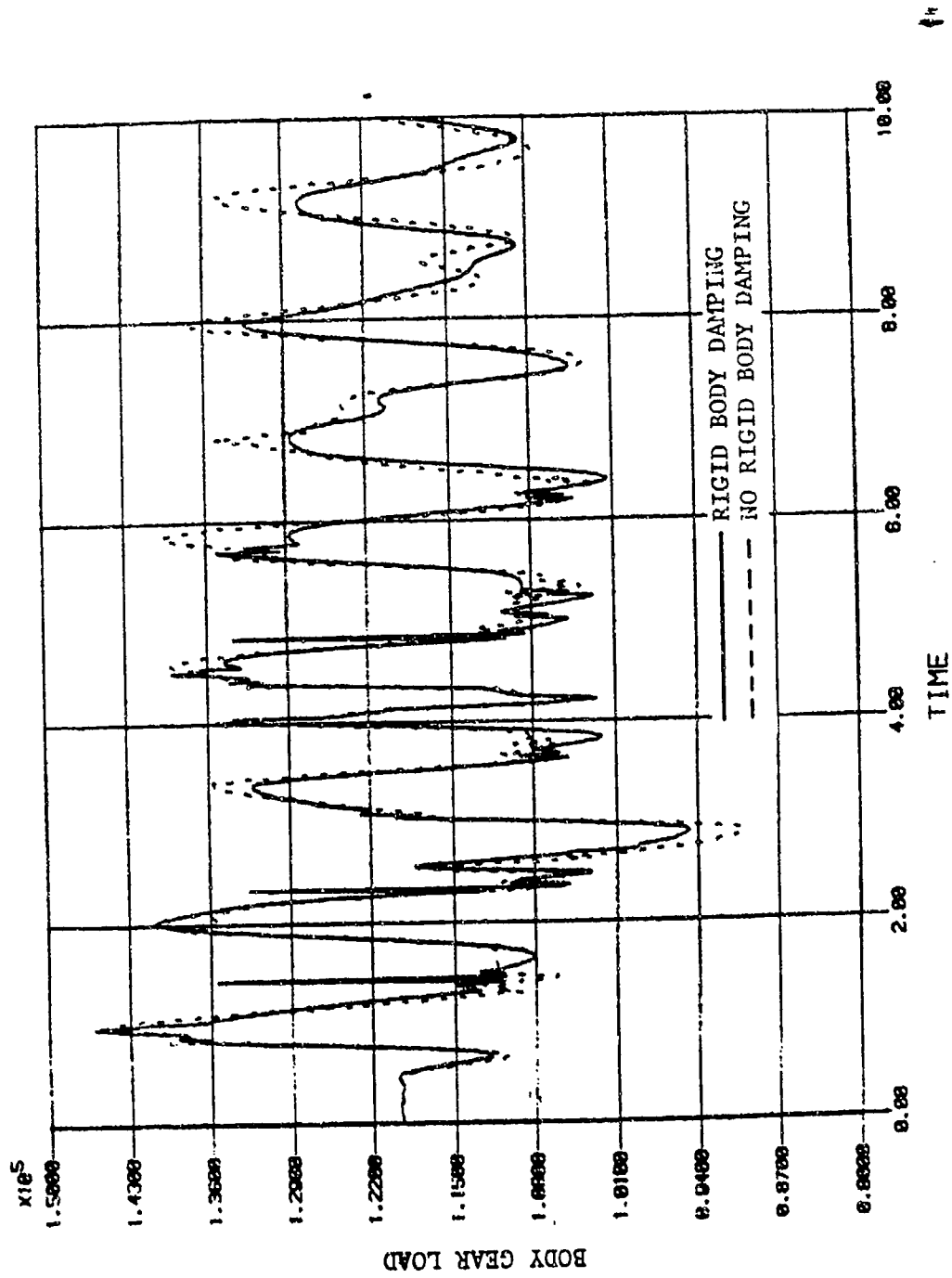

Figure 21 Effect of Rigid Body Damping on Body Gear Load

Table 3

CRITICAL TAXI CONDITIONS
FOR SINGLE BUMP ENCOUNTER

CLASS REPAIR	MAX NOSE LOAD	MAX NOSE LOAD	CRITICL VELOCITY	TIME OF CRITICAL NG LOAD	NG PRE-CHARG	GROSS WEIGHT	BRAKES MU=0.4	REVERSE THRUST 80000 LBS MAX
	LBS	%DLL	FPS	SEC	PSI	LBS	YES/NO	YES/NO
A	124200	63	113	2.97	150	836000	NO	NO
B	158800	81	114	1.02	150	836000	NO	NO
C	179700	91	41	4.42	150	836000	NO	NO
C	147900	75	117	2.99	150	836000	NO	NO
E	201100	102	39	4.62	150	836000	NO	NO
E	164400	83	105	1.54	150	836000	NO	NO
A	122500	62	47	3.90	150	666000	YES	NO
B	158500	81	146	1.48	150	666000	YES	NO
C	166100	84	42	4.29	150	666000	YES	NO
E	187200	95	41	4.68	150	666000	YES	NO
A	139900	71	49	3.69	150	666000	YES	YES
B	163300	83	121	1.33	150	666000	YES	YES
C	174900	89	43	1.50	150	666000	YES	YES
E	196200	99.7	47	3.89	150	666000	YES	YES

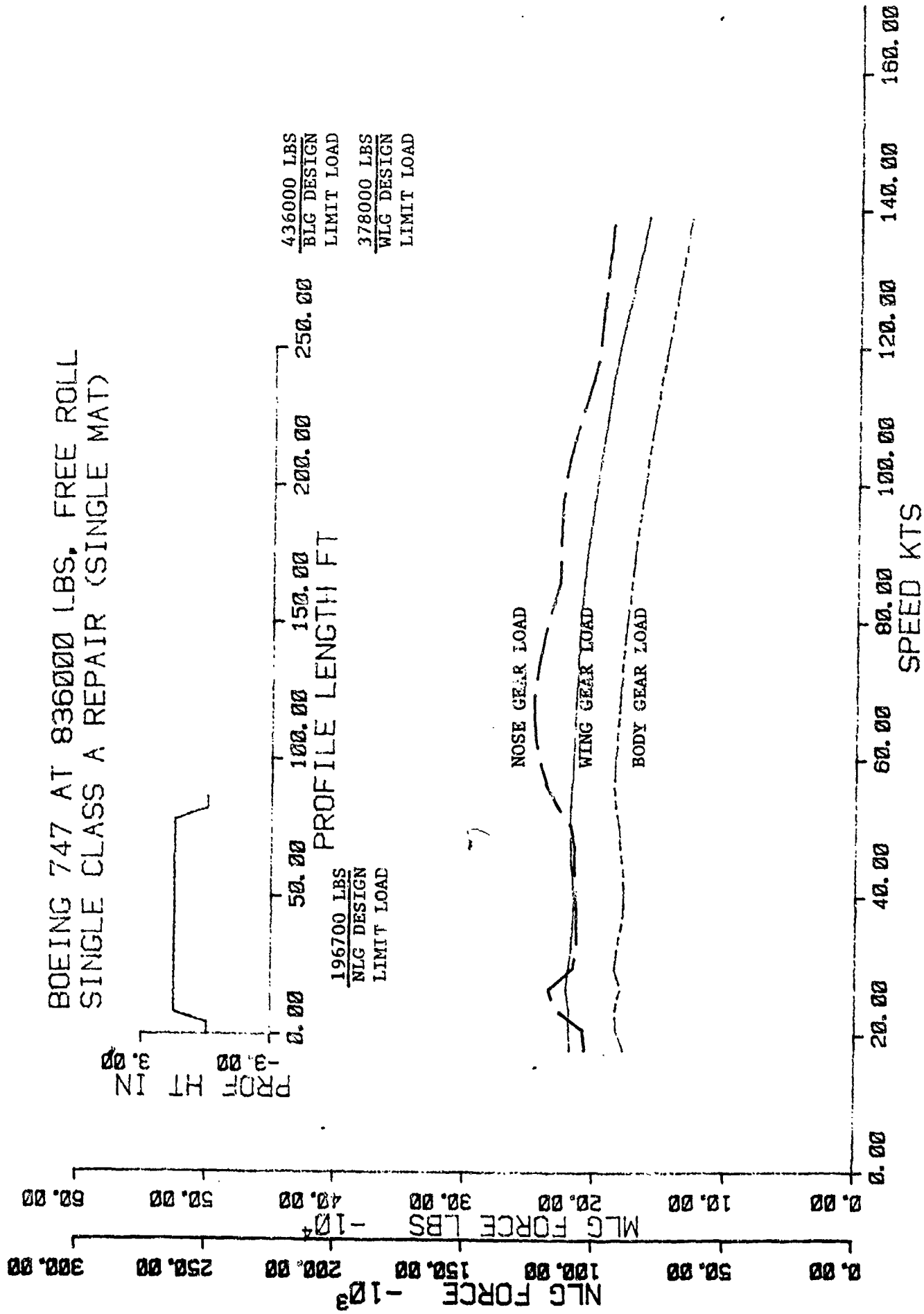

Figure 22 Velocity Analysis - Free Roll Over Class A Repair at 836000 lbs GW

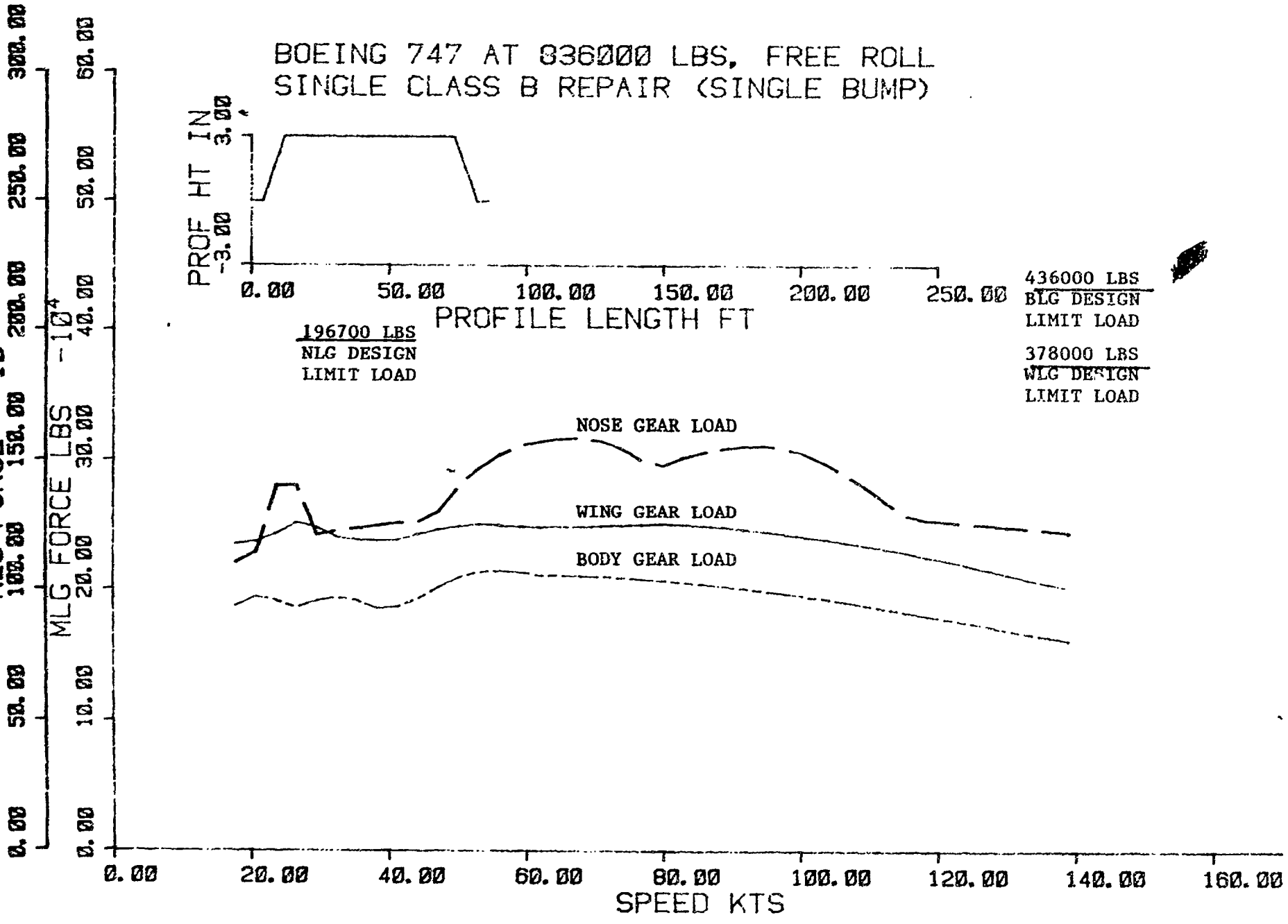

Figure 23 Velocity Analysis-Free Roll Over Class B Repair at 836000 lbs GW

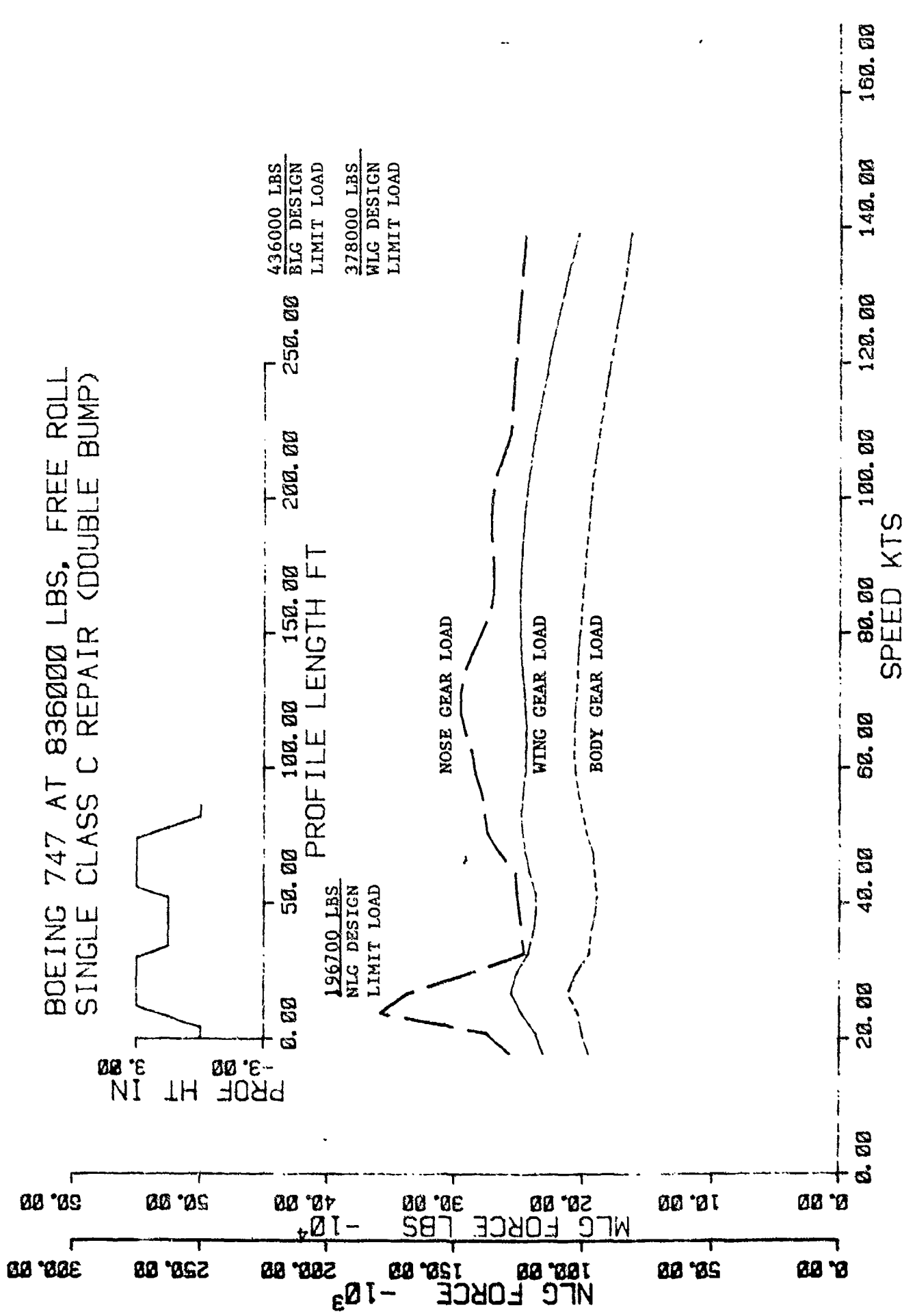

Figure 24 Velocity Analysis-Free Roll Over Class C Repair at 836000 lbs GW

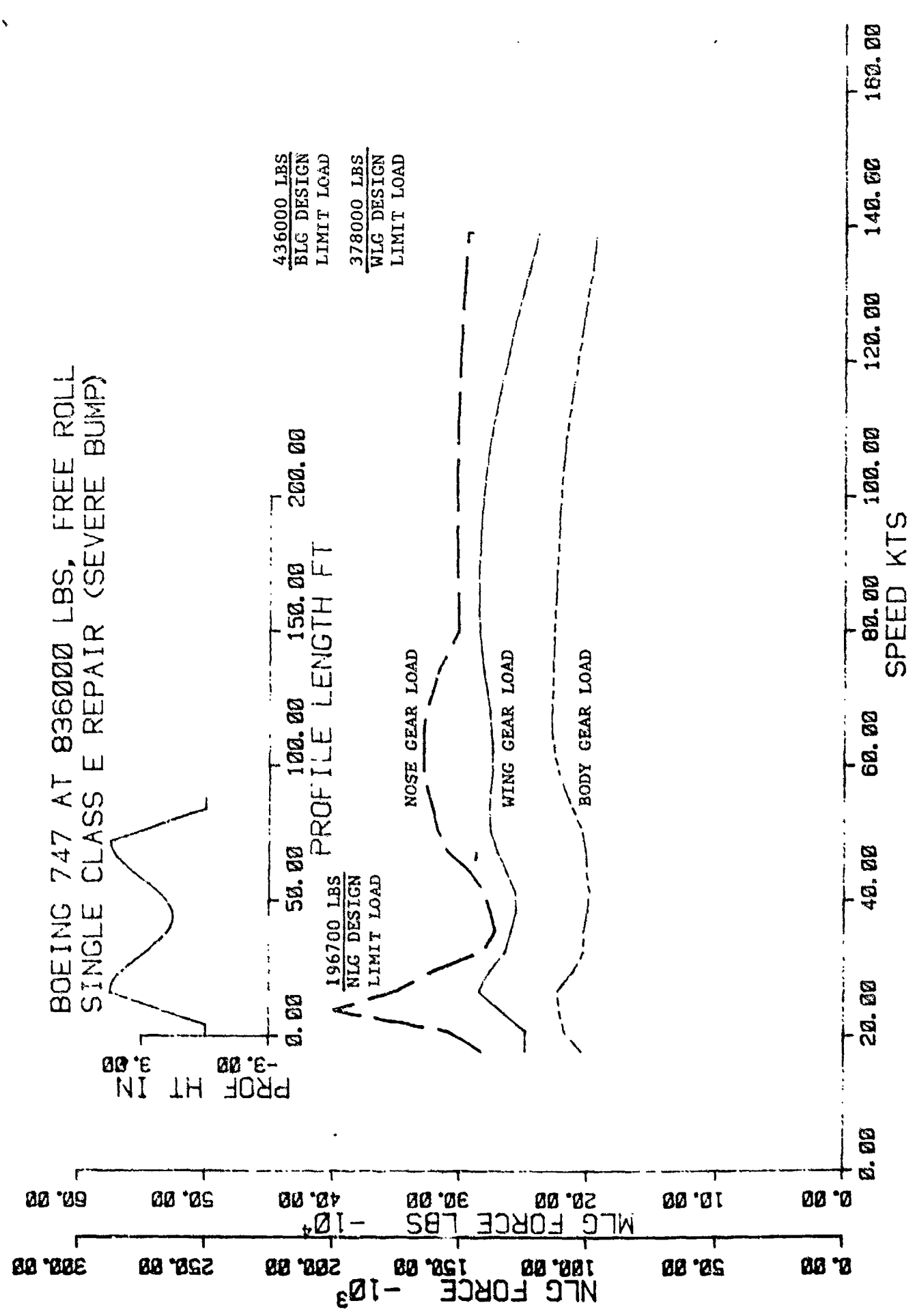

Figure 25 Velocity Analysis-Free Roll Over Class E Repair at 836000 lbs GW

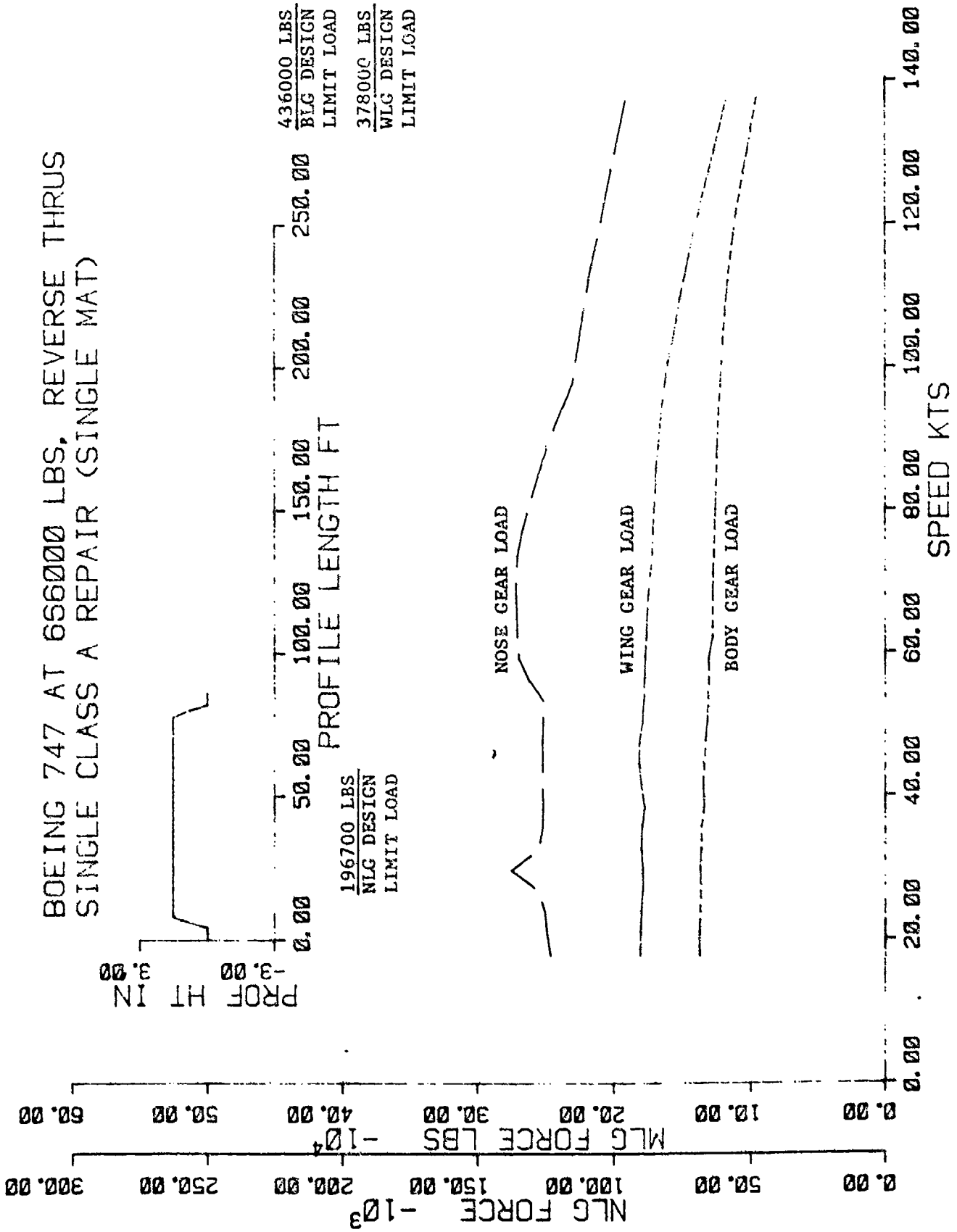

Figure 26 Velocity Analysis-Reverse Thrust Braked Roll Over Class A Repair at 666000 lbs GW

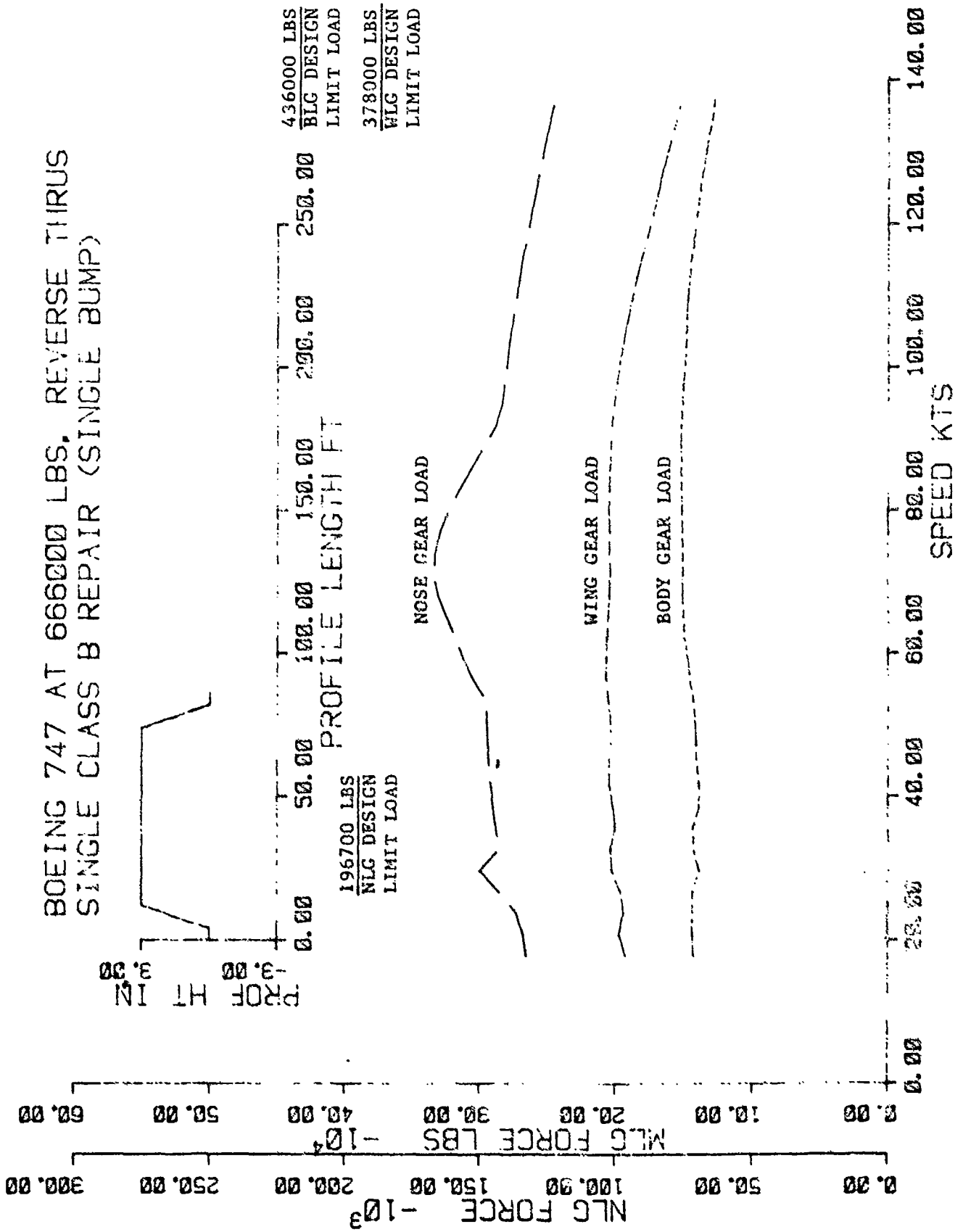

Figure 27 Velocity Analysis-Reverse Thrust Braked Roll Over Class B Repair at 666000 lbs GW

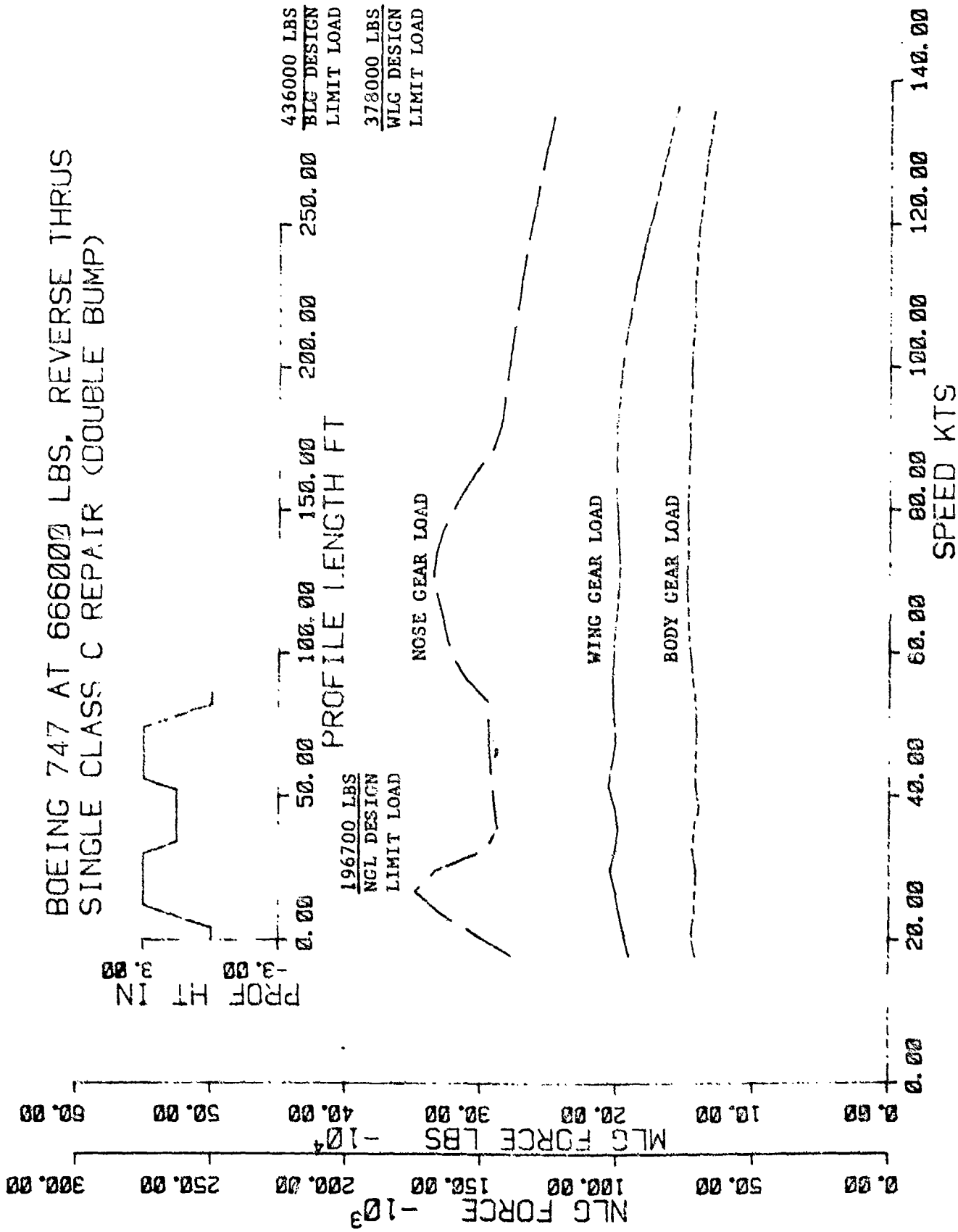

Figure 28 Velocity Analysis-Reverse Thrust Braked Roll Over Class C Repair at 666000 lbs GW

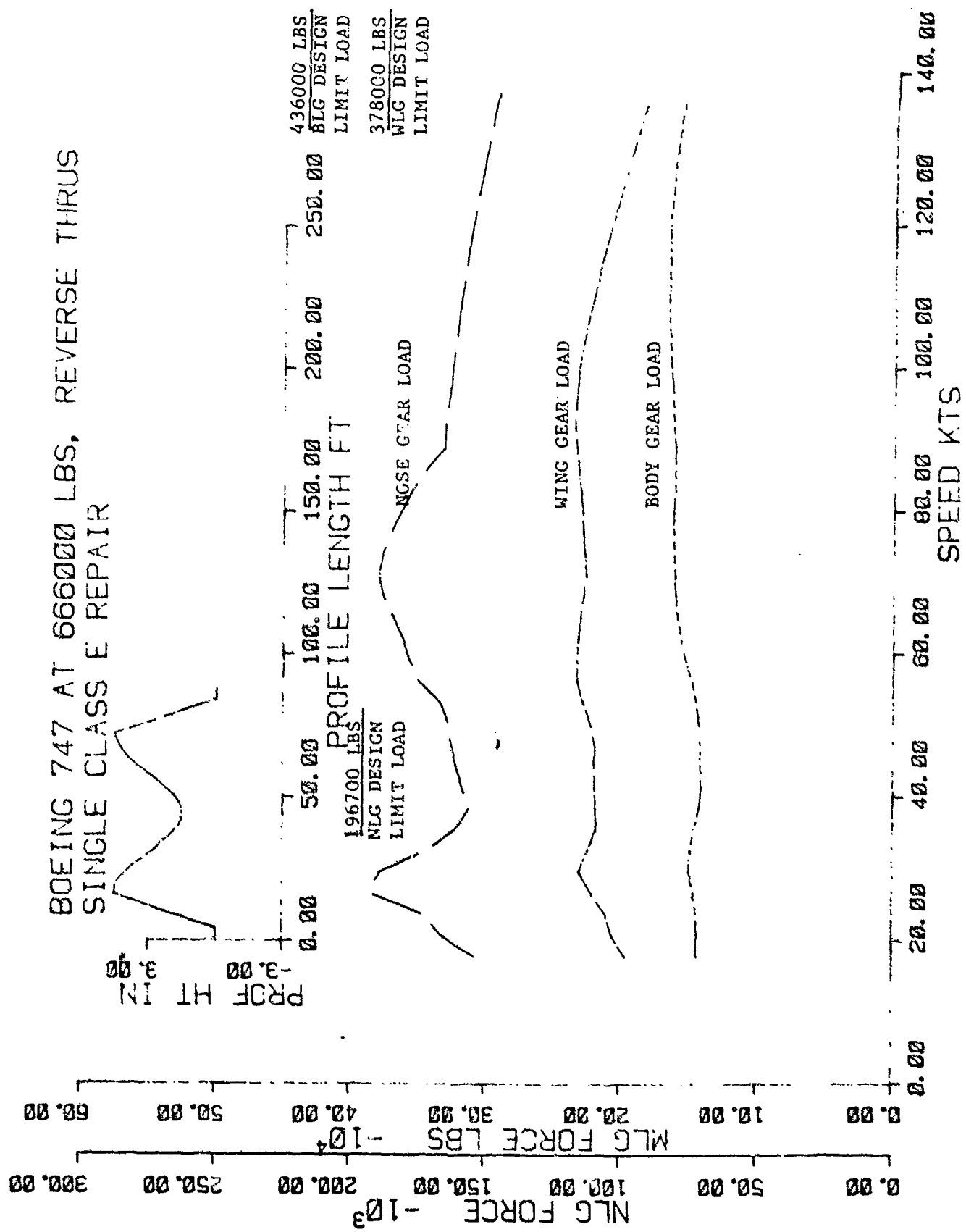

Figure 29 Velocity Analysis-Reverse Thrust Braked Roll Over Class E Repair at 666000 lbs GW

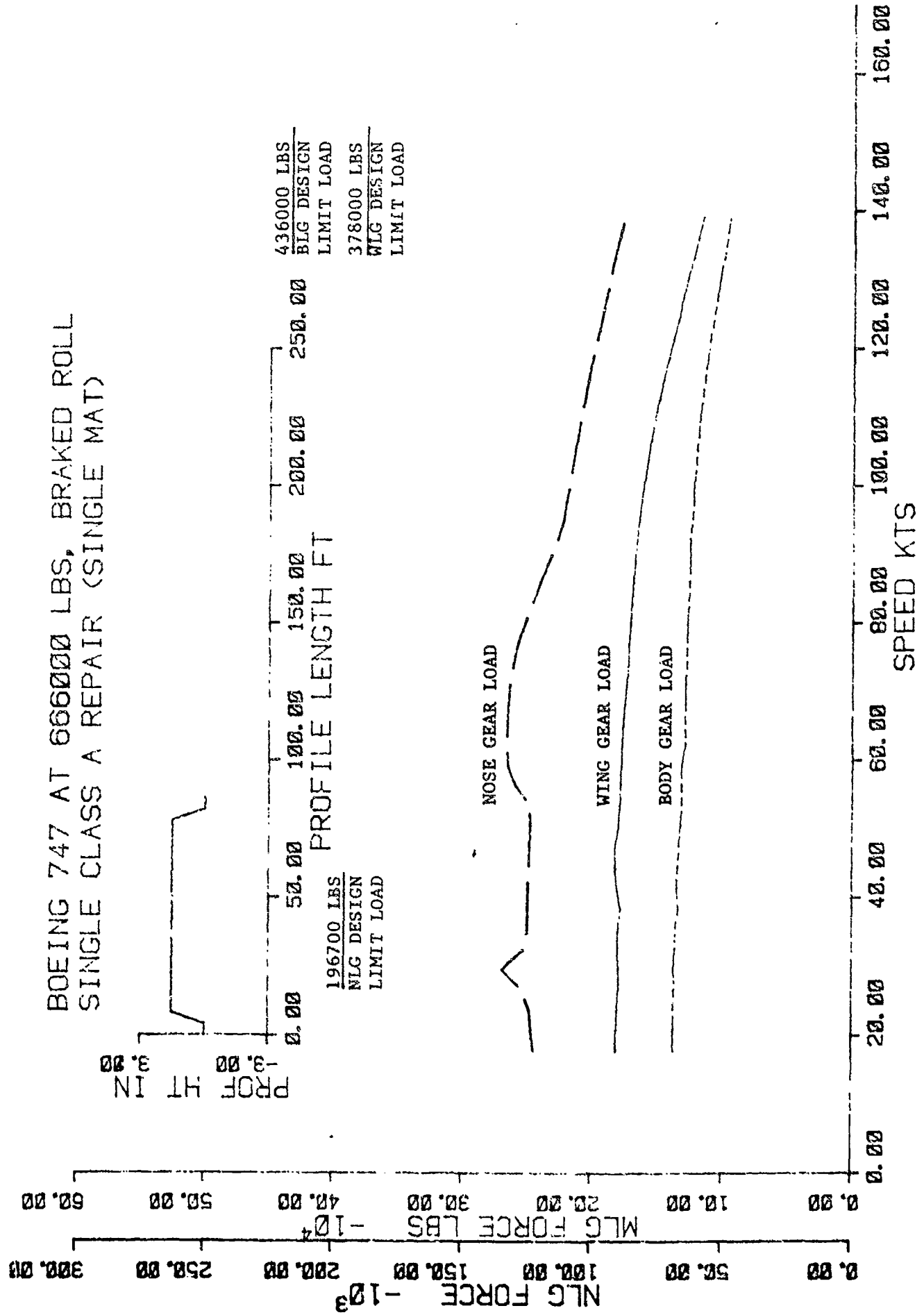

Figure 30 Velocity Analysis-Braked Roll Over Class A Repair at 666000 lbs GW

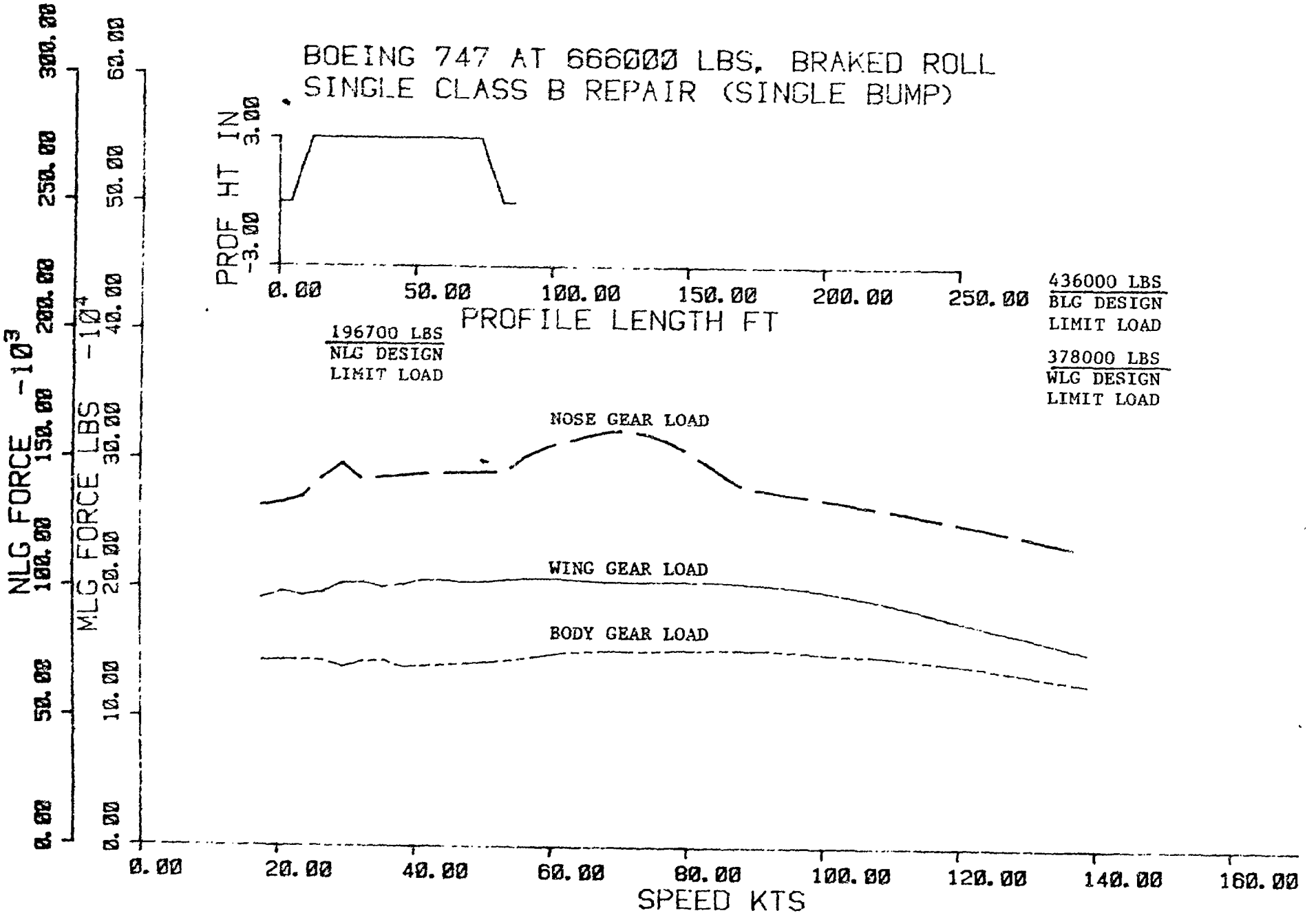

Figure 31 Velocity Analysis-Braked Roll Over Class B Repair at 666000 lbs GW

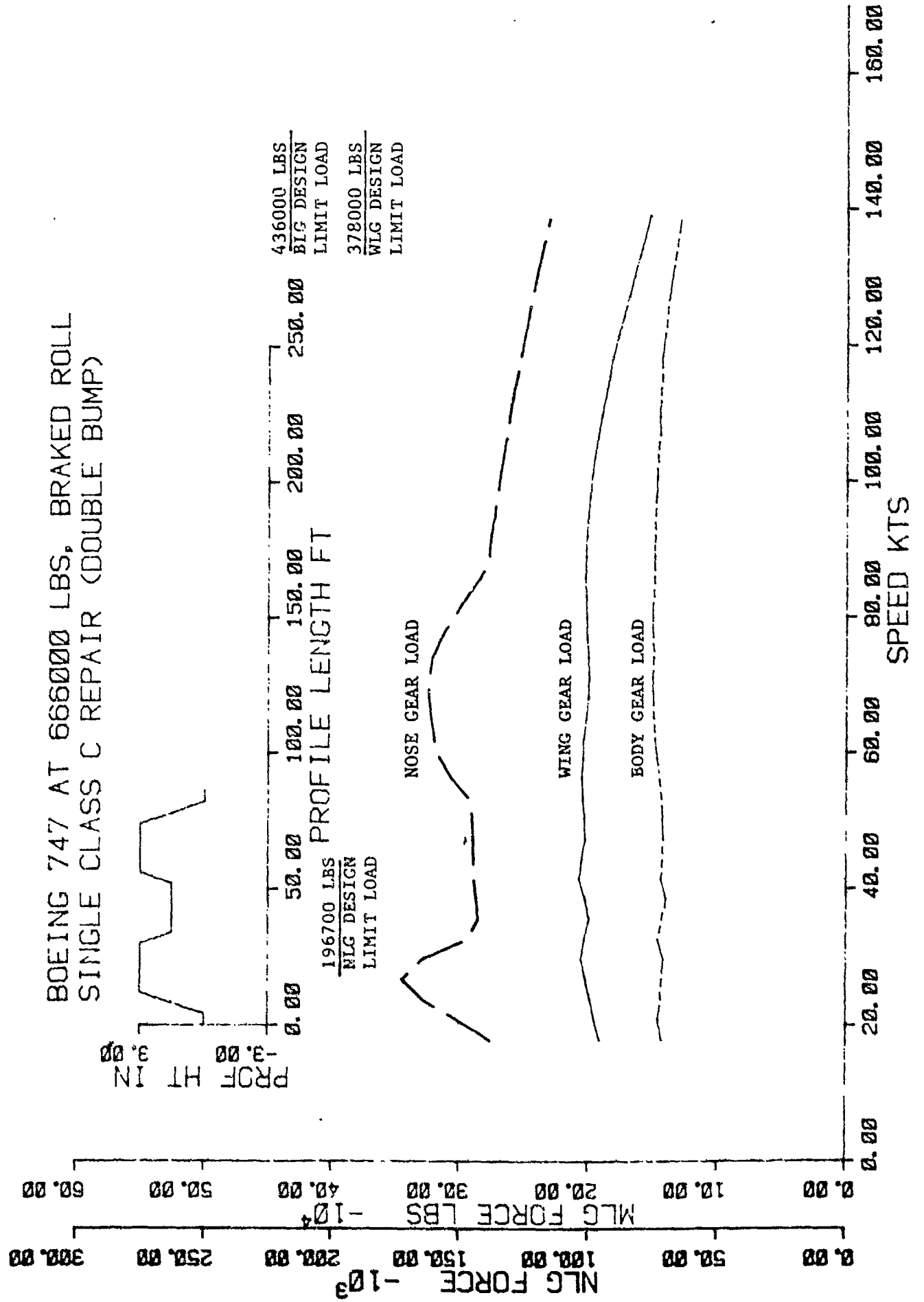

Figure 32 Velocity Analysis-Braked Roll Over Class C Repair at 666000 lbs GW

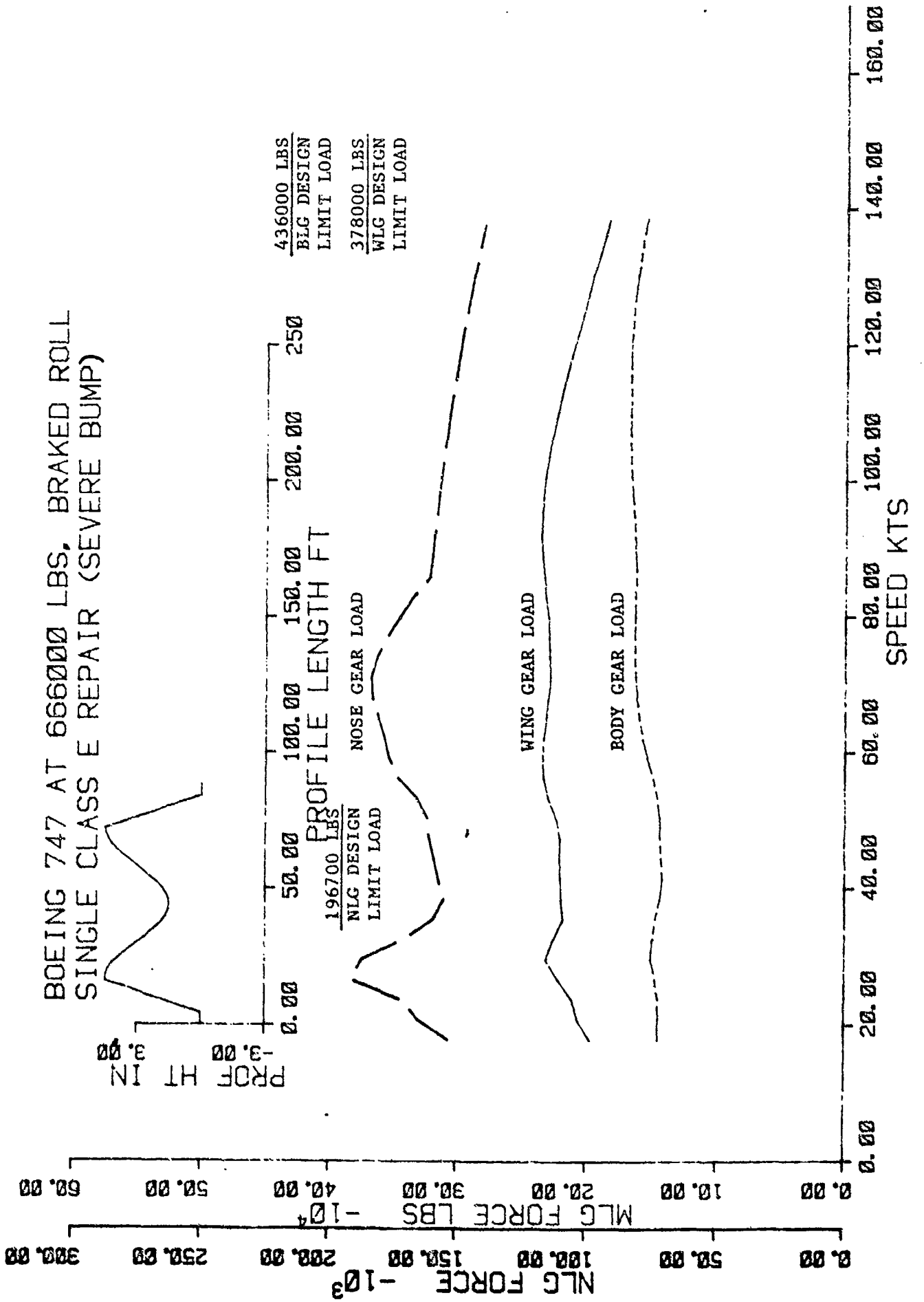

Figure 33 Velocity Analysis-Braked Roll Over Class E Repair at 666000 lbs GW

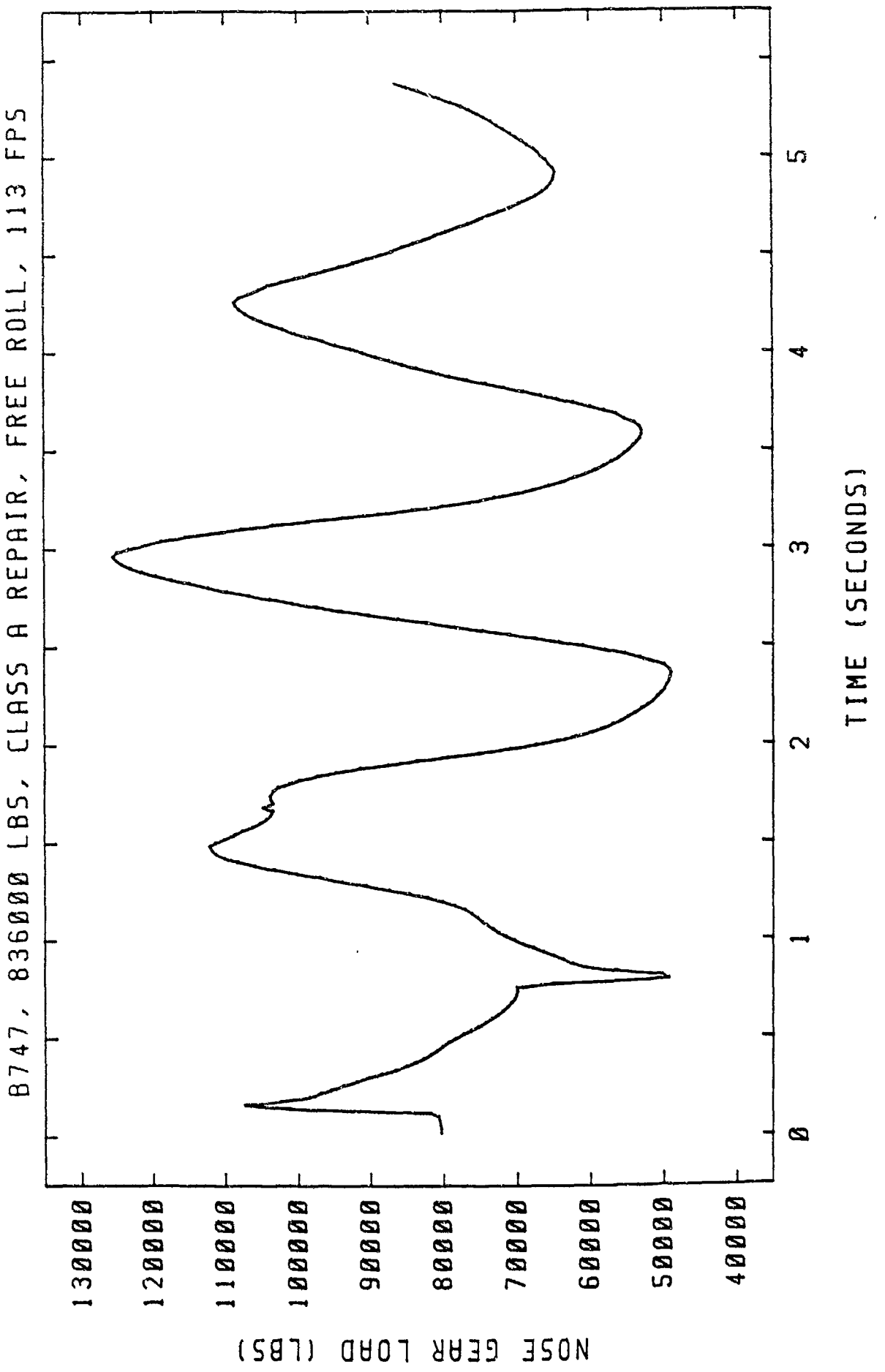

Figure 34 Nose Gear Load vs Time-Free Roll Over Class A Repair at Critical Velocity

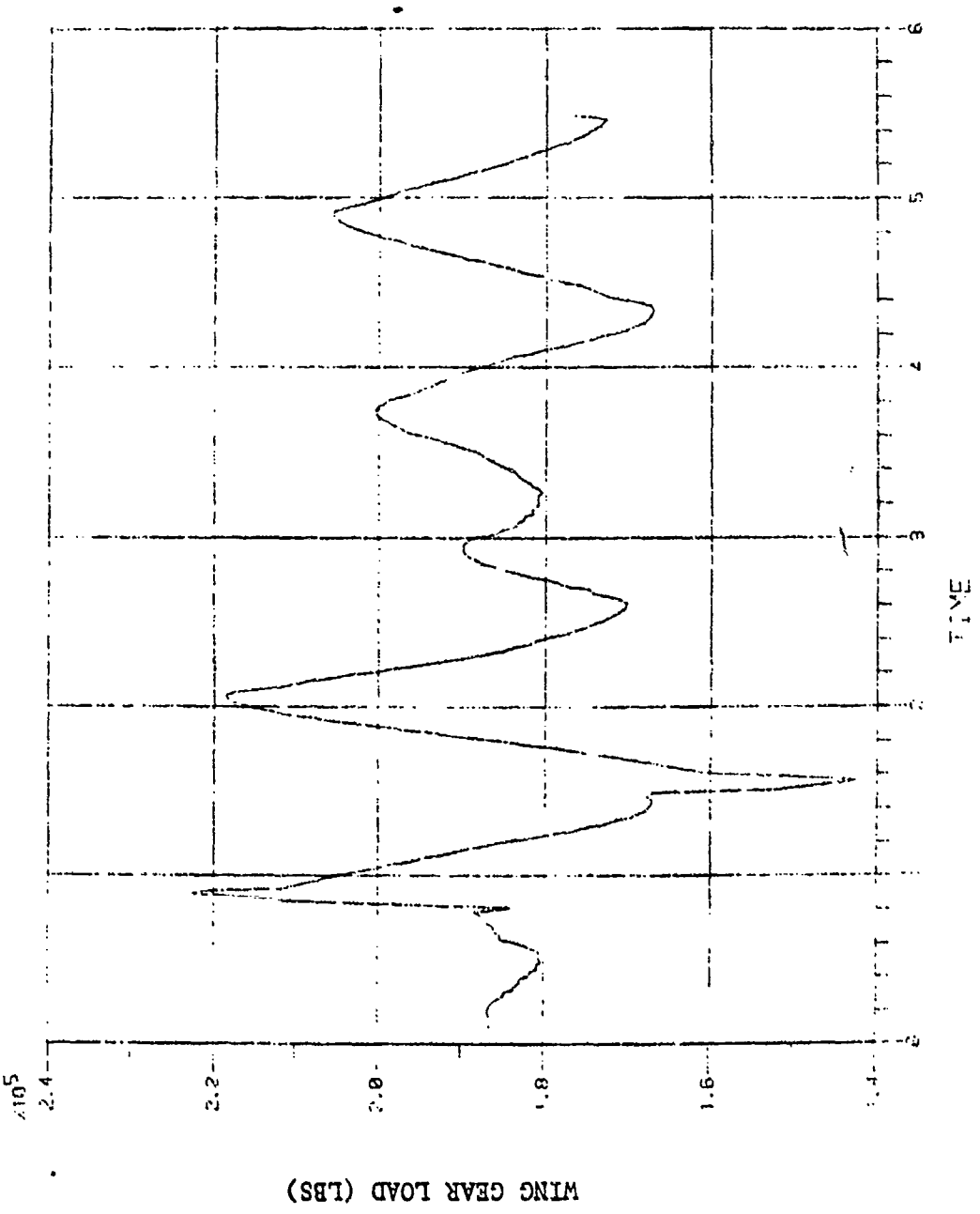

Figure 35 Wing Gear Load vs Time-Free Roll Over Class A Repair at Critical Velocity

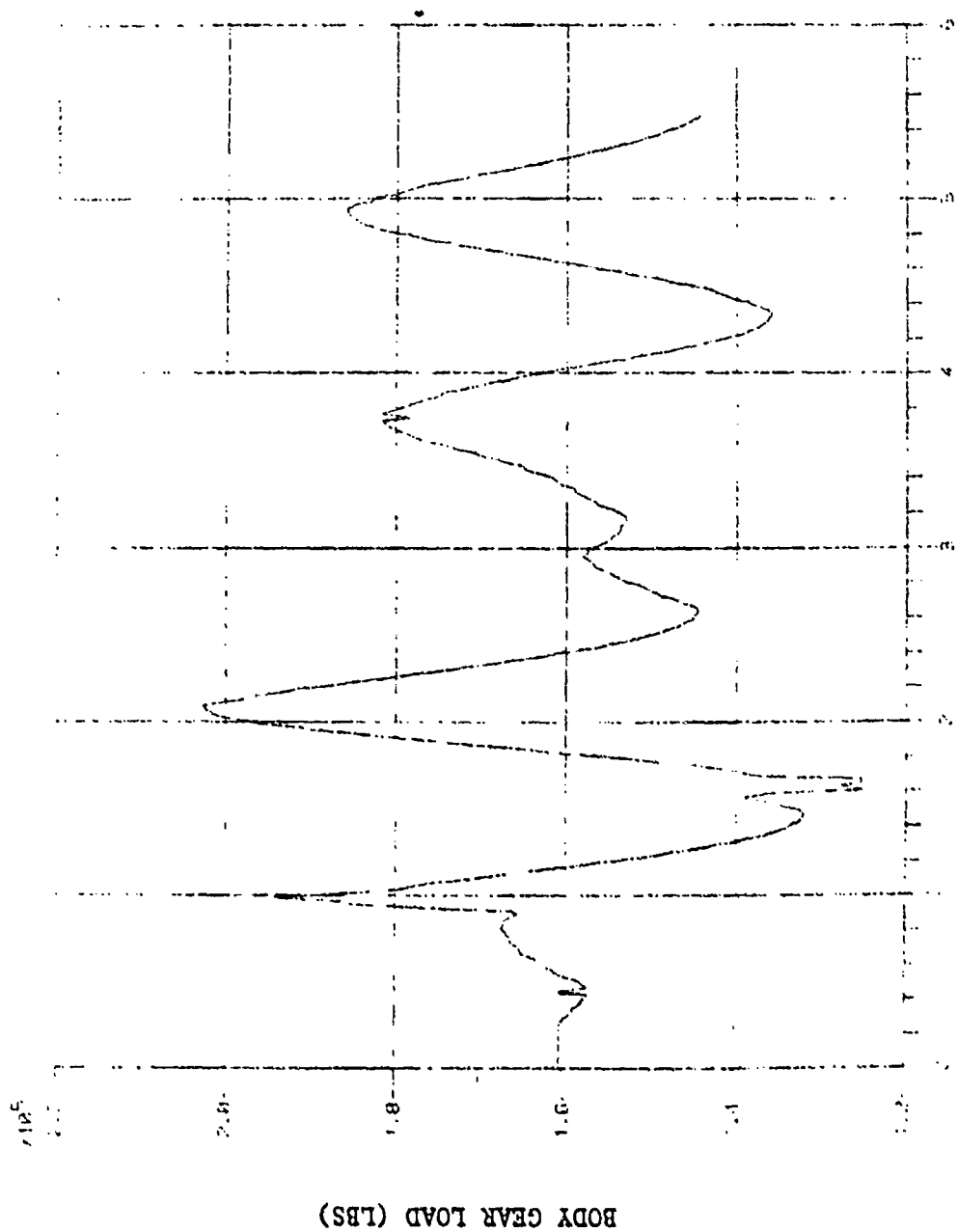

Figure 36 Body Gear Load vs Time-Free Roll Over Class A Repair at Critical Velocity

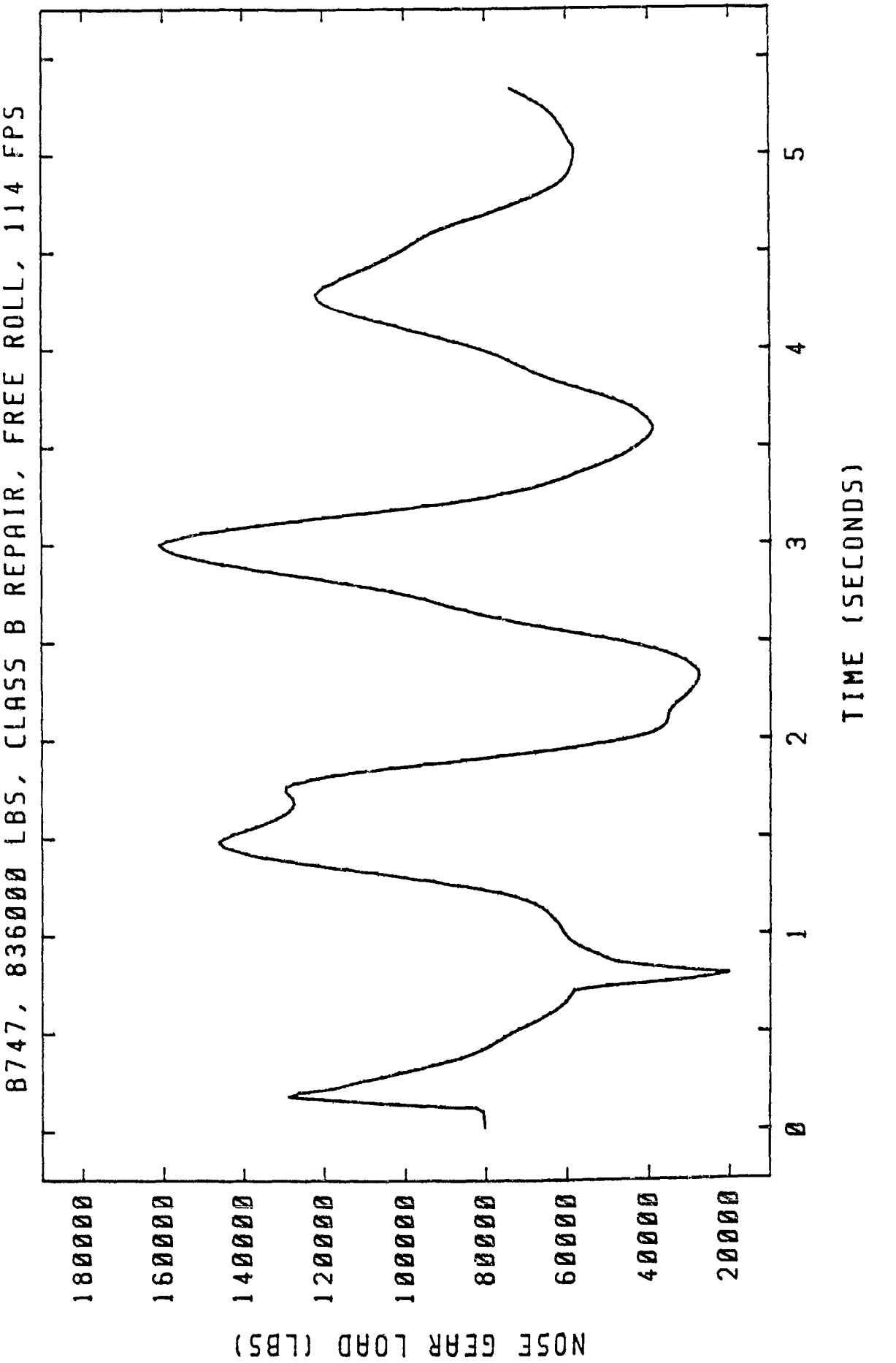

Figure 37 Nose Gear Load vs Time-Free Roll Over Class B Repair at Critical Velocity

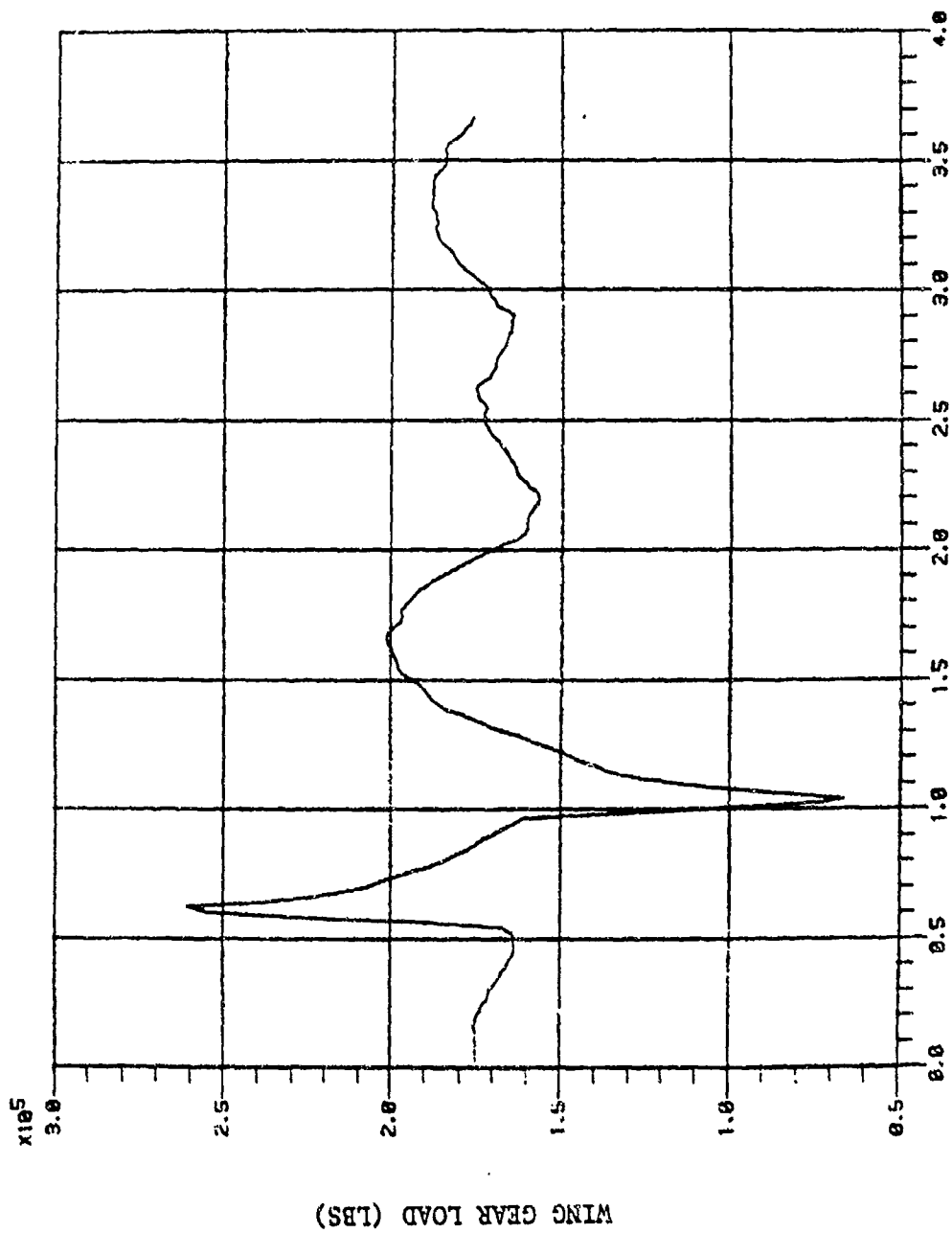

Figure 38 Wing Gear Load vs Time-Free Roll Over Class B Repair at Critical Velocity

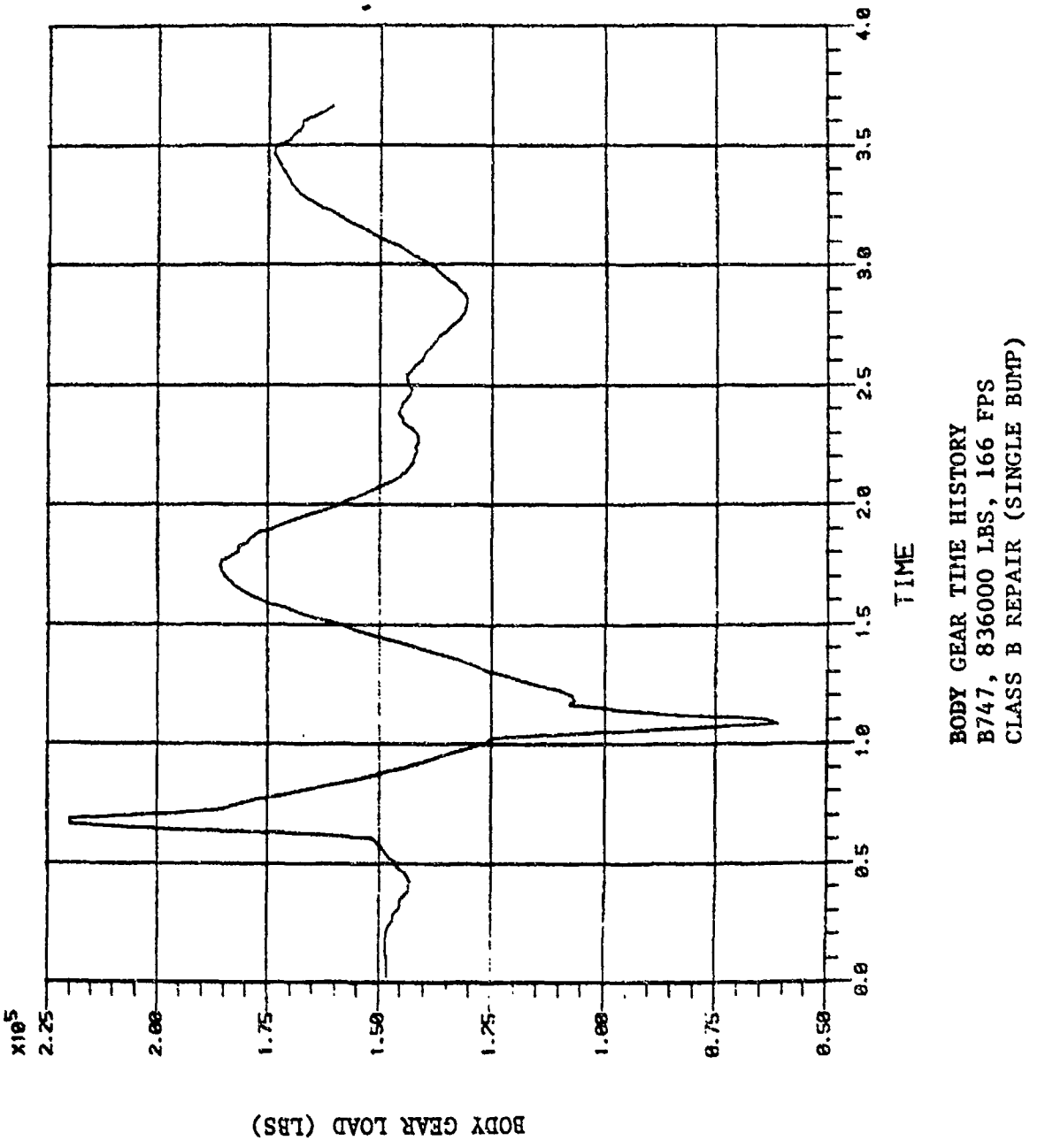

Figure 39 Body Gear Load vs Time-Free Roll Over Class B Repair at Critical Velocity

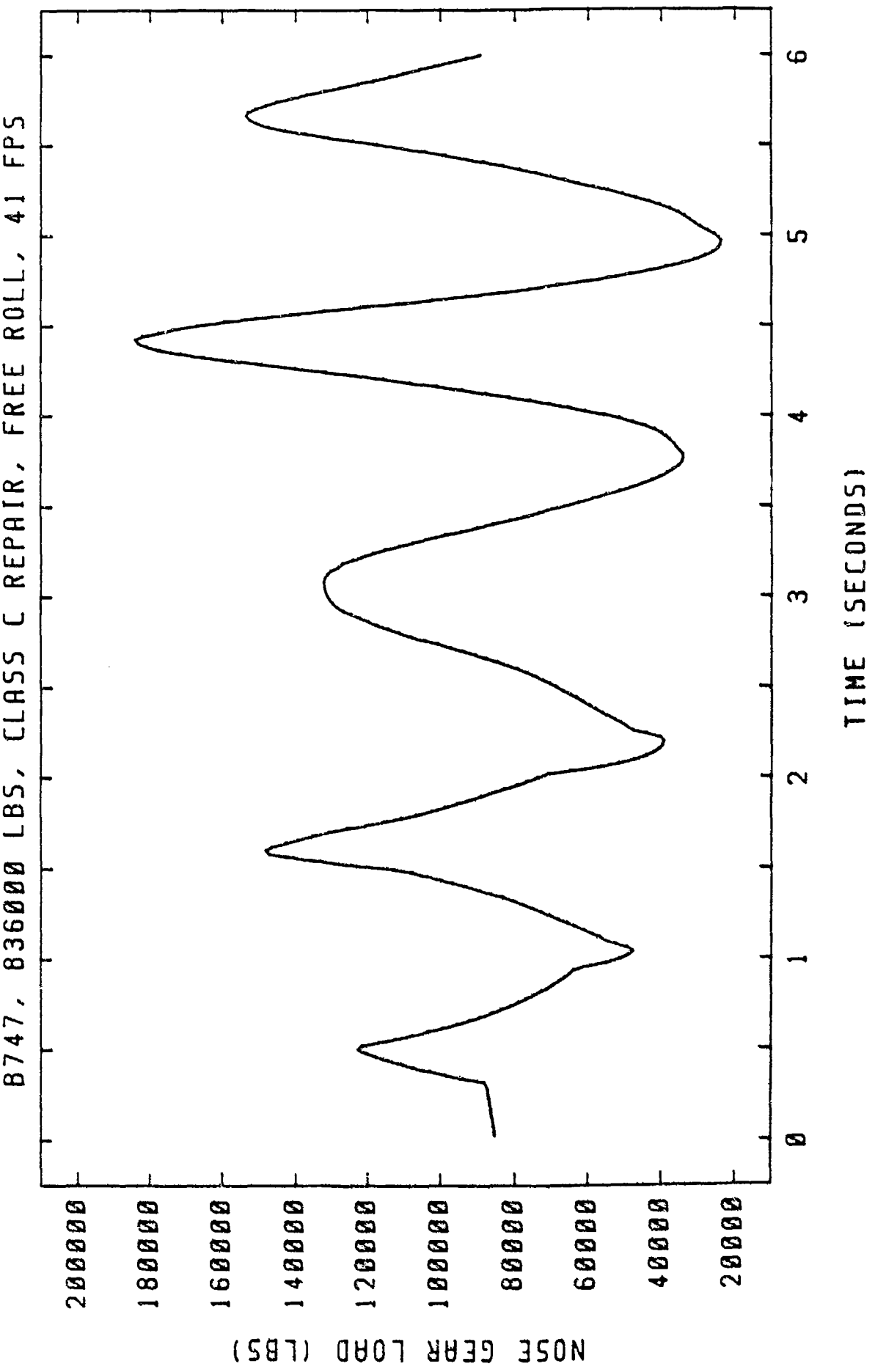

Figure 40 Nose Gear Load vs Time-Free Roll Over Class C Repair at Critical Velocity

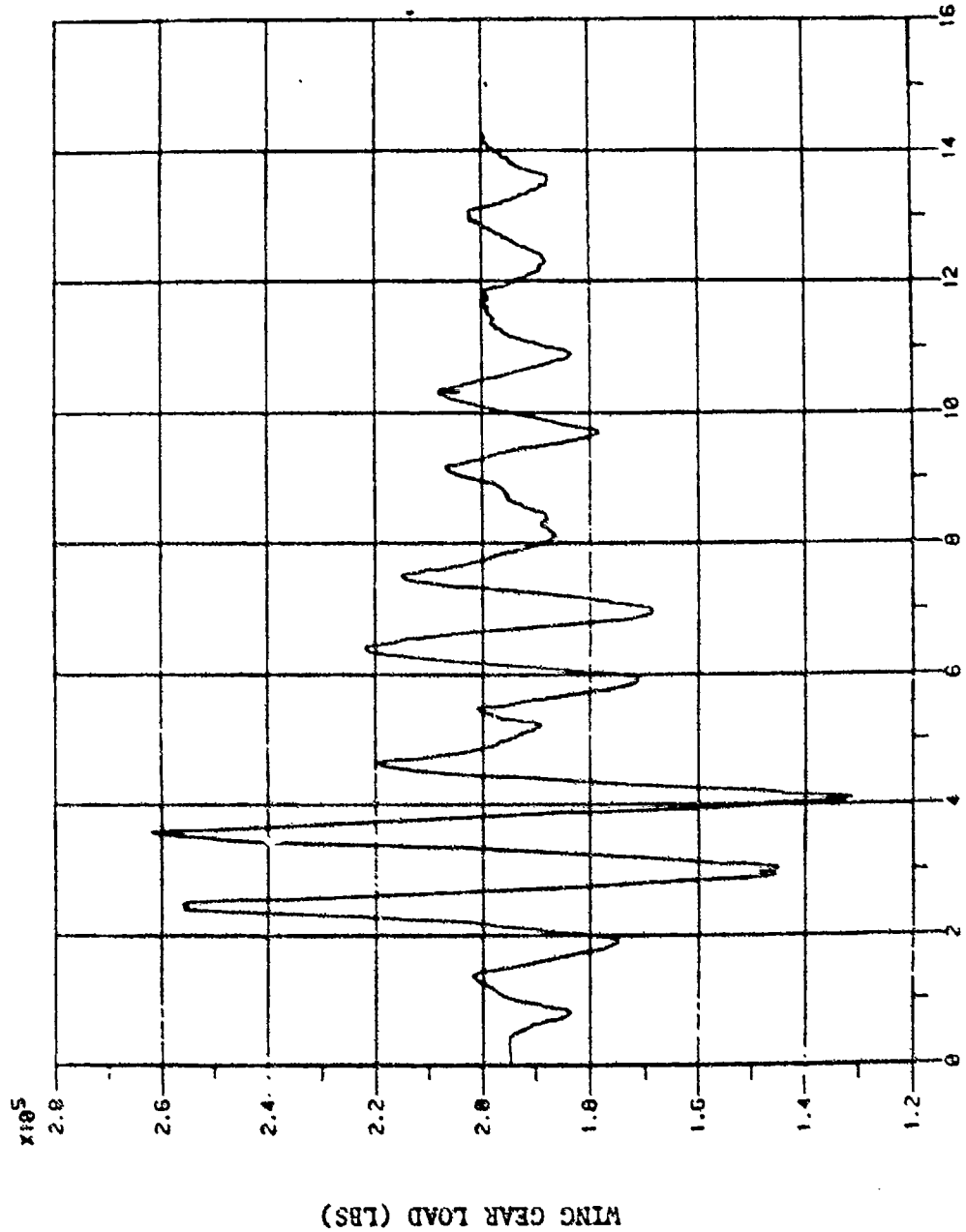

Figure 41 Wing Gear Load vs Time-Free Roll Over Class C Repair at Critical Velocity

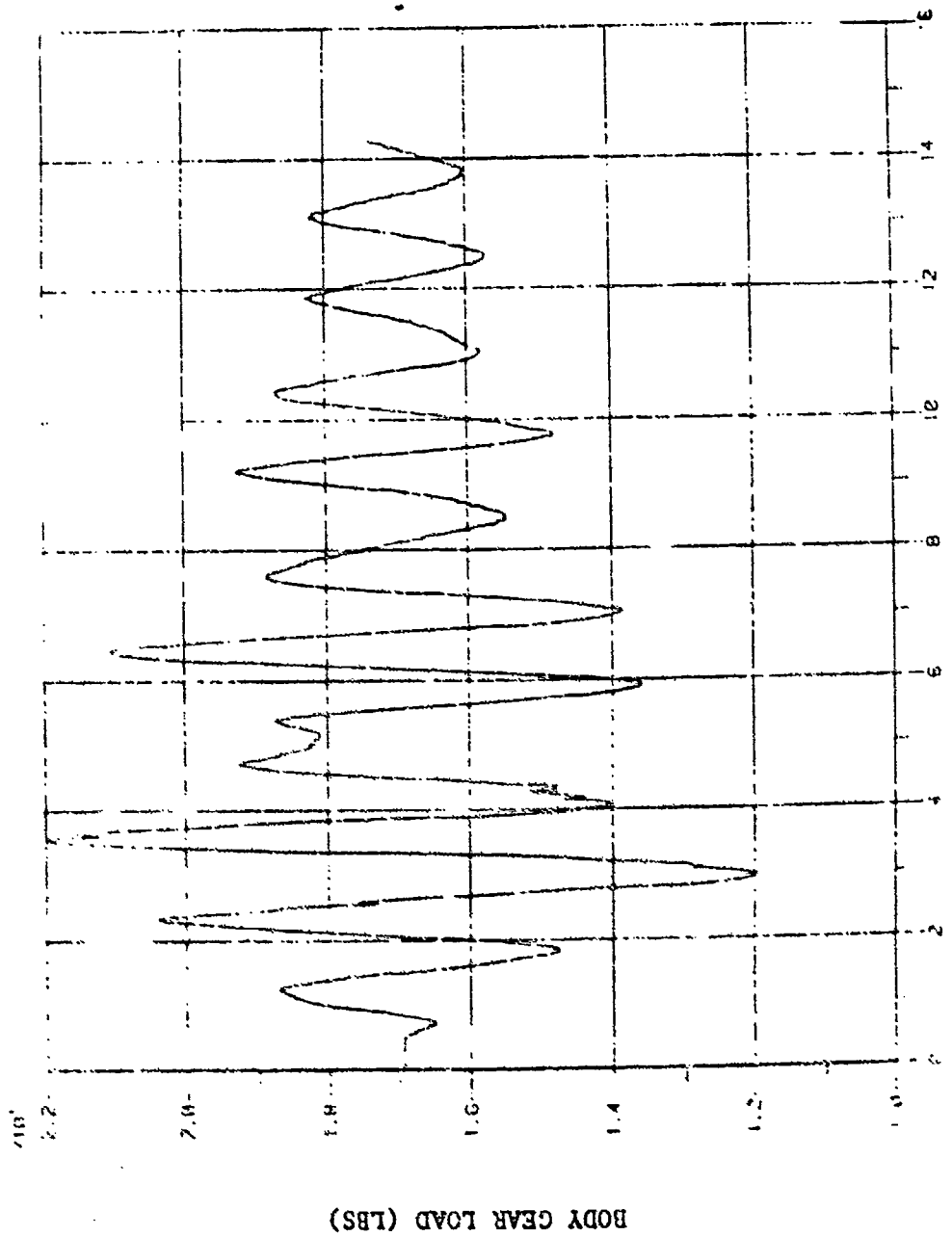

Figure 42 Body Gear Load vs Time-Free Roll Over Class C Repair at Critical Velocity

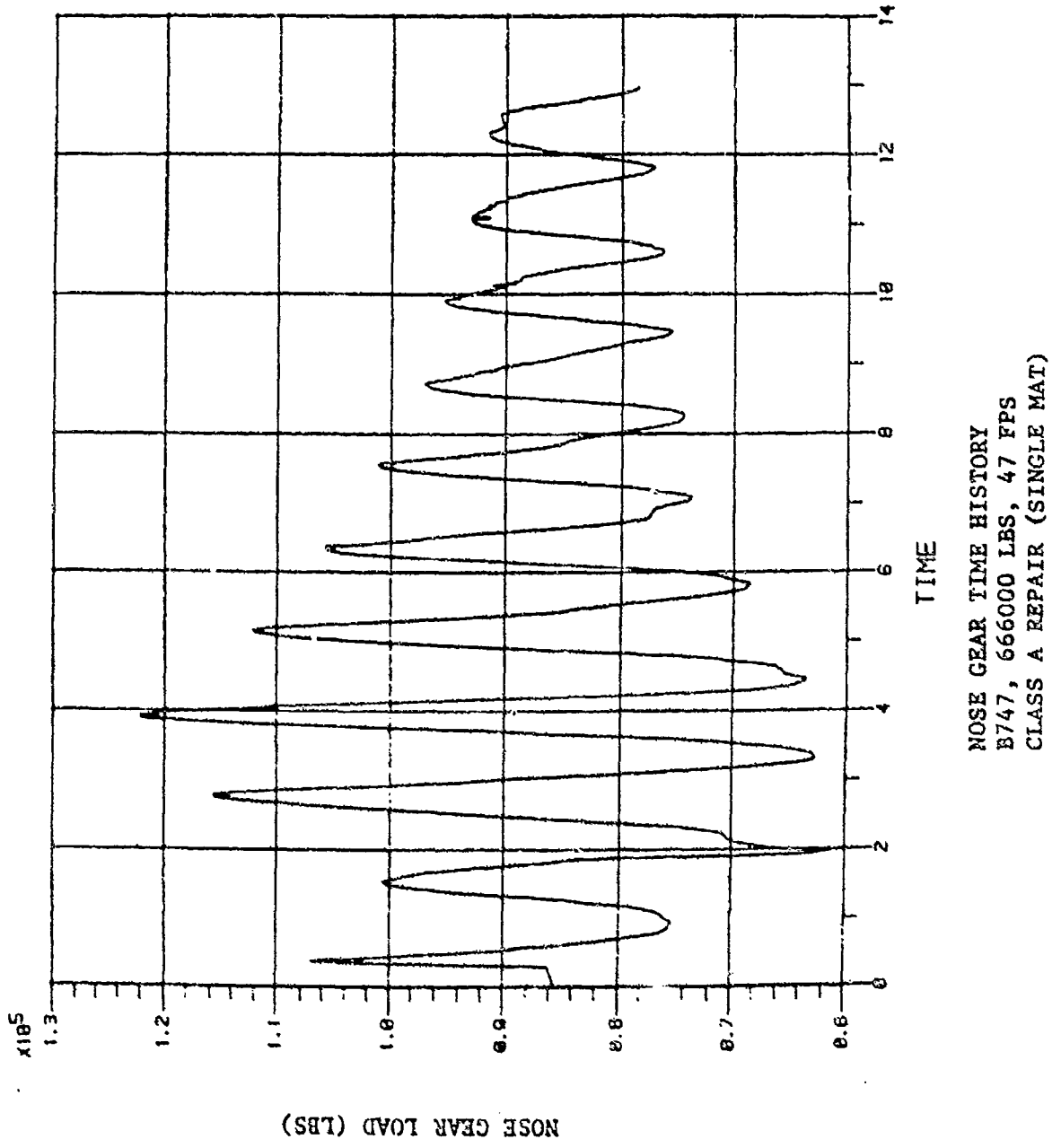

Figure 43 Nose Gear Load vs Time-Reverse Thrust Braked Roll Over Class A Repair at Critical Velocity

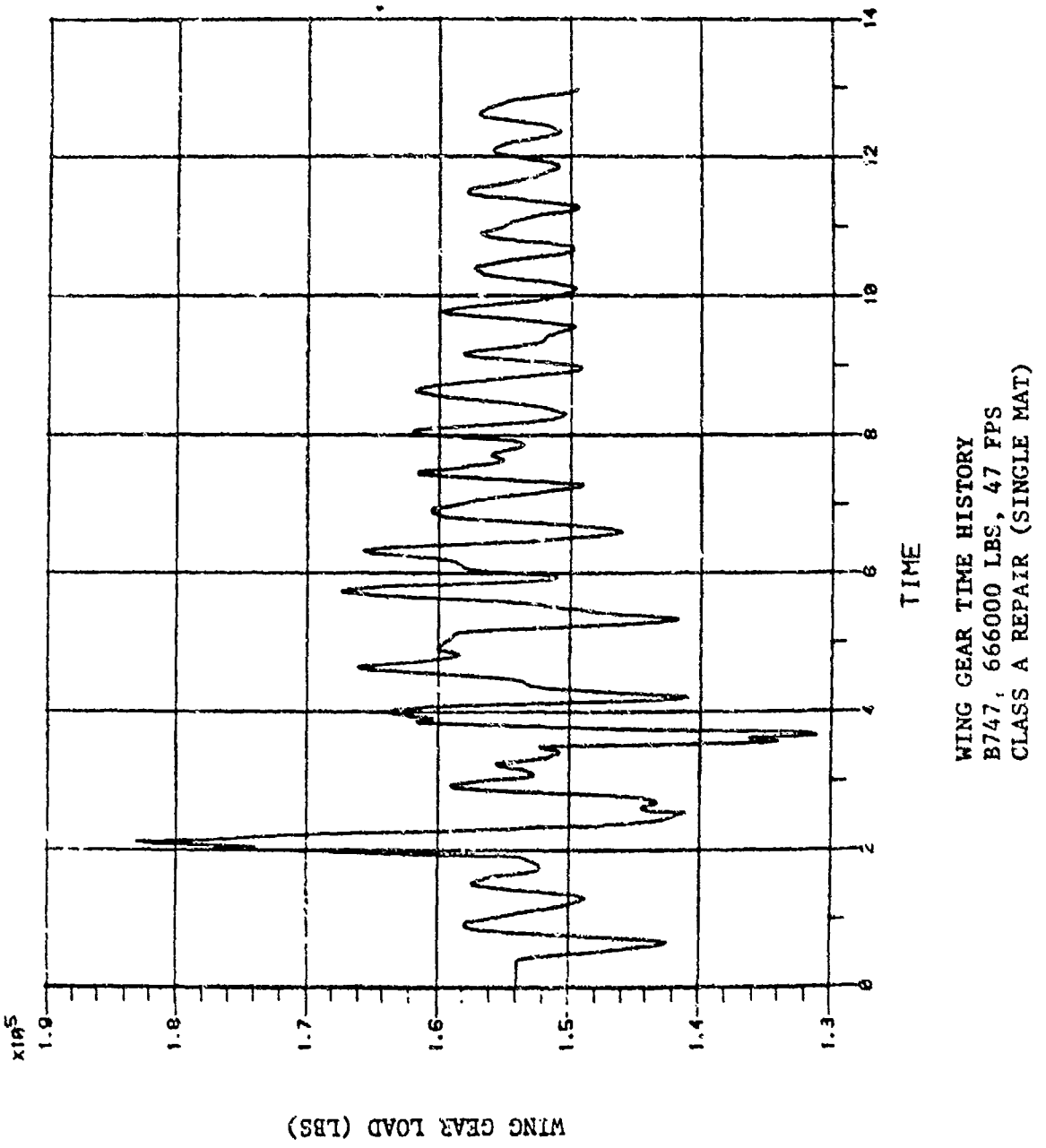

Figure 44 Wing Gear Load vs Time-Reverse Thrust Braked Roll Over Class A Repair at Critical Velocity

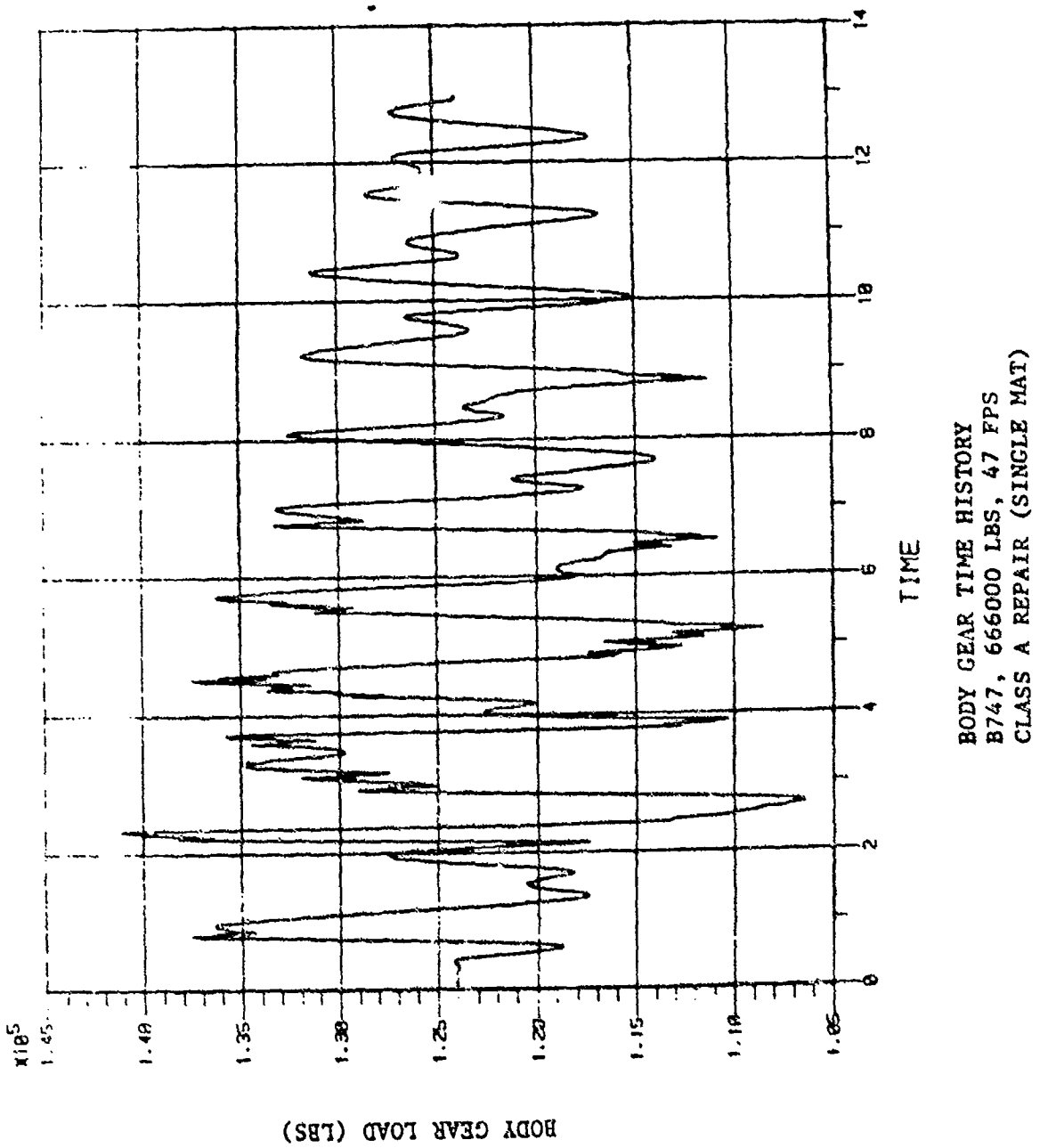

Figure 45 Body Gear Load vs Time-Reverse Thrust Braked Roll Over Class A Repair at Critical Velocity

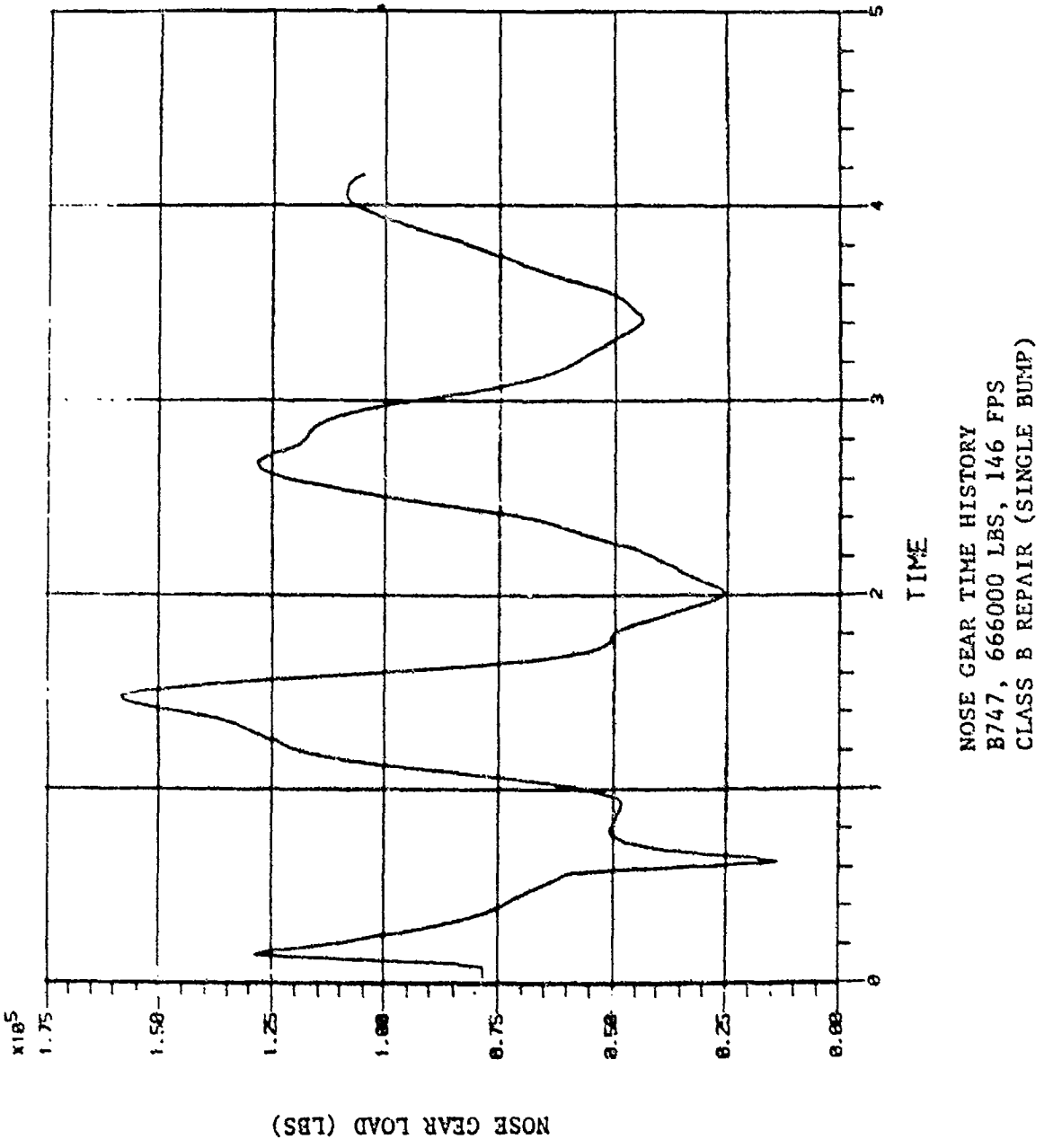

Figure 46 Nose Gear Load vs Time-Reverse Thrust Braked Roll Over Class B Repair at Critical Velocity

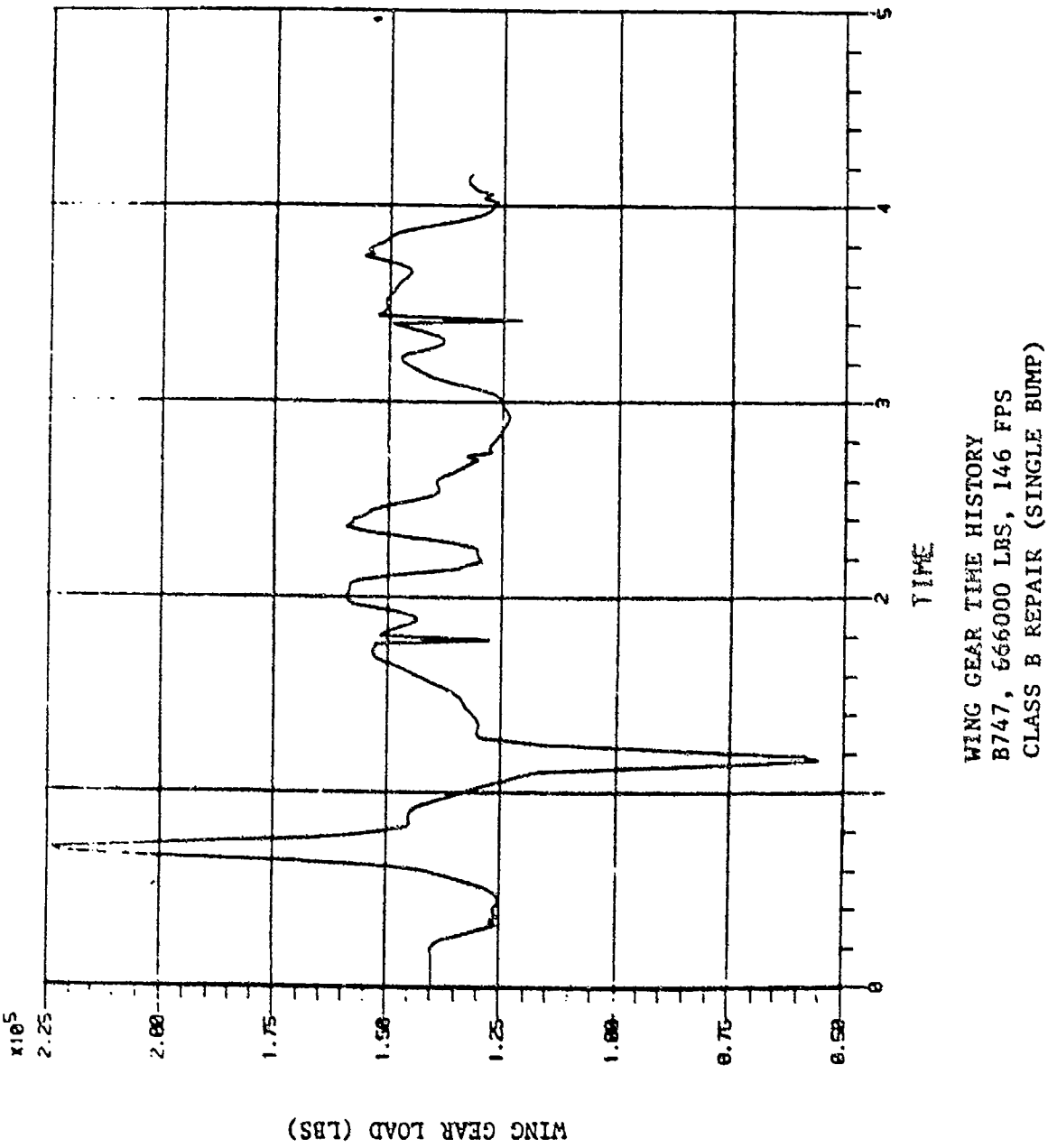

Figure 47 Wing Gear Load vs Time-Reverse Thrust Braked Roll Over Class B Repair at Critical Velocity

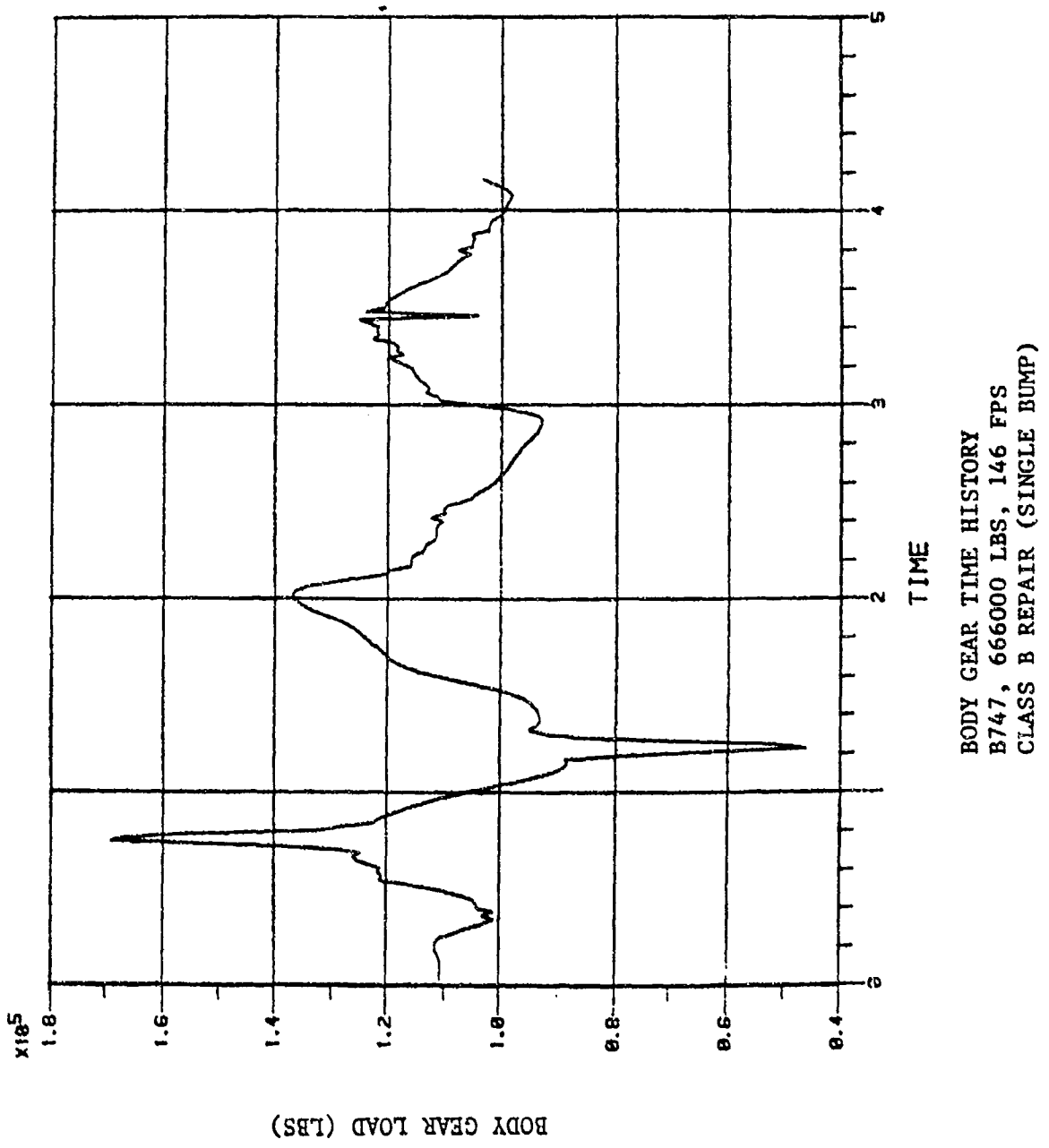

Figure 48 Body Gear Load vs Time-Reverse Thrust Braked Roll Over Class B Repair at Critical Velocity

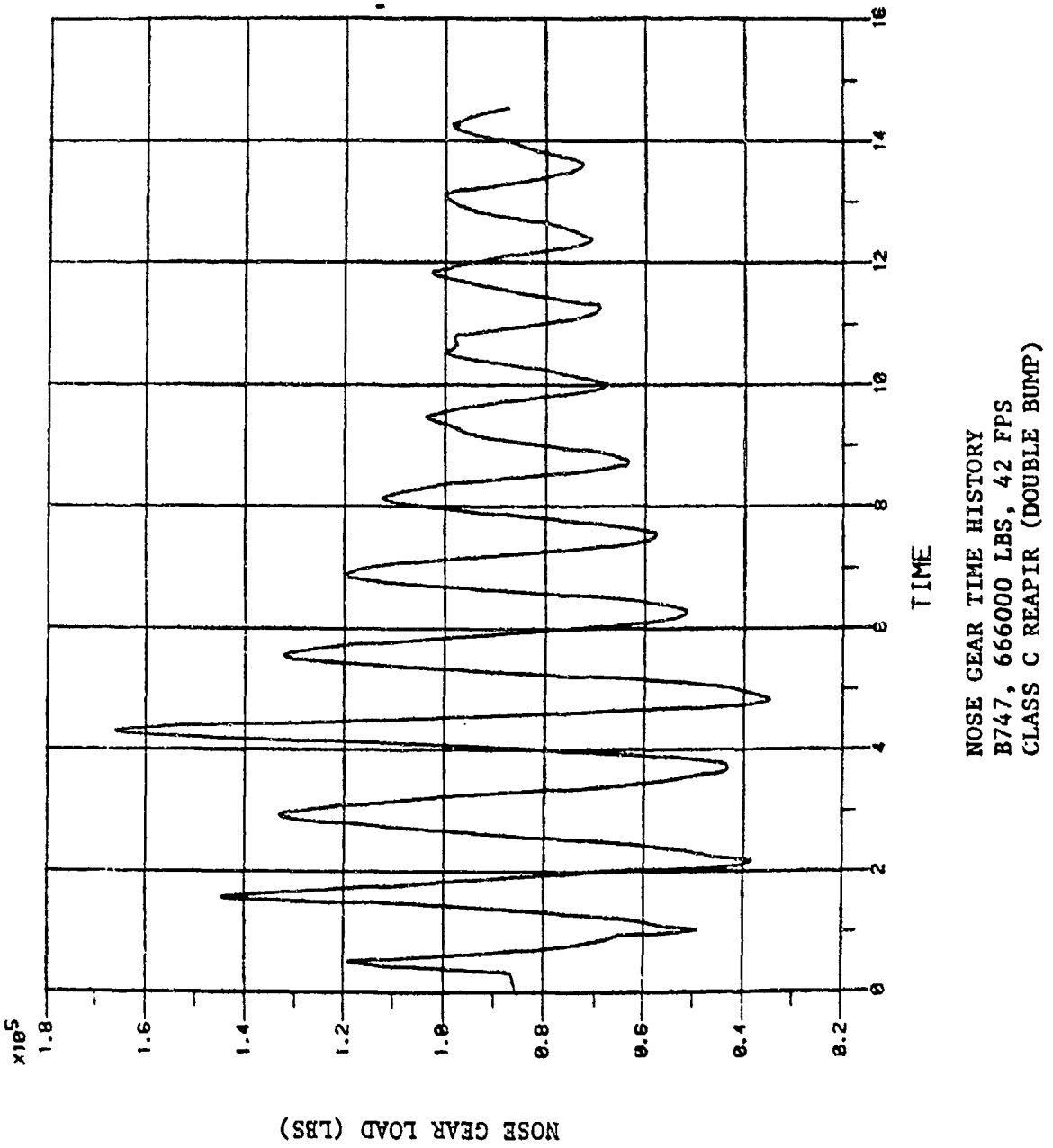

Figure 49 Nose Gear Load vs Time-Reverse Thrust Braked Roll Over Class C Repair at Critical Velocity

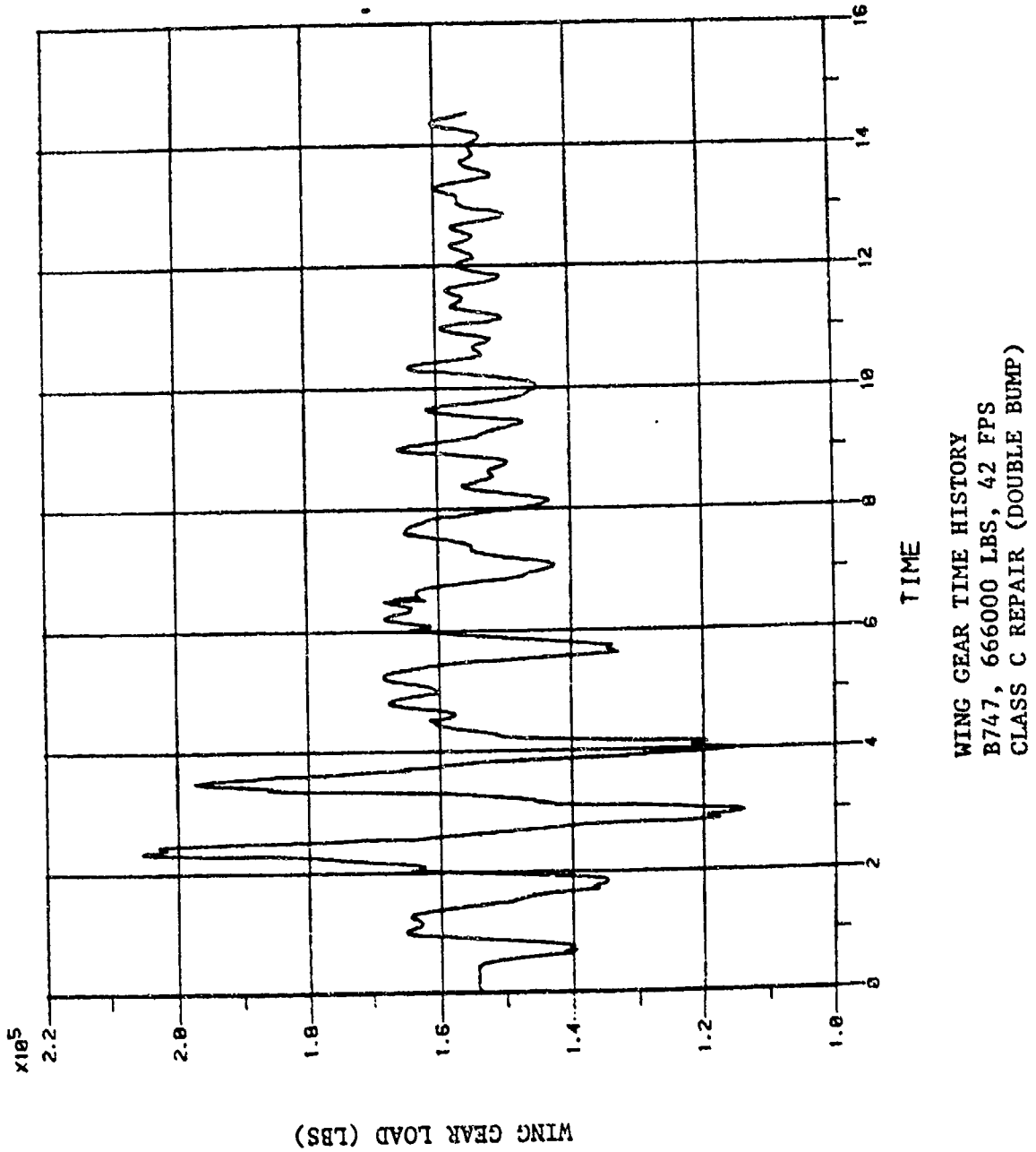

Figure 50 Wing Gear Load vs Time-Reverse Thrust Braked Roll Over Class C Repair at Critical Velocity

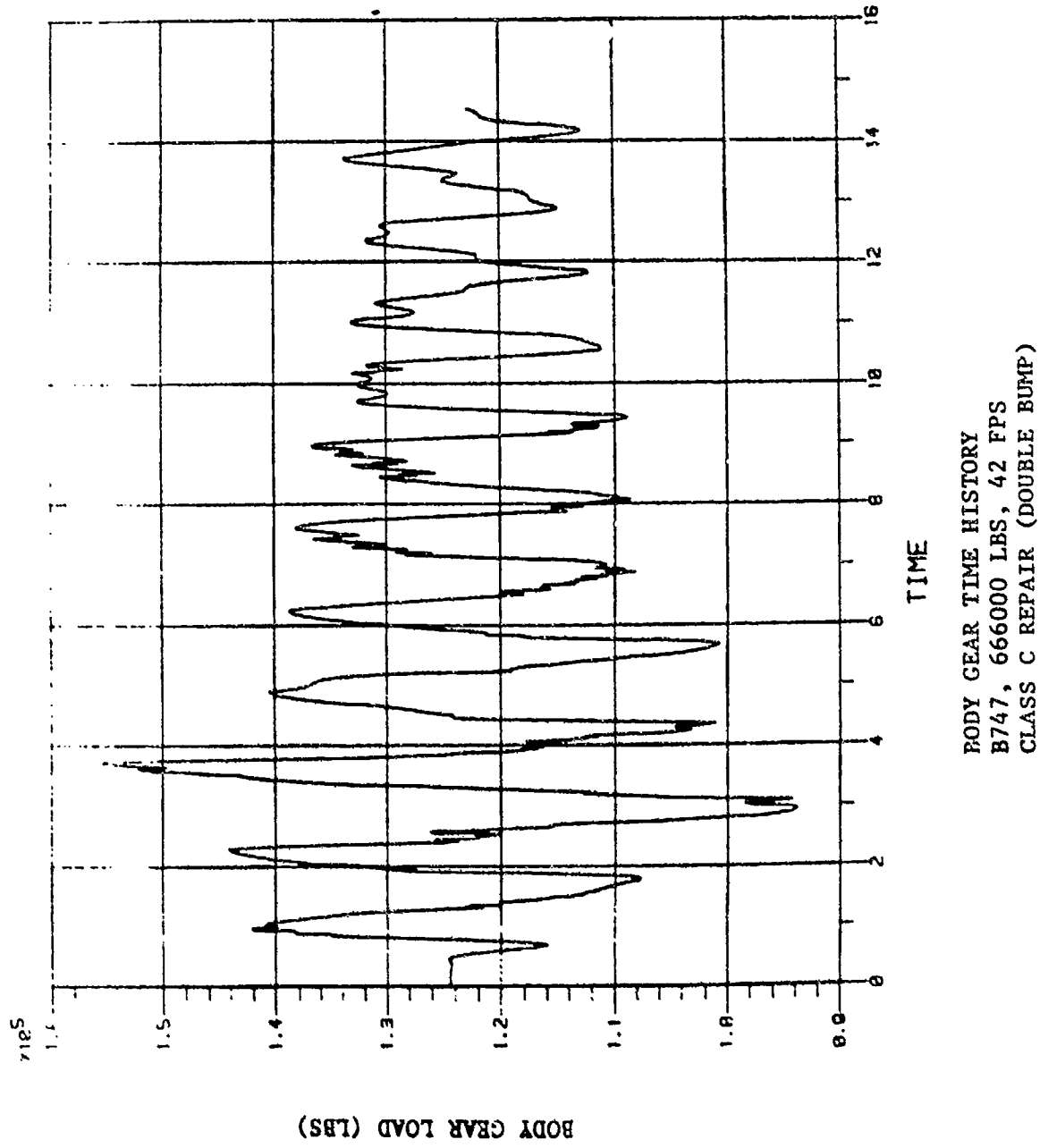

Figure 51 Body Gear Load vs Time-Reverse Thrust Braked Roll Over Class C Repair at Critical Velocity

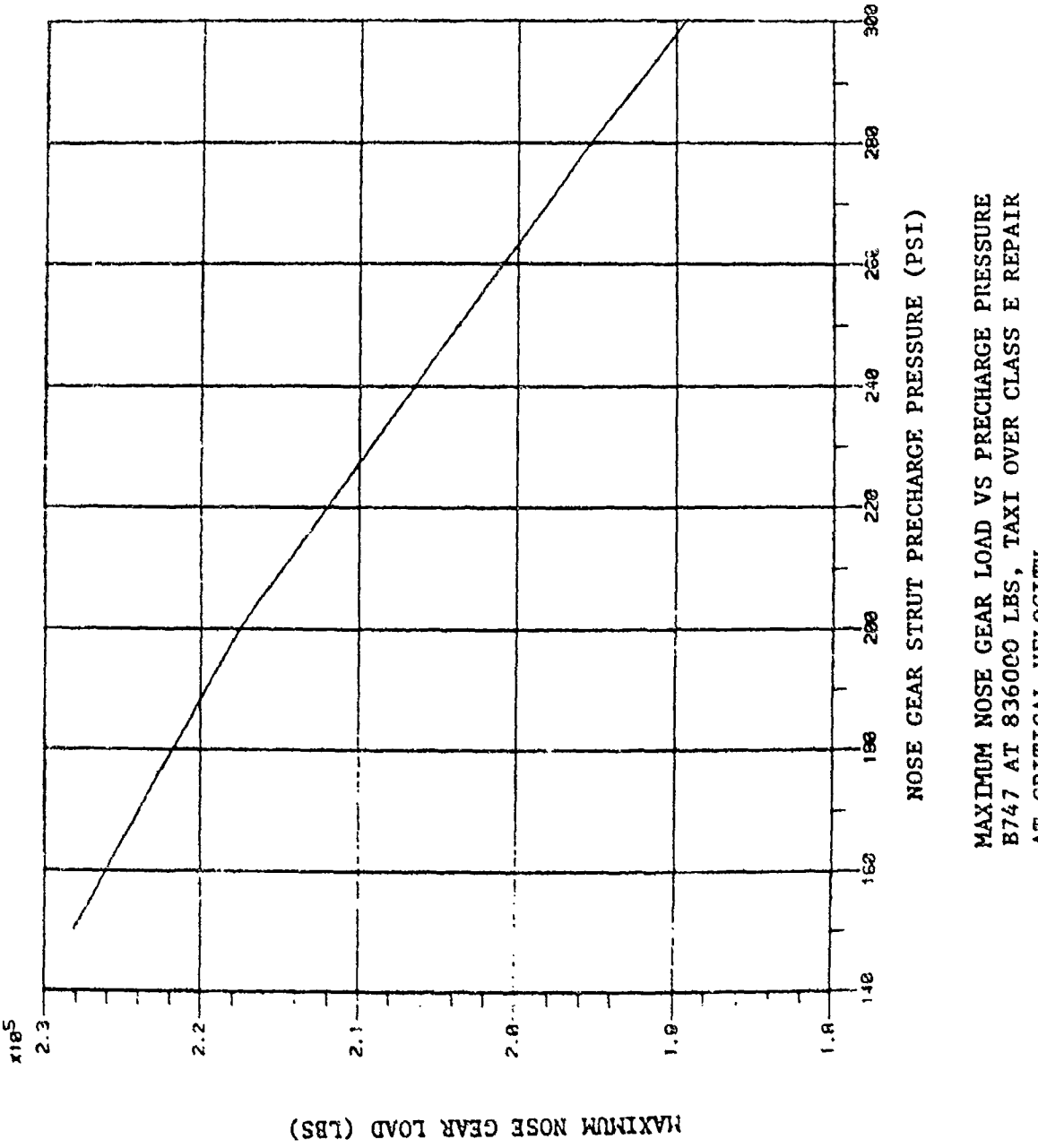

Figure 52 Effect of Strut Pressure on Maximum Nose Gear Load

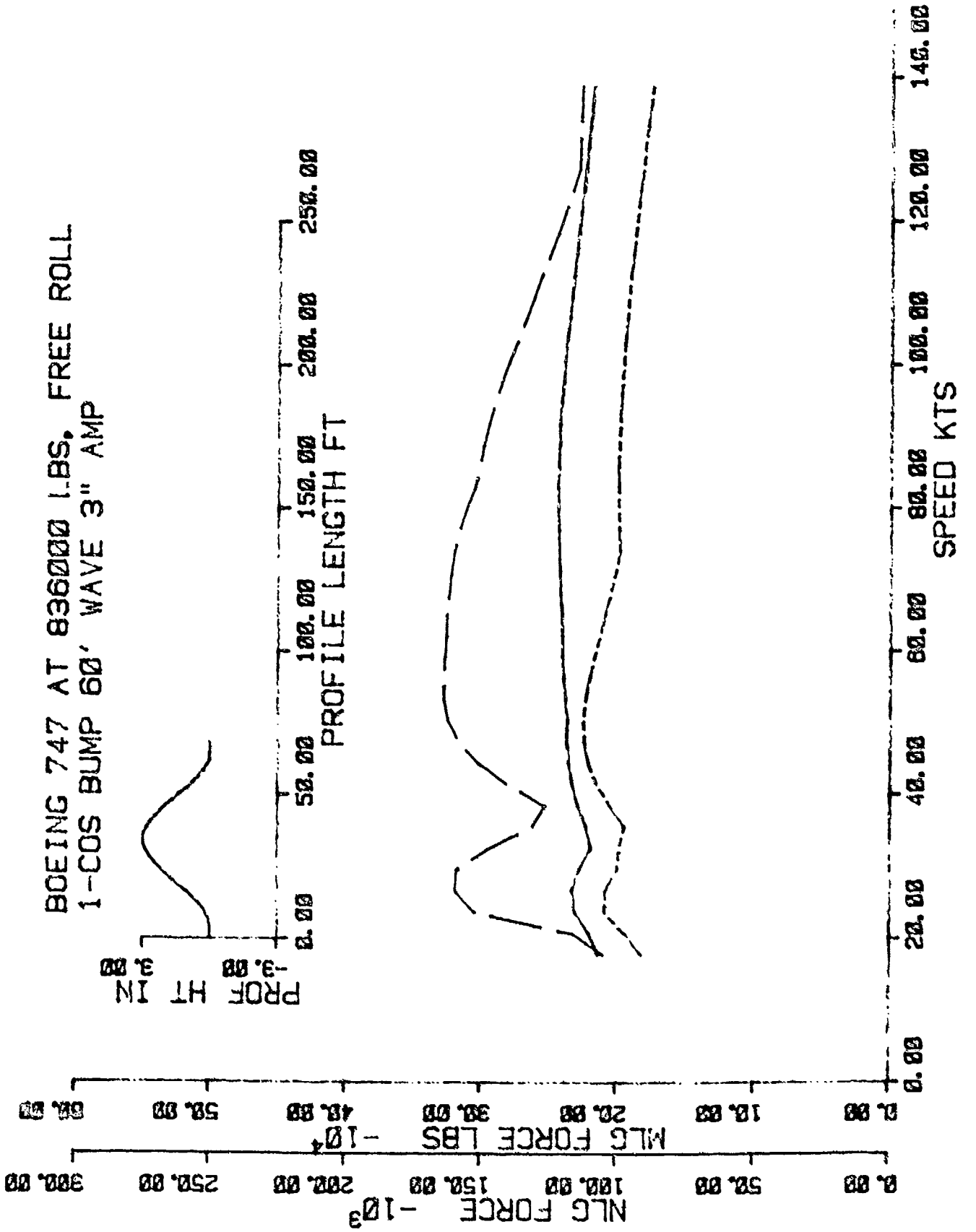

Figure 53 Velocity Analysis-Free Roll Over One-Minus-Cosine at 836000 lbs GW

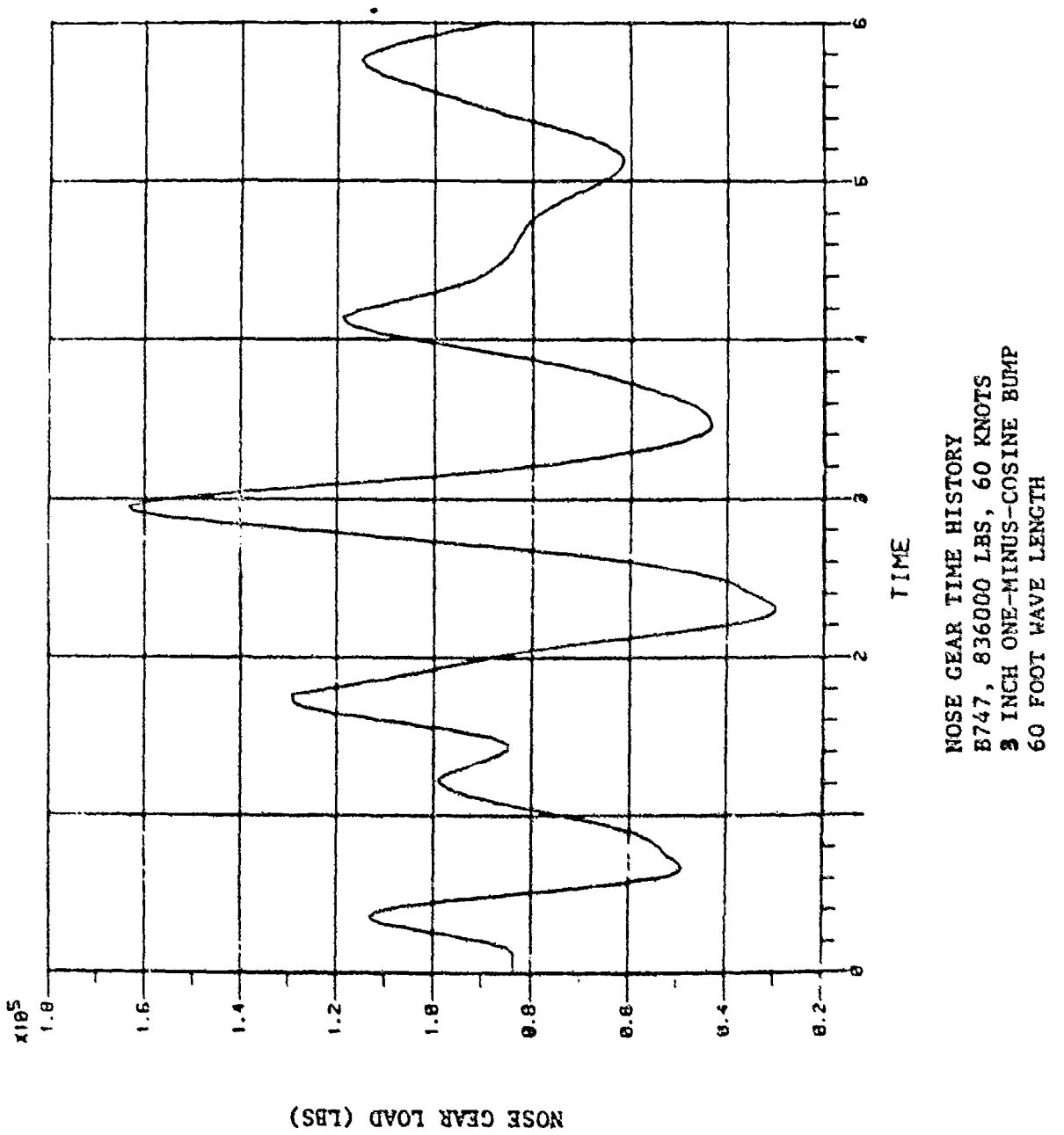

Figure 54 Nose Gear Load vs Time-Free Roll Over One-Minus-Cosine at 836000 lbs GW

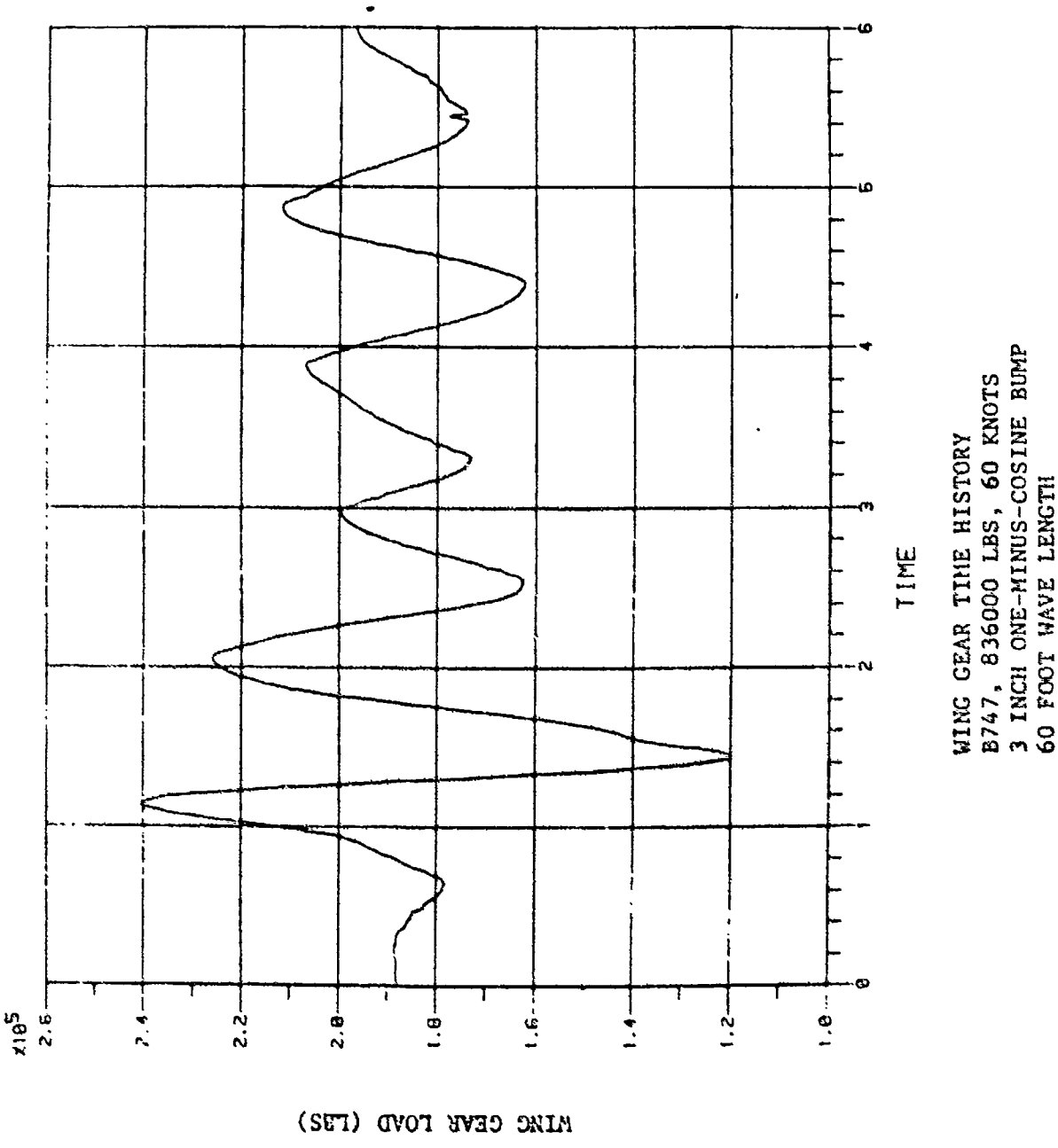

Figure 55 Wing Gear Load vs Time-Free Roll Over One-Minus-Cosine at 836000 lbs GW

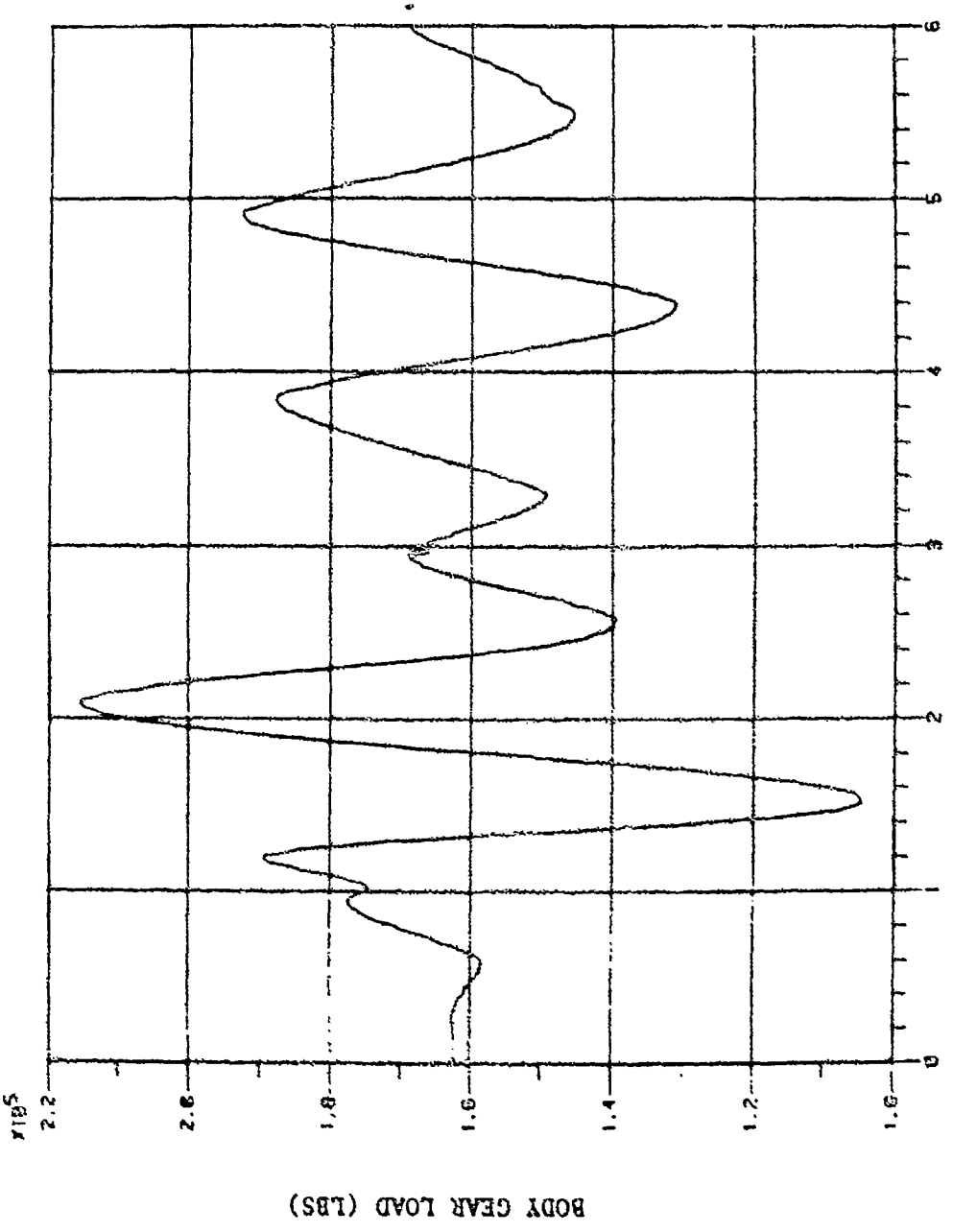

Figure 56 Body Gear Load vs Time-Free Roll Over One-Minus-Cosine at 836000 lbs GW

Table 4

MINIMUM SPACING IN FEET FOR
TRAVERSING TWO REPAIR PROFILES

SECOND PROFILE (TYPE)	FIRST PROFILE (TYPE) A	B	C	E*
A	0	0	0	100
B	0	400	200	400
C	0	400	200	400
E*	400	400	500	500

* E profile must not be traversed at speeds between 20 and 40 knots.

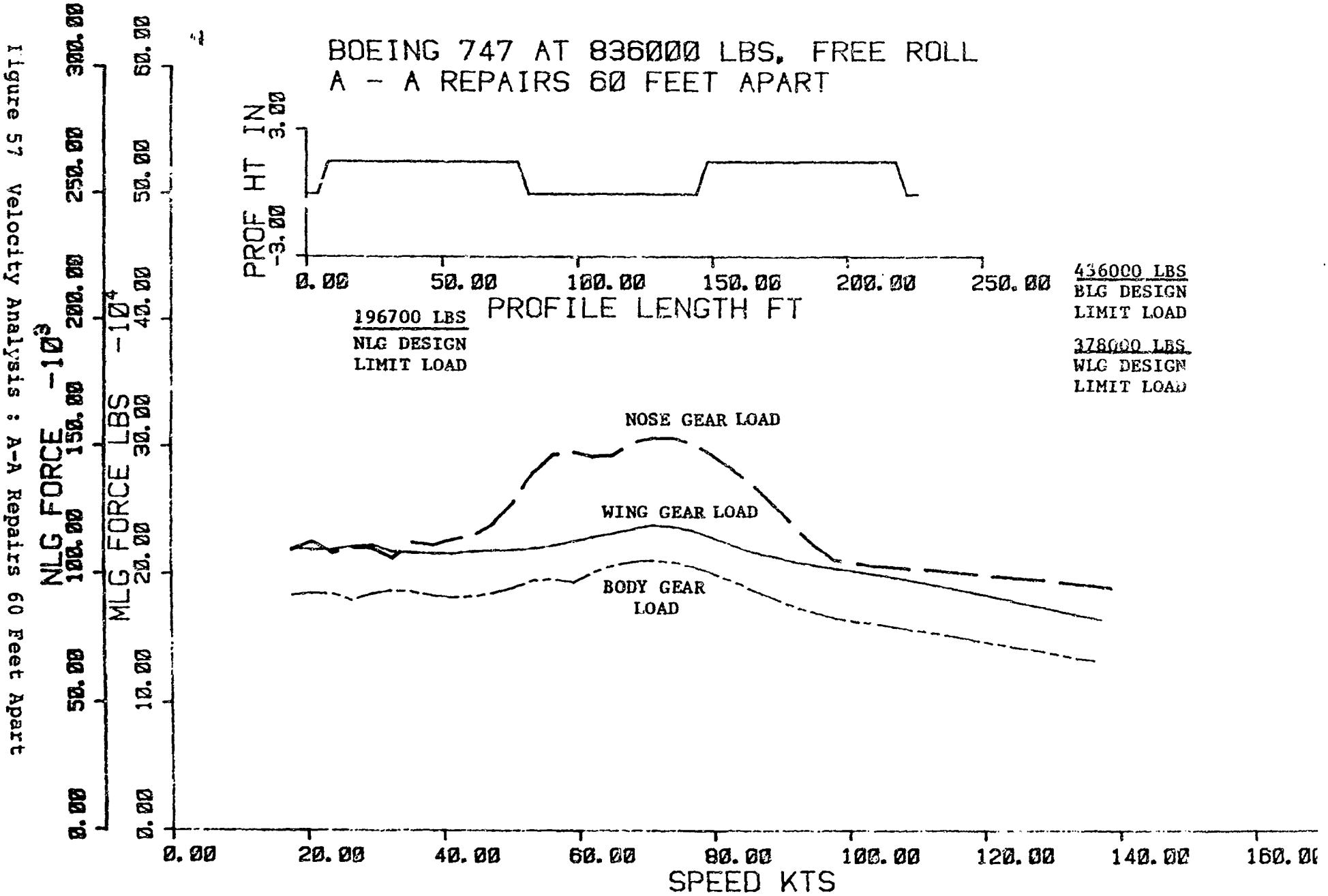

Figure 57 Velocity Analysis : A-A Repairs 60 Feet Apart

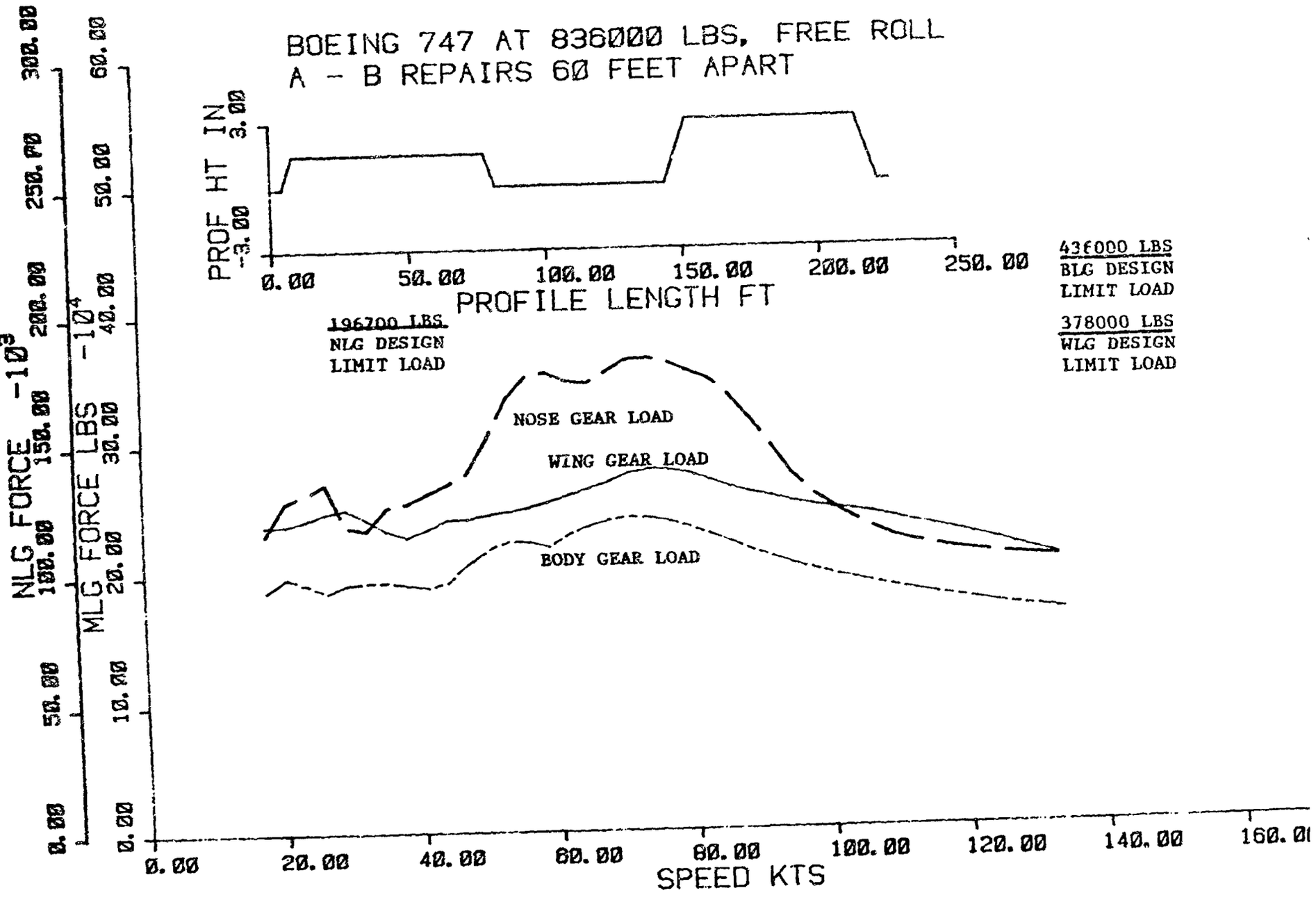

Figure 58 Velocity Analysis : A-B Repairs 60 Feet Apart

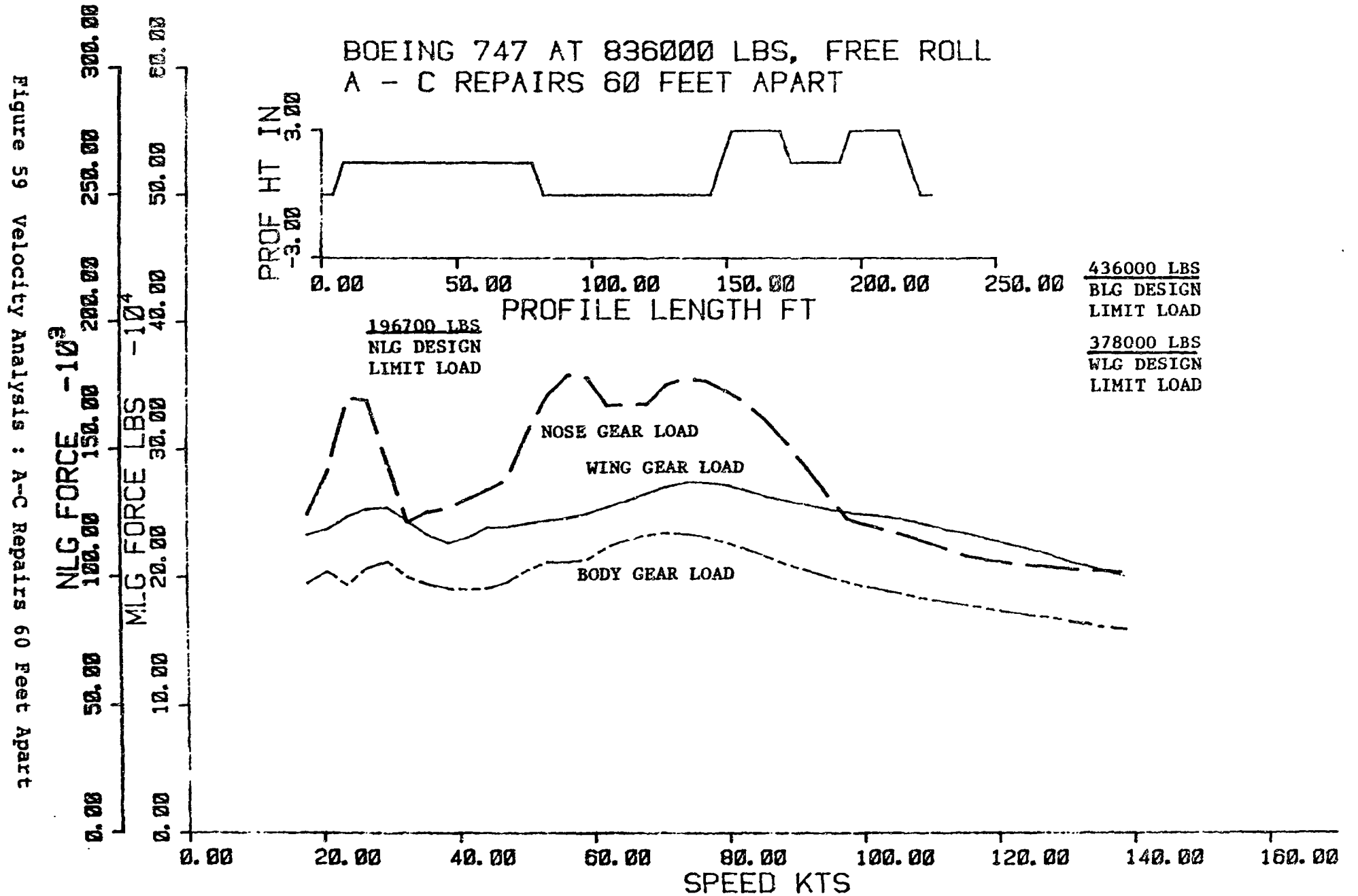

Figure 59 Velocity Analysis : A-C Repairs 60 Feet Apart

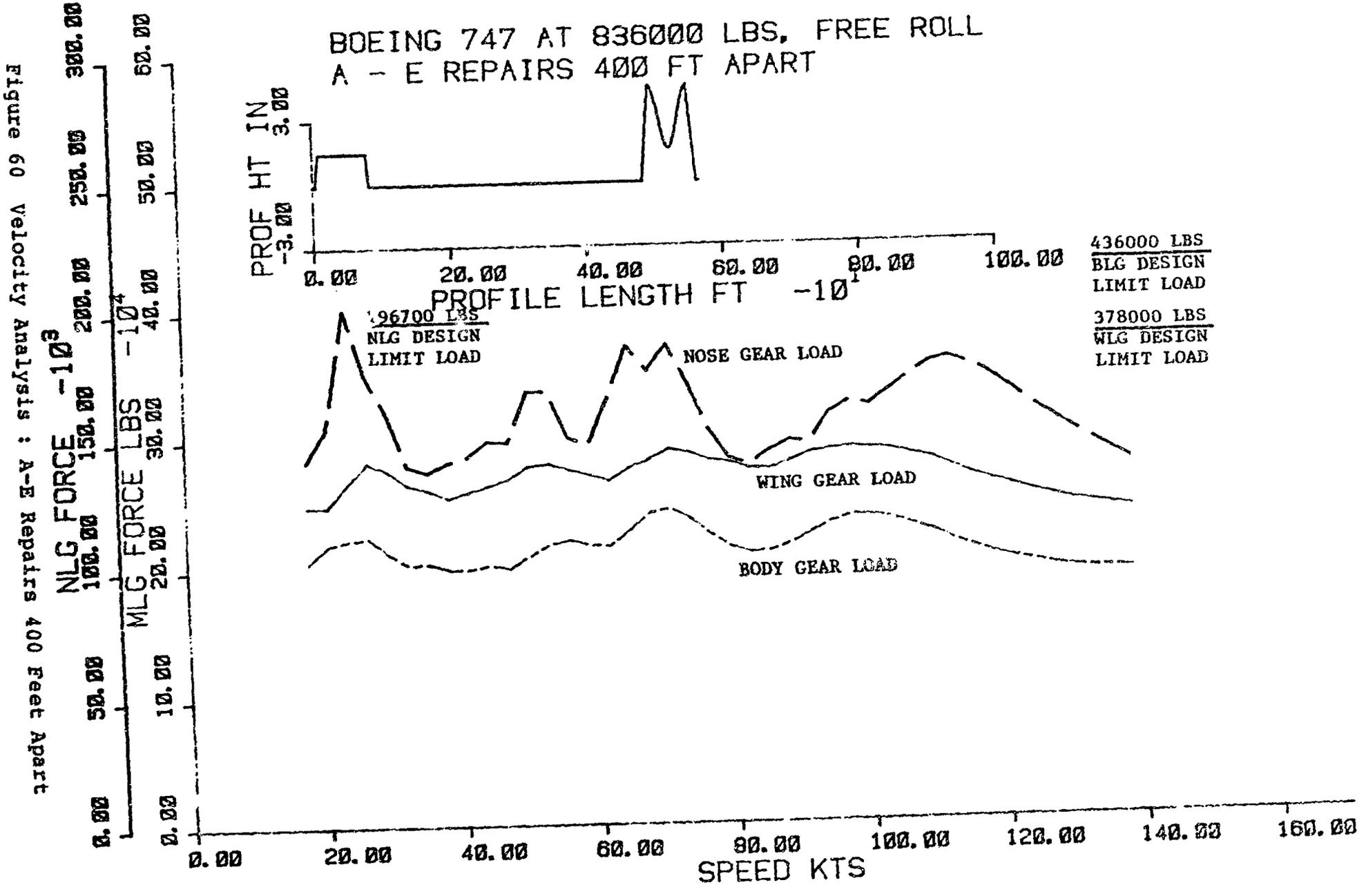

Figure 60 Velocity Analysis : A-E Repairs 400 Feet Apart

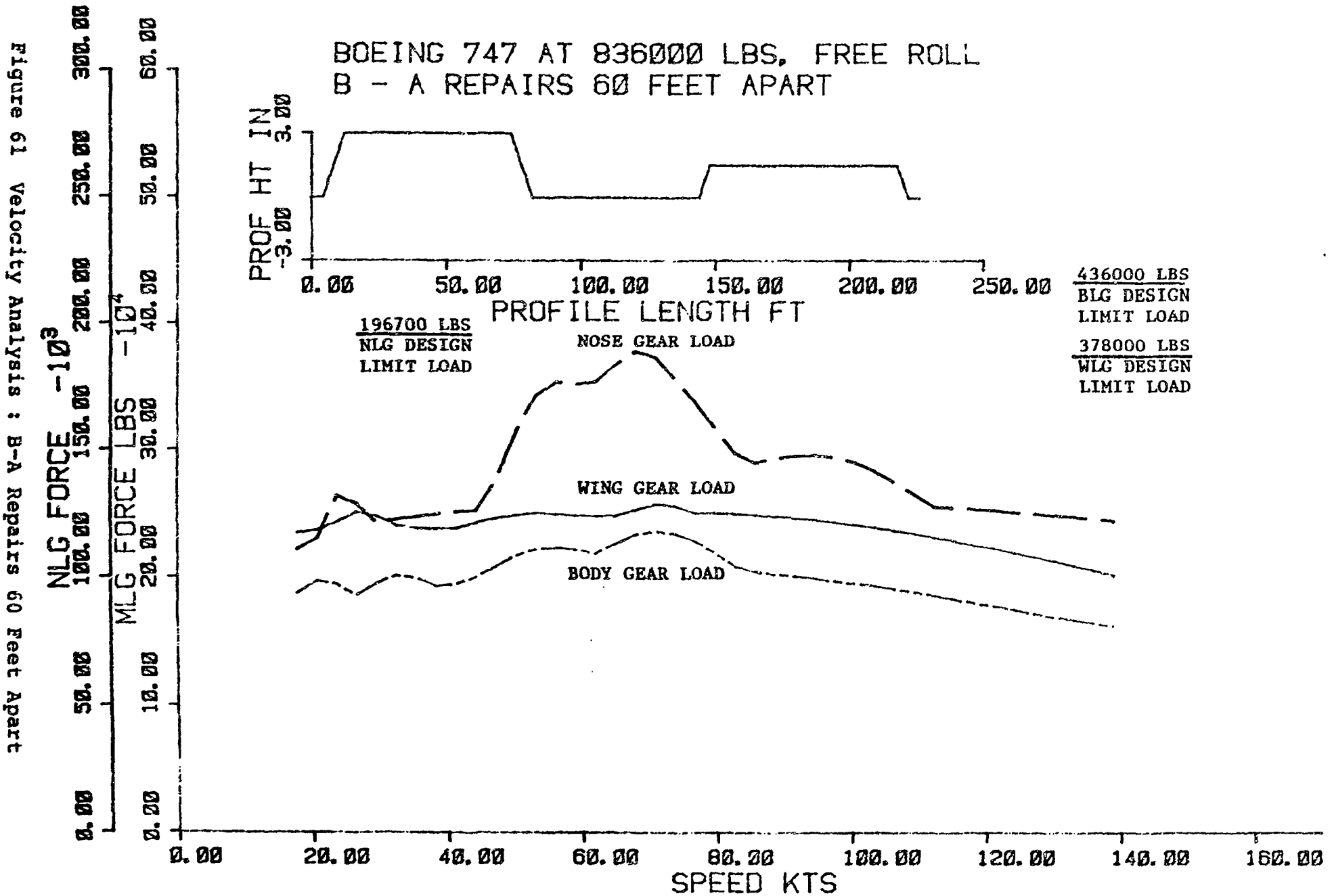

Figure 61 Velocity Analysis : B-A Repairs 60 Feet Apart

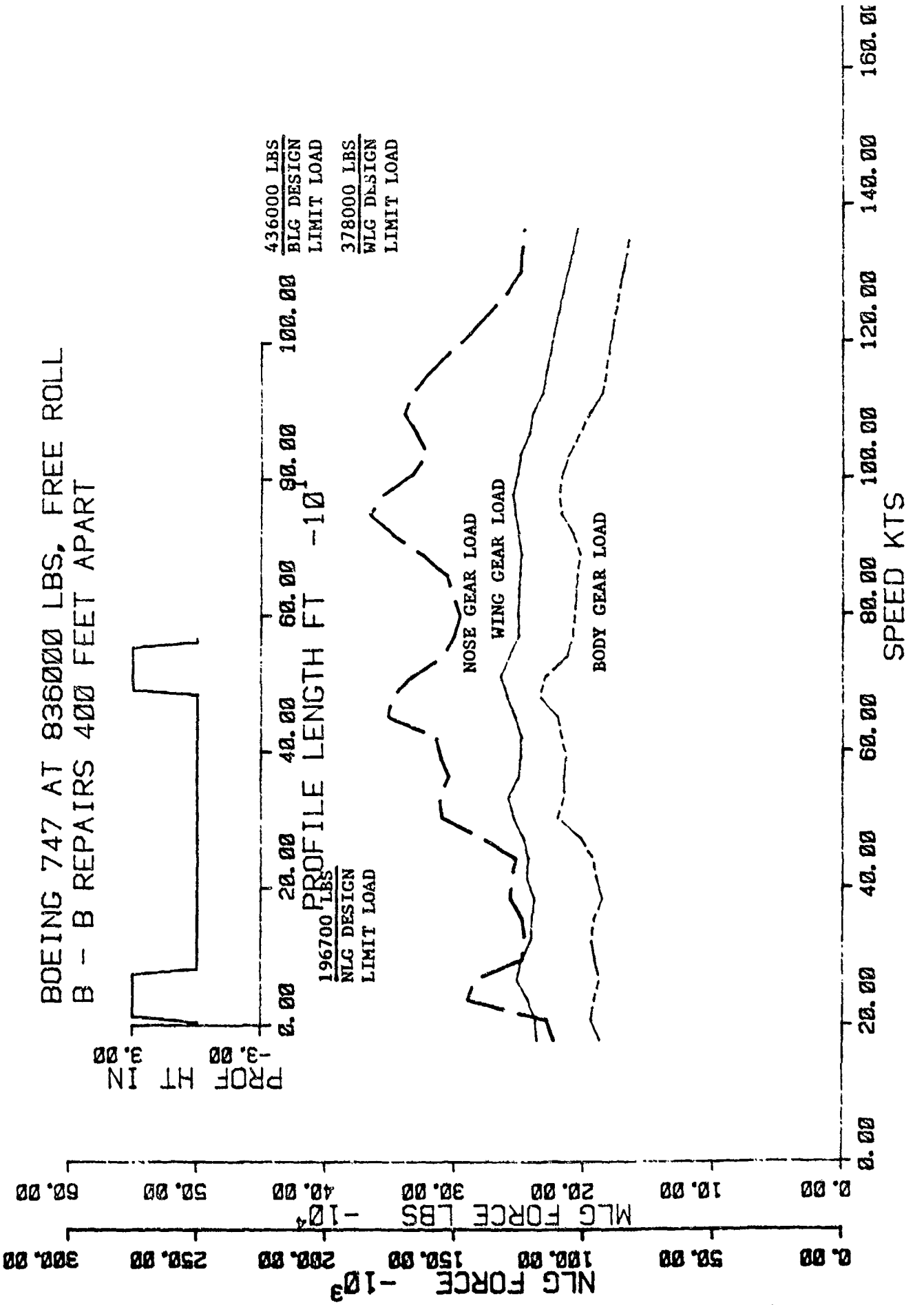

Figure 62 Velocity Analysis : B-B Repairs 400 Feet Apart

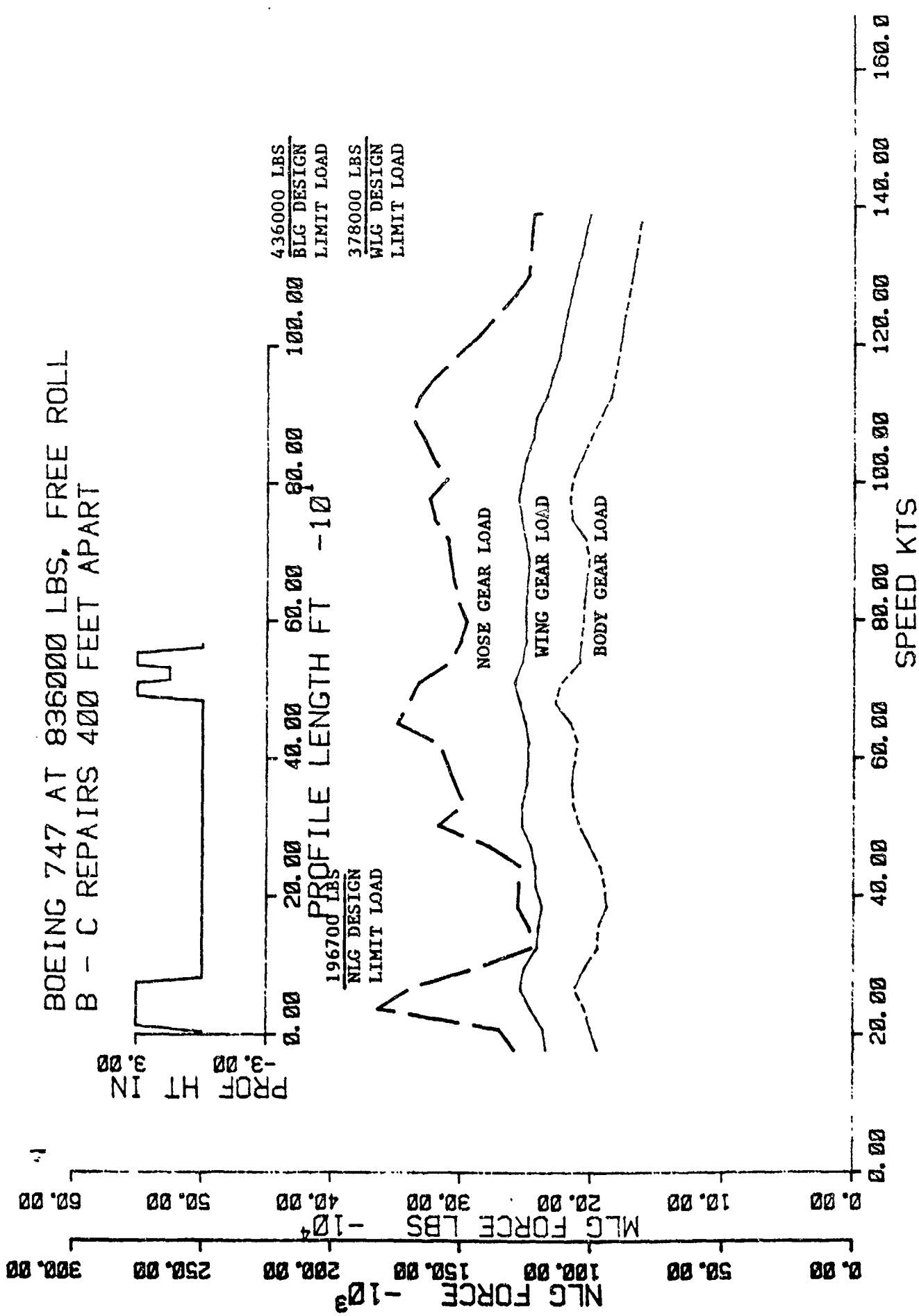

Figure 63 Velocity Analysis : B-C Repairs 400 Feet Apart

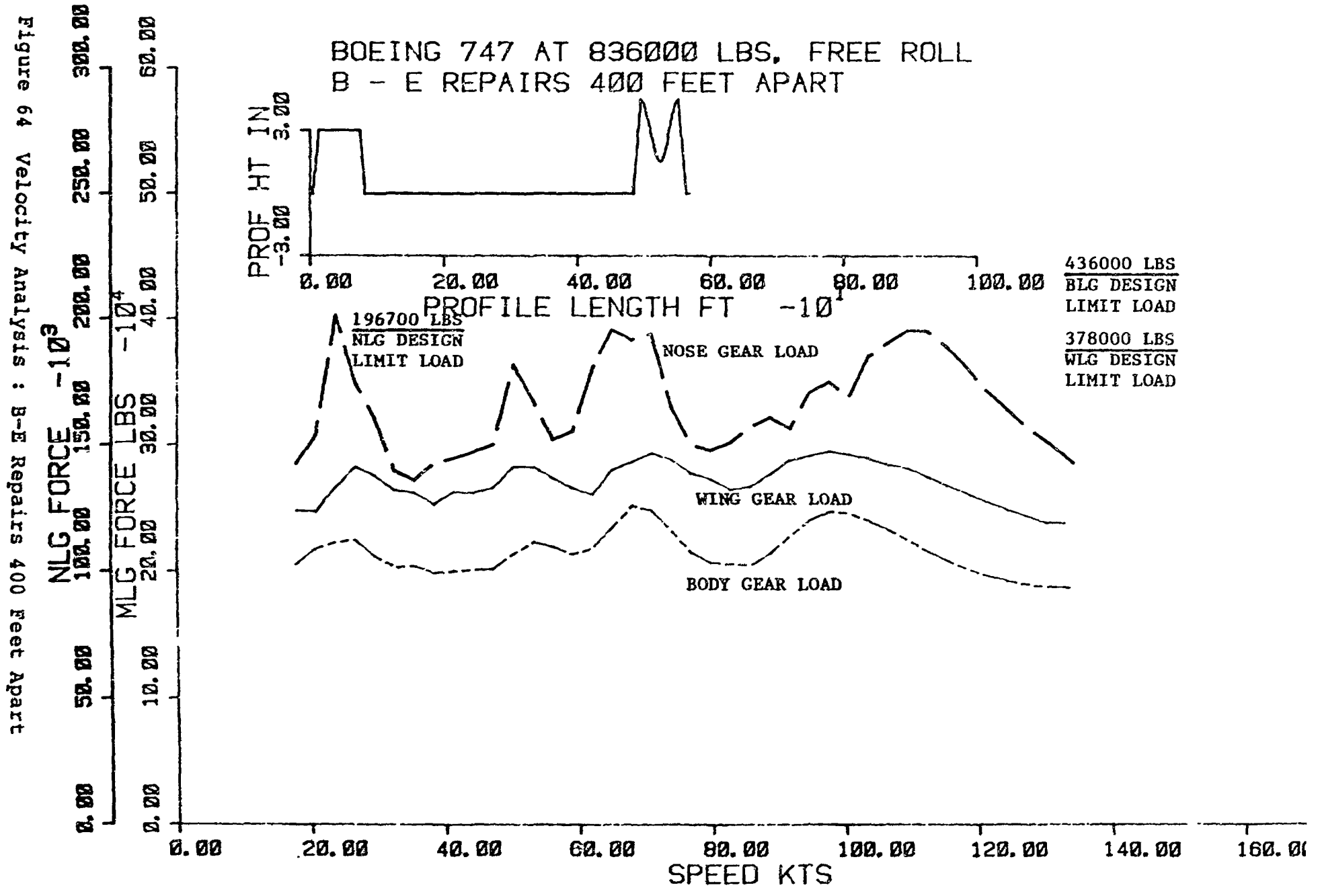

Figure 64 Velocity Analysis : B-E Repairs 400 Feet Apart

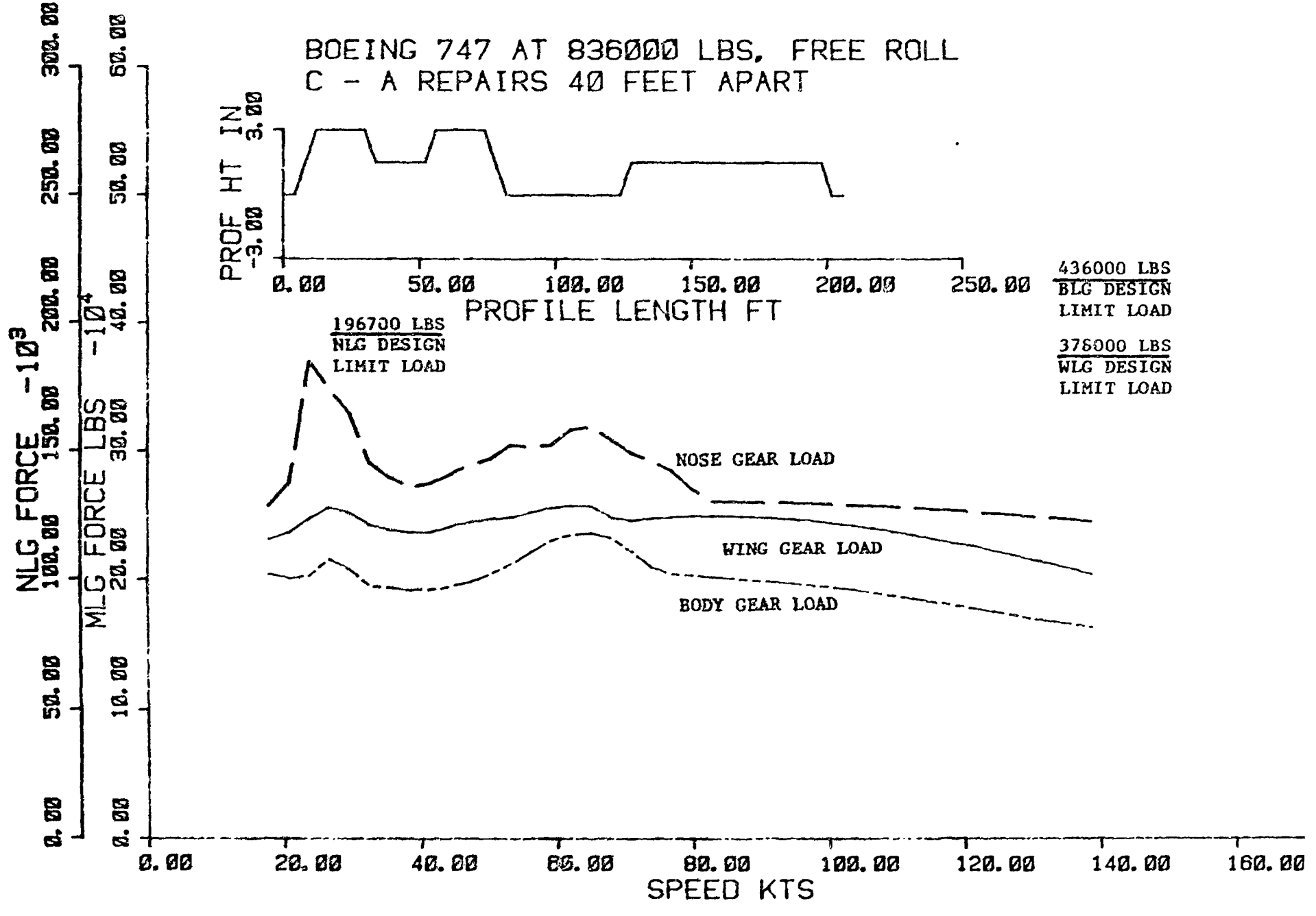

Figure 65 Velocity Analysis : C-A Repairs 40 Feet Apart

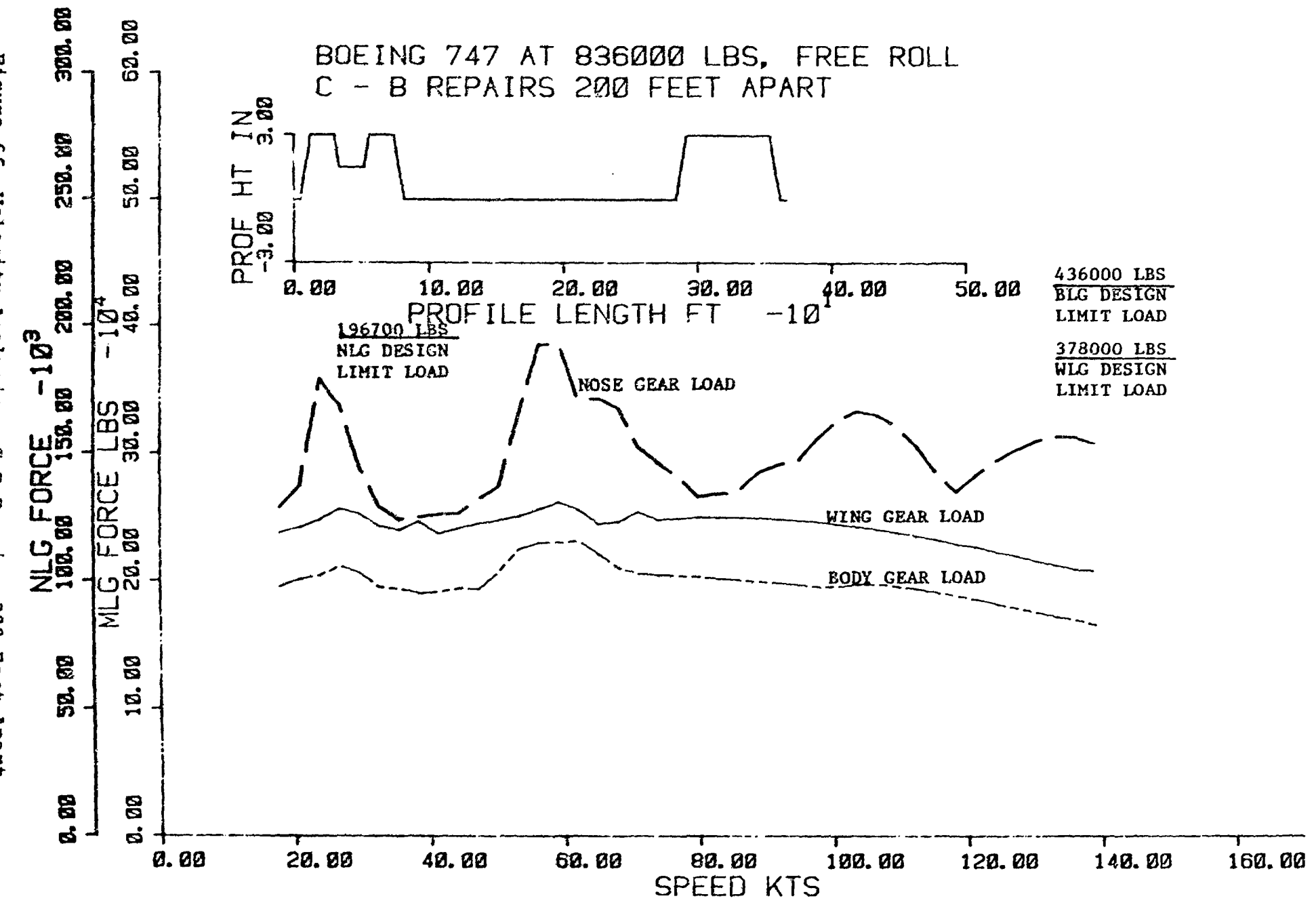

Figure 66 Velocity Analysis : C-B Repairs 200 Feet Apart

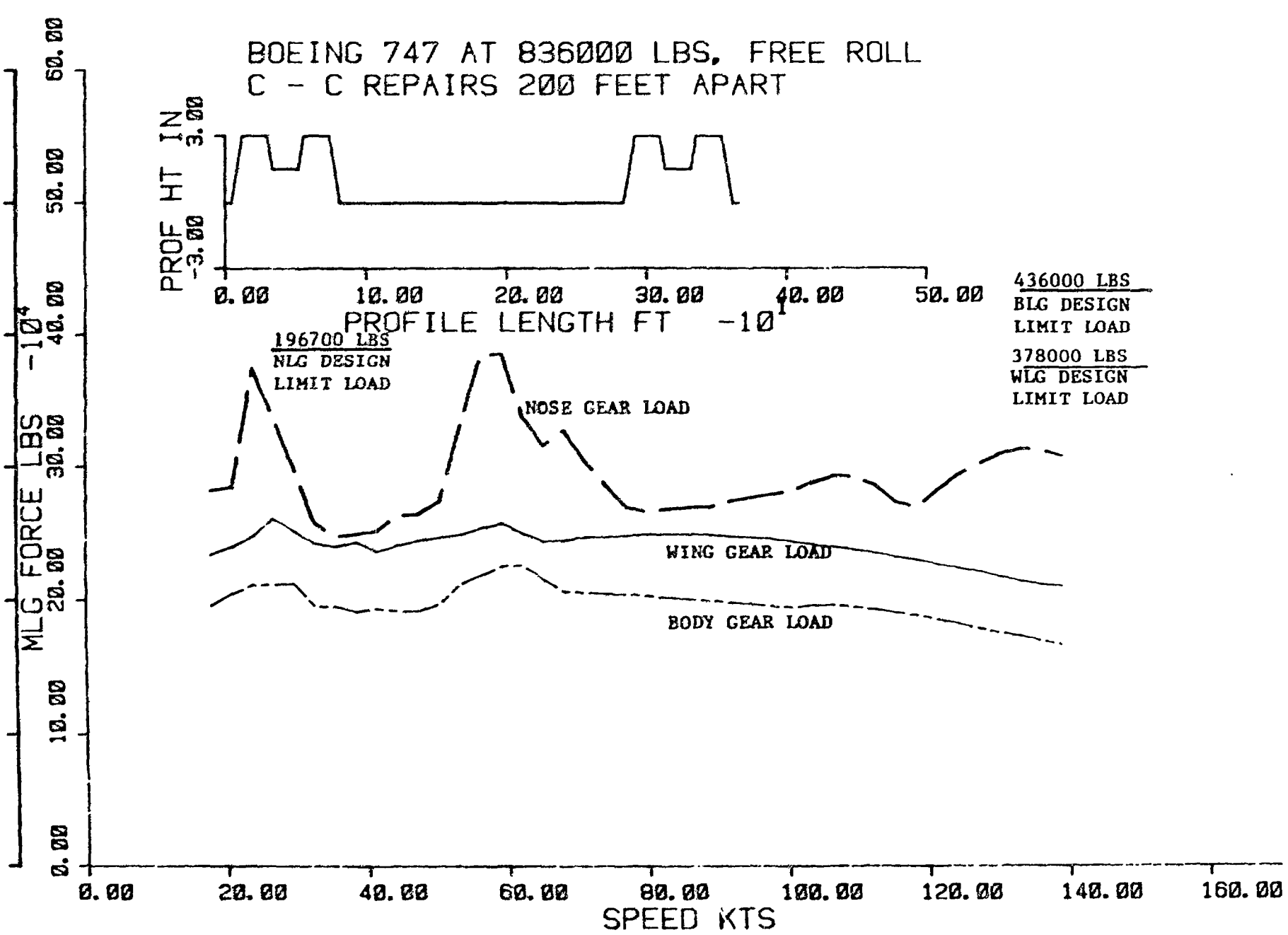

Figure 67 Velocity Analysis : C-C Repairs 200 Feet Apart

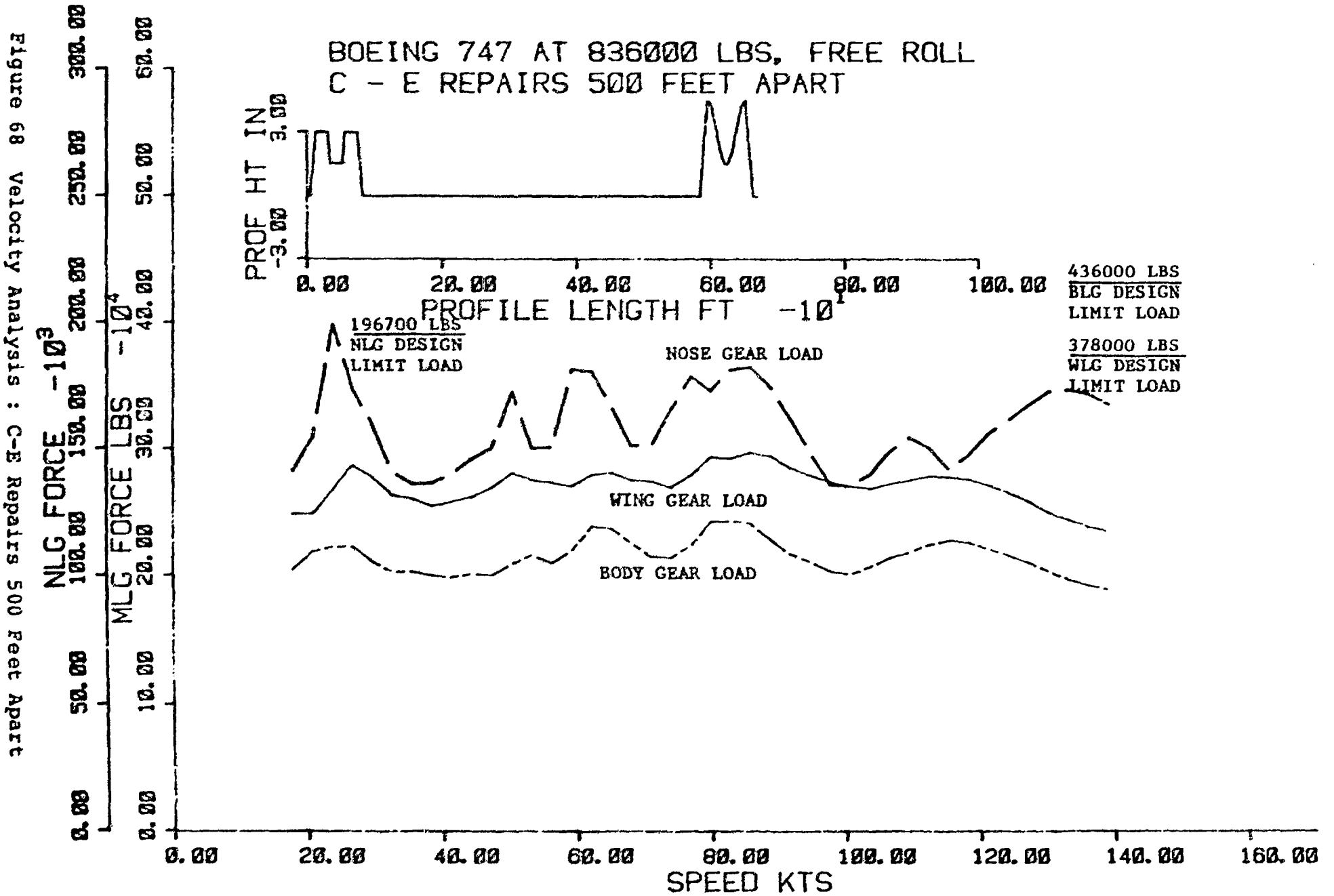

Figure 68 Velocity Analysis : C-E Repairs 500 Feet Apart

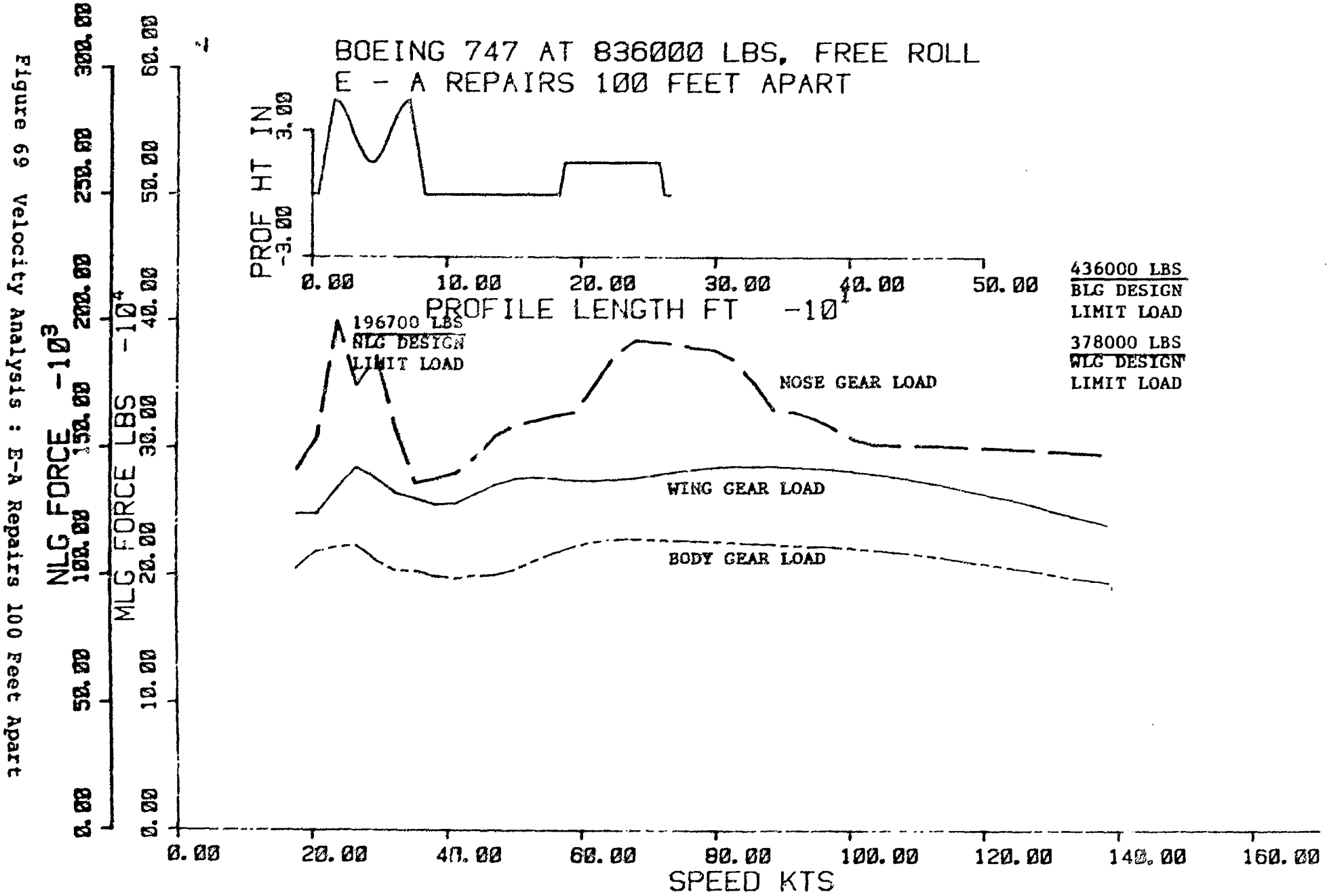

Figure 69 Velocity Analysis : E-A Repairs 100 Feet Apart

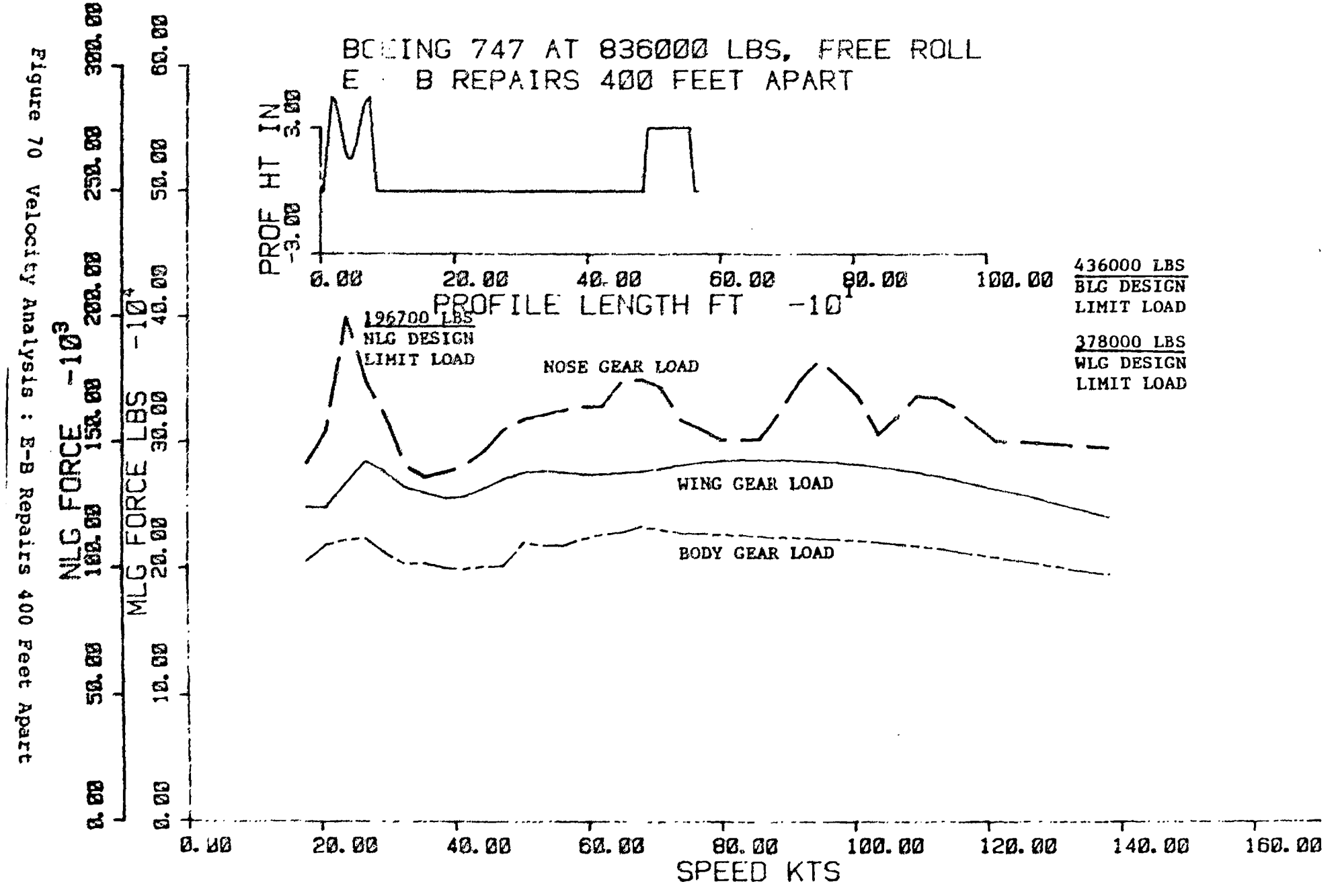

Figure 70 Velocity Analysis : E-B Repairs 400 Feet Apart

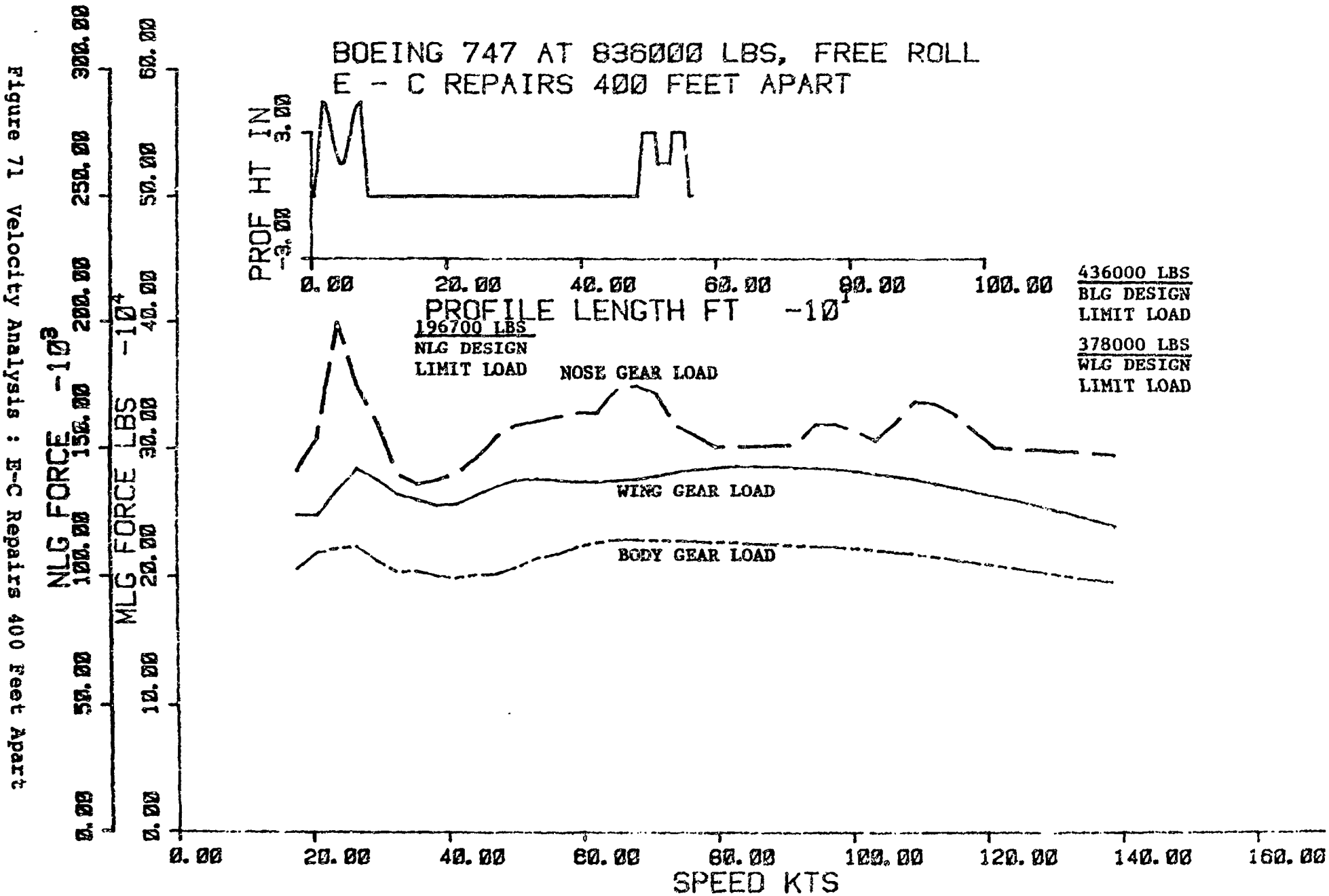

Figure 71 Velocity Analysis : E-C Repairs 400 Feet Apart

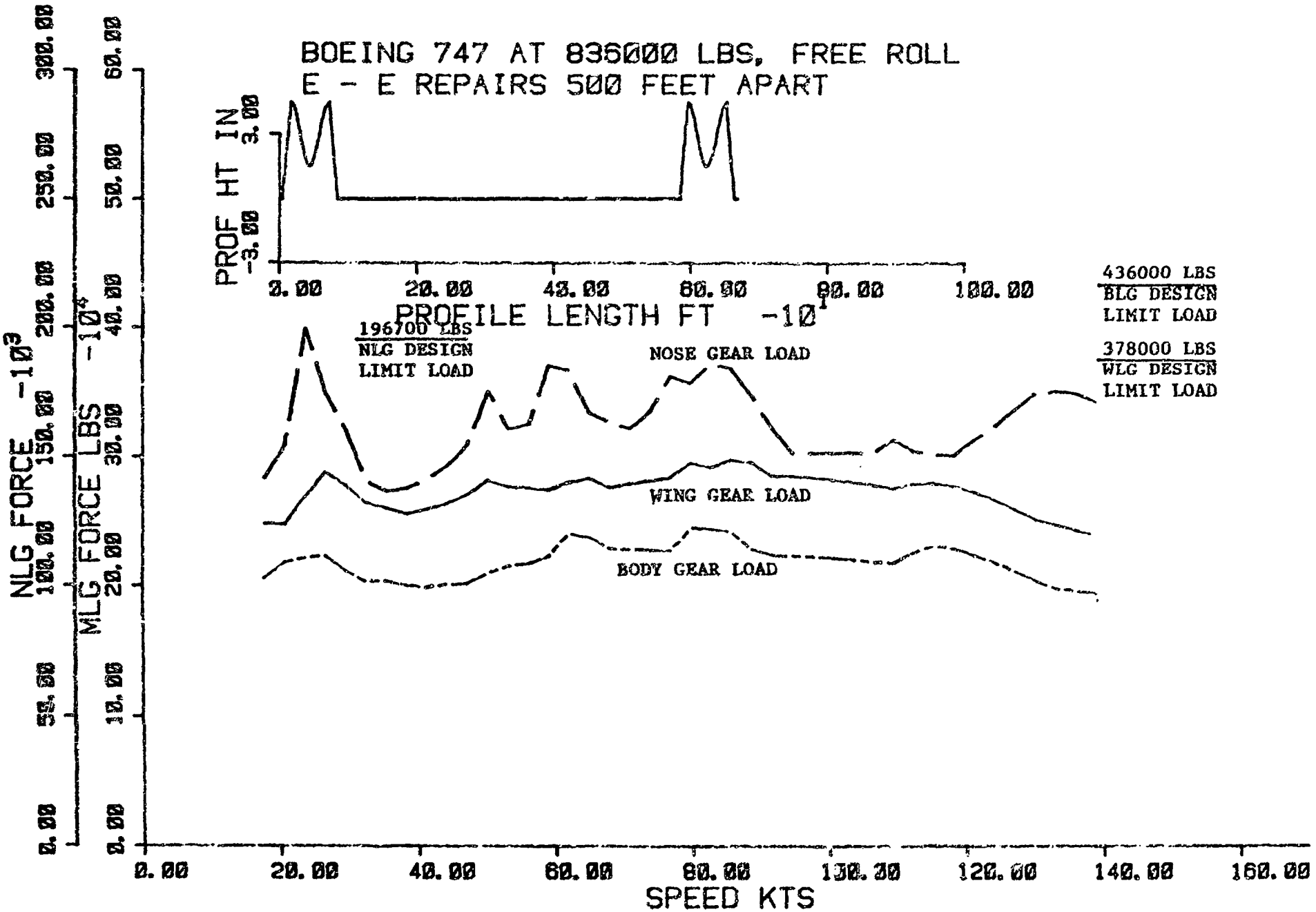

Figure 72 Velocity Analysis : E-E Repairs 500 Feet Apart